THE UNIVERSITY OF OKLAHOMA

GRADUATE COLLEGE

DOWNHOLE DYNAGRAPH MEASUREMENT

A THESIS

SUBMITTED TO THE GRADUATE FACULTY

in partial fulfillment of the requirements for the

degree of

MASTER OF SCIENCE

By

GLENN DOUGLAS ALBERT

Norman, Oklahoma

1986

DOWNHOLE DYNAGRAPH MEASUREMENT

A THESIS

APPROVED FOR THE DEPARTMENT OF AEROSPACE, MECHANICAL

AND NUCLEAR ENGINEERING

By

[redacted]

ACKNOWLEDGEMENTS

The author would like to thank his committee members, Drs. J. C. Purcupile, W. R. Upthegrove, and J. G. Bredeson for their critique of this report. Special thanks to Dr. Purcupile for fostering creative thinking and instilling the desire, in this author, to take on challenge. Also for his practical direction through the course of this project.

Also to Carl Adams for his assistance with the hardware development and Jesus Chacin for his work prior to the author's involvement, and continuous assistance and support throughout.

Thanks also to Chevron Oil Field Research Company for funding the project and providing the well and services needed for the downhole test.

Finally, to my beautiful wife, Joy, and loving children Jennifer and Blake, who are motivational by existance and whose support and loving tolerance made the successful completion of this project a reality.

GLENN D. ALBERT
December, 1986

ABSTRACT

While various mathematical models exist for predicting downhole forces and motion in sucker rod type pumping systems, none have been thoroughly verified with actual measurements. In fact, downhole force measurements were last made in 1942.

This report documents the development and use of a downhole data acquisition system designed and built to dynamically measure force and displacement at the bottom of the hole.

The system consists of a microcomputer, memory storage, power supply, and transducers, designed to fit collectively in a volume slightly over one inch in diameter by five feet in length.

Downhole dynagraphs and other data recovered from over one mile in the ground are presented.

TABLE OF CONTENTS

LIST OF ILLUSTRATIONS

LIST OF ILLUSTRATIONS (CONT'D)

DOWNHOLE DYNAGRAPH MEASUREMENT

CHAPTER I

INTRODUCTION

In the oil production industry there is a graphic method for observing the general pumping conditions, of an artificial lift type well, known as a dynagraph. A dynagraph is a display of the polish rod load versus the position in the pump stroke and is normally plotted over a single pump cycle as shown in Figure 1.1. For the past 60 years the dynagraph has been useful in measuring well performance and diagnosing trouble conditions downhole. More

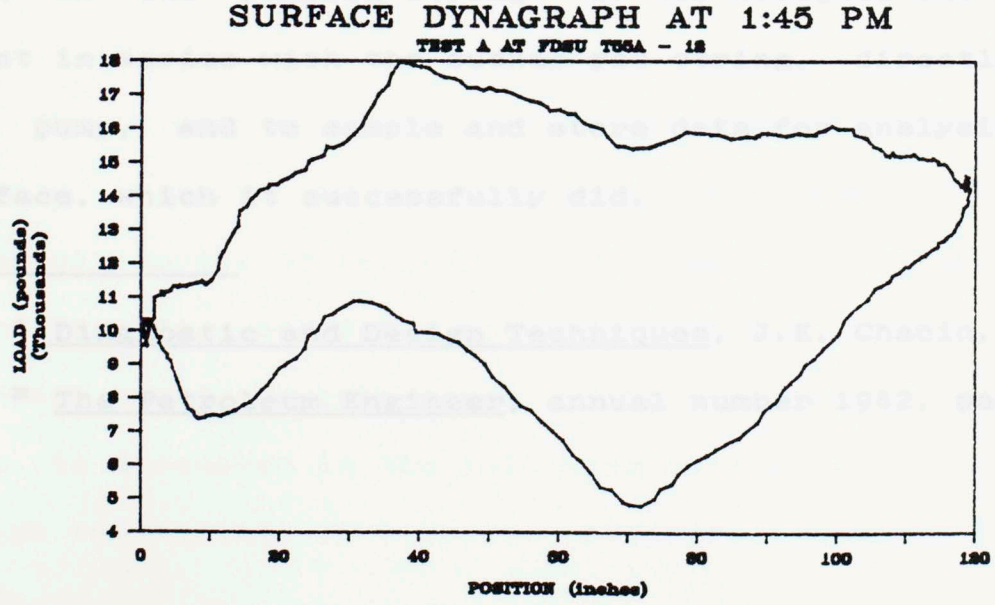

Figure 1.1 Surface dynagraph FDSU T55A - 12, 08-28-86

recently surface dynagraph data, with other well-specific parameters, has served as input to mathematical models for predicting downhole behavior, particularly a predicted dynagraph at the pump (which is located at the well bottom). Various computer programs to perform this task have been written (reference 1), none of which have been thoroughly verified empirically. In fact, no downhole measurements have been taken since 1942 by Lamberger and Langer (reference 2).

The task of this research was to conceive and build a modern apparatus to take downhole data to support or refute said models.

The resultant apparatus is a microcomputer-based data acquisition system that takes real-time measurements of multiple parameters, under the constraints of a downhole section in the pumping string. It was designed and built to mount in series with the sucker rod string, directly above the pump, and to sample and store data for analysis at the surface, which it successfully did.

---

[1] Diagnostic and Design Techniques, J.E. Chacin, 1986

[2] The Petroleum Engineer, annual number 1942, page 206.7

CHAPTER II

DESIGN SPECIFICATION

The primary motivation for this project was the need for experimental data to support Jesus Chacin's doctoral research work and computer program for predicting downhole behavior. As a result, the early design needs were already defined and the product definition resulted from our combined thoughts and discussions on what was important and feasible. Subsequent meetings with both Jesus and our mutual advisor, Dr. John C. Purcupile helped establish a good, practical approach to achieving these goals, specifically the hardware implementation.

2.1 Goals

The objective was to produce an apparatus that could be readily attached in series with the sucker rod, sent to crude oil depths of roughly 7,000 feet, withstand 10,000 pound tensile, and 2,000 pound compressive loads, and, of course, yield accurate data. (the quality and quantity of data is discussed in the following section). The inherent design constraints were space, pressure, temperature, and time.

2.2 Constraints

2.2.1 Space

Recognizing the potential hazard of introducing an unproven foriegn object into a well, standard oil field hardware was selected to contain the apparatus and attach it in the string. The standard Harbison-Fisher tubes and connectors detailed in appendix B are readily available in a variety of sizes and lengths and were the selection for this project. The dimension of primary concern and the main spatial constraint was the diameter of the tube which is 1.312 inches (1-5/16 inches, 33 mm). The design was virtually unconstrained in length though it was desirable to keep it short for handling and testing, and a stock length was desired to minimize cost.

2.2.2 Pressure

The apparatus had to be sealed to protect the electrical circuits and transducers from the external fluid being pumped. Having specified an adequate limit for the maximum depth of expected operation of 7,000 feet, the apparatus would have to withstand 3,000 psi static pressure and another 10% dynamic variation from pumping accelerations of approximately 0.10 g. The apparatus was designed and tested to 5,000 psi, sufficiently greater than the 2,500 to 3,000 psi experienced in the downhole test.

2.2.3 Temperature

The geothermal gradient in the first few miles of the crust of the earth is +1.6 degrees F per 100 feet (starting at 50 degrees just below the surface), with some variation for localized geothermal sources. At 7,000 feet a temperature of just over 160 degrees F could be expected which was an initial guideline for the temperature constraint. However, another line of constraint of great significance is the allowable operating temperature of the electrical components which are generally available in three temperature grades; 70, 85, and 125 degrees C. Besides the substantially higher cost of the higher temperature grade devices, initial parts sourcing revealed the availability of the chosen memory chips (to be discussed in the controller section) in only the lowest grade which forced the temperature specification of the apparatus to match. The temperature limitations of all other devices used, electrical and mechanical, would meet or exceed this limit of 70 degrees C.

2.2.4 Time

Today's low power, silicon technology provides the capacity for data storage of thousands of bytes on a single chip. The approach of a self-contained electronic apparatus with memory was conceptually superior to, and more practical than a tethered subassembly that received power, and trans-

mitted data over thousands of feet of cables, as was done in 1942. The device would then naturally be battery operated and, due to the exhaustable nature of batteries, this posed a time limitation on the useful duration of application of the apparatus.

A typical workover crew can run 7,000 feet of sucker rod, up or down, in one to two hours. Without adding to the fluid level from the surface it can take a well of this depth two to three hours to stabilize. If measurements of a stabilized well were desired and the apparatus were to require power the entire time it was in the ground, than a minimum of seven hours of battery life would be required. With the use of CMOS (Ceremic Metal Oxide Semiconductor) electrical components, wherever possible in the design, for extremely low power dissipation, the application of the only high-temperature dry cells (see Chapter 3.2) found on the market would exceed this duration goal by a factor of ten.

An added plus for the battery requirements here is the selection of the memory devices (GI-28C64 8kx8 EEPROM) which, are not only CMOS but also non-volatile, which means that once written to, they retain data indefinitely without presence of power. The benefit of this choice of memory is that the batteries need only last through the completion of the data taking period. Under normal operation this has little significance because of the excessive capacity of the batteries. But this feature is extremely valuable in the

event of a mishap that would strand the apparatus underground for several days, or if it were damaged during removal or dissassembly.

The Development section explains more fully how each of these constraints was addressed, designed and/or tested for before the downhole test.

CHAPTER III

DEVELOPMENT

The block diagram of the system in Figure 2.1 shows the three basic elements of the design; transducers, controller, and battery pack. The physical containment or case, with strain gages mounted to its inner wall, is itself a transducer.

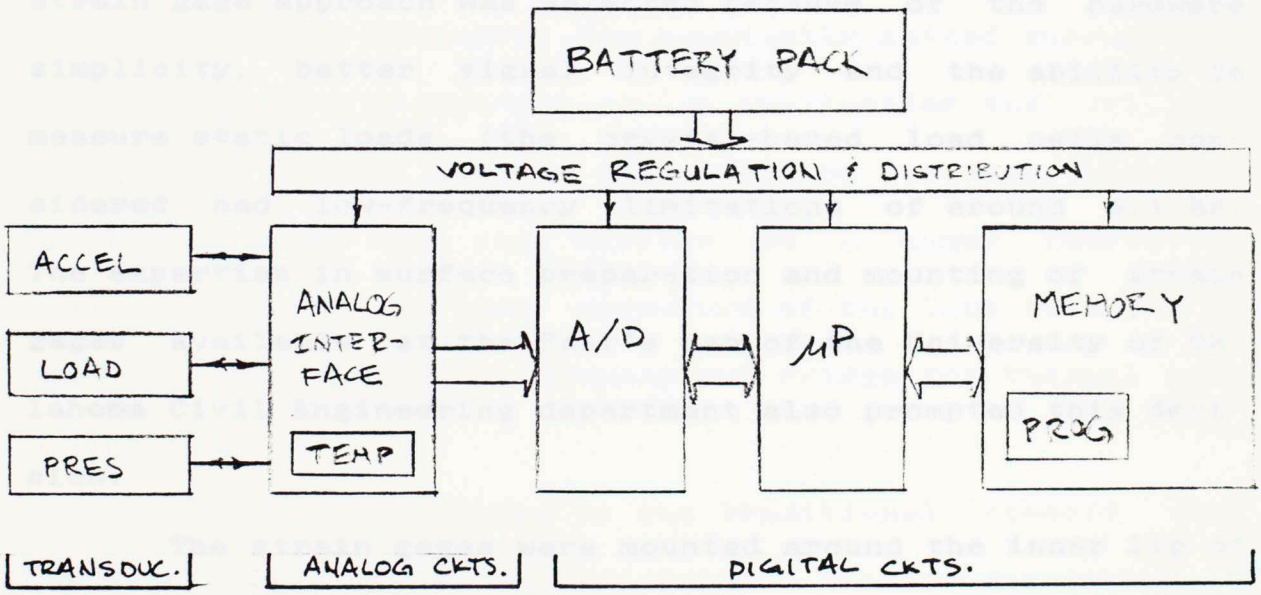

Figure 3.1 System Block Diagram

3.1 Transducers

Four variables, two primary and two secondary, are transduced within the apparatus: axial load, axial acceleration (to derive displacement), external pressure on the ap-

paratus, and internal temperature. The primary variables, load and displacement, were given the greatest development priority but since temperature and pressure could be readily obtained and it was not initially known in the development, whether these variables would have any affect on the primary transducers, it was decided to monitor these two environmental parameters as well.

3.1.1 Load

Two alternatives were considered for sensing load; a strain gage assembly or a piezo-electric load cell. The strain gage approach was selected because of the hardware simplicity, better signal integrity and the abililty to measure static loads (the crystal-based load cells considered had low-frequency limitations of around 0.1 Hz. The expertise in surface preparation and mounting of strain gages available at the Fear's Lab of the University of Oklahoma Civil Engineering department also prompted this decision.

The strain gages were mounted around the inner lip of the 12 inch section of tubing, as shown in Figure 3.2, that was chosen to contain all of the transducers. The first mounting attempt produced the strain sensing element used in the downhole test. Four strain gages were mounted to insure adequate testing.

The benefit of having multiple gages was that a high

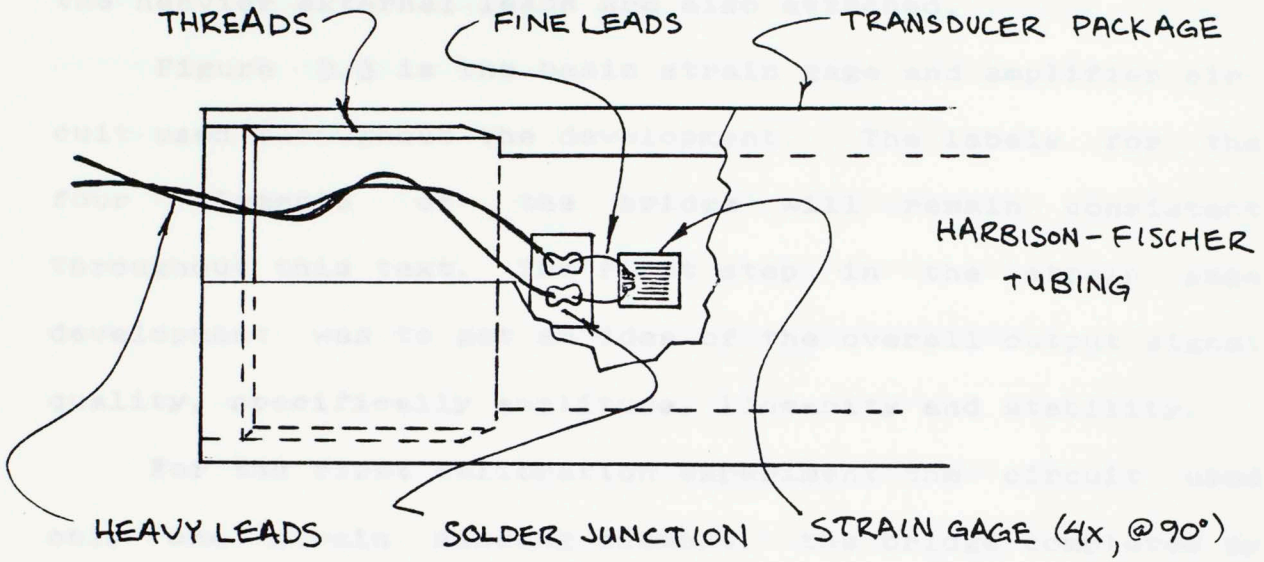

Figure 3.2 Strain gage mounting location.

degree of output linearity was eventually gained through the development of a Wheatstone bridge application that utilized two active strain gages, which will be discussed shortly. Two strain gages were also mounted on a dummy sample of steel that fit the inner curvature of the tube to serve as inactive legs used in the Wheatstone bridge for thermal compensation.

The Wheatstone bridge is the traditional circuit used for strain gage signal amplification. A brief discussion of this and the mentioned concept of thermal compensation is provided in Appendix A.

The gages were mounted reasonably close to the end of the tubing for ease of surface preparation and gage placement and also for access with a soldering iron to solder the fine gage leads to a surface pad (see Figure 3.2) to which

the heavier external leads are also attached.

Figure 3.3 is the basic strain gage and amplifier circuit used throughout the development. The labels for the four elements of the bridge will remain consistent throughout this text. The first step in the strain gage development was to get an idea of the overall output signal quality, specifically amplitude, linearity and stability.

For the first calibration experiment the circuit used only one strain sensing element, the bridge completed by three circuit resistors (see Figure 3.3). At this point in the development it was safe enough to assume negligable temperature variation in the lab so no attempt was made to compensate the circuit thermally.

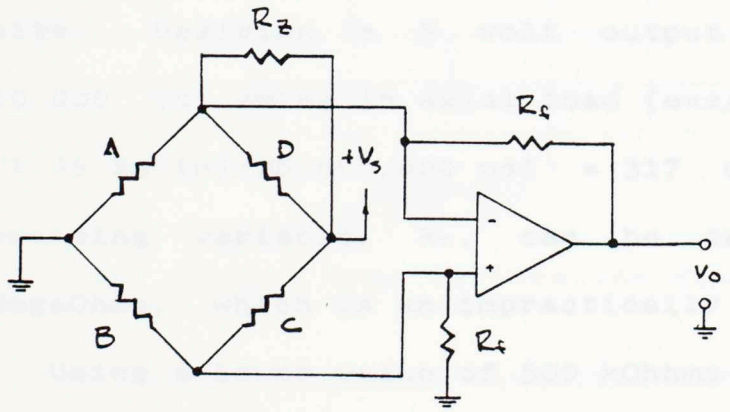

Figure 3.3 Basic Strain Gage Circuit Configuration

The equation for the output of this this circuit is:

Eq. 1 $V_o = (V_s/2) * a * e * (R_f/R_s)$

where V_o=output voltage, V_s=supply voltage, a=gage factor, e=strain, R_f=feedback resistance, and R_s=strain gage resistance.

The gage factor accounts for the fact that the change in R_s, though linear, is not directly proportional to the change in e. This factor is generally between 1 and 2 and was assumed to be 1.5 for the initial analysis that follows.

The A/D converter was already designed at this point and the input range was specified as 0 to 5 volts. Therefore it was the goal to condition all transducer signals to be within that range and preferable span a large percentage of the 5 volt swing for maximum resolution of the digital data.

R_s was given as 350 Ohms, and V_s was a factory recommended 5.0 volts. Desiring a 5 volt output swing for roughly a 10,000 lb swing in axial load (e=s/E =(L/A)/e =(10,000 lb /1.05 sq in)/30,000,000 psi = 317 uinch/inch), the only remaining variable, R_f, can be calculated as roughly 1.5 MegaOhms, which is an impractically large circuit value. Using a lower value of 500 kOhhms was still a concern, producing a differential amplifier gain of over 1000, large enough to yield unwanted stray effects in the output.

The first calibration data is shown in Figure 3.4. Readily apparant from this data are two forms of error, nonlinearity and, of greater concern, a 200 mV shift in the

operating point occurring in just the short time between taking the two columns of data. Further observation during this test revealed subsequent shifts of greater than 500 mV and a sensitivity to air movement in the vicinity of the circuit.

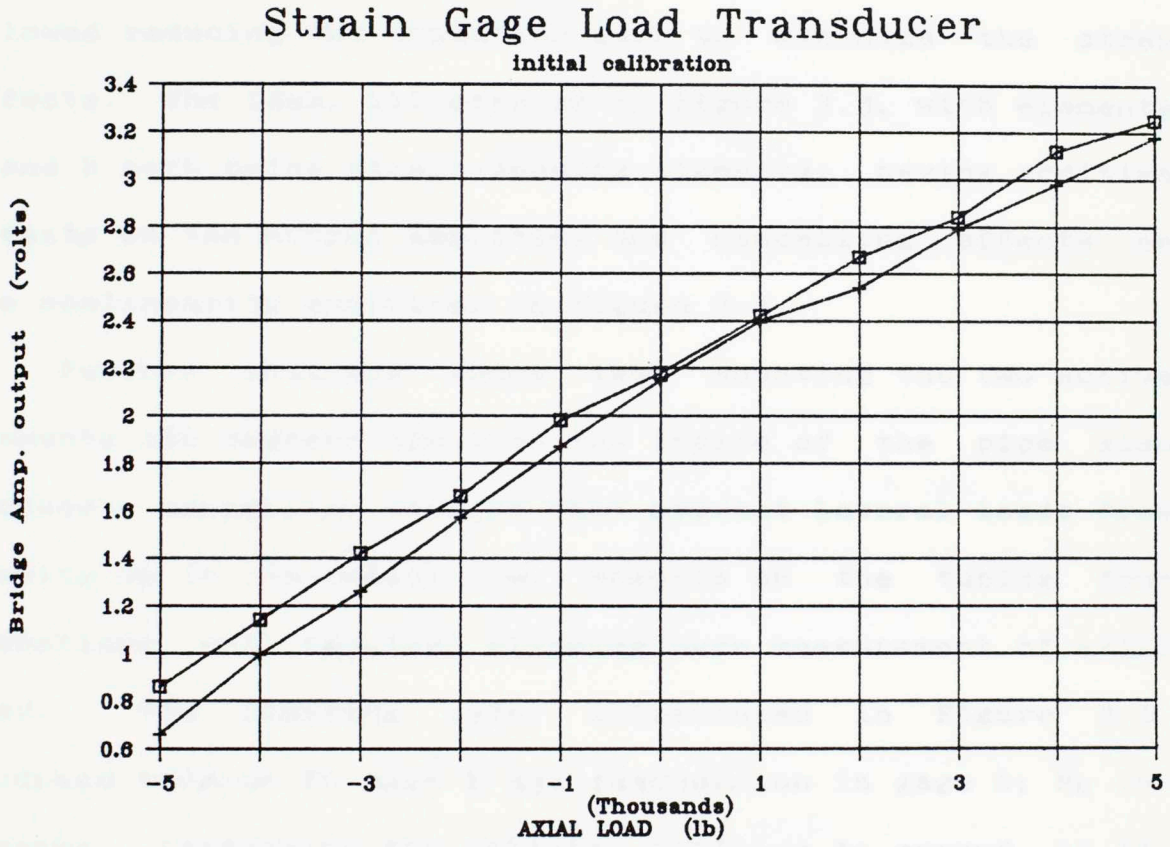

Figure 3.4 Single Gage Calibration Results

The two most important design decisions made, regarding the strain gage load transducer, resulted from the outcome of this first experiment.

First, the lead lengths in the elements of the bridge had to be made as short as possible because a 0.01 Ohm change in any part of the bridge produces a 150 mV change in the output. So, for the next step in development, all four

legs of the bridge would be mounted close together (ie, up inside the tube, near the strain gages).

Second, needing to reduce the gain of the amplifier and yet wanting a larger output swing, a method was devised to double the output of the bridge, before the amplifier, which allowed reducing the amplifier gain to minimize the stray effects. The idea, illustrated by Figure 3.3, with elements B and D both being strain-sensing elements, having additive effects on the output amplitude and cancelling effects on the nonlinearity exhibited in Figure 3.4.

Further analysis shows that mounting the two active elements 180 degrees apart on the inside of the pipe also produces cancelling effects that prevent lateral loads from showing up in the output (ie. moments on the tubing from vibrations and bending) allowing pure measurement of axial load. The limiting case, illustrated in Figure 3.5, produces tension in gage B and compression in gage D; R_B increases, increasing the voltage, relative to ground, at the plus op-amp input, and R_D decreases which, by decreasing the voltage across R_D that is referenced to +V, also increases the minus op-amp input, producing no net change at the output. In the other limiting case where the tubing is rotated 90 degrees, both gages are near the neutral fiber and they experience no change. For intermediate cases, gages B and D are always equidistant from the neutral fiber and consequently experience equal and opposite strain, producing no

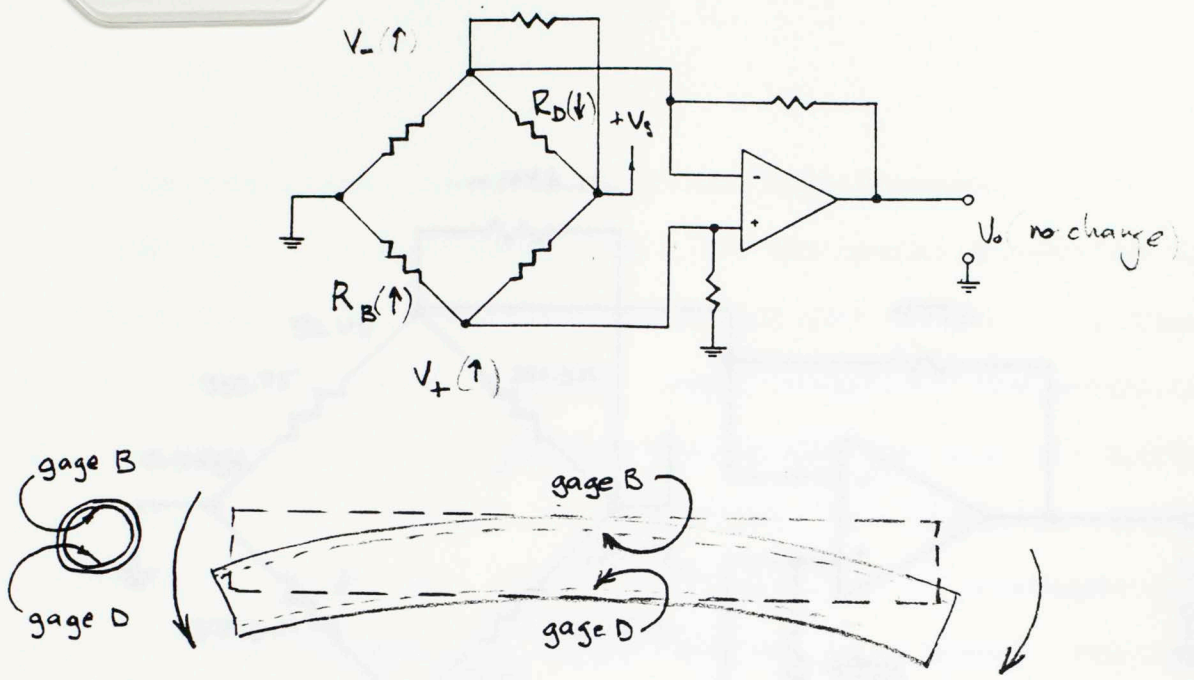

Figure 3.5 Gage Mounting for Lateral Load Insensistivity

net effect on the output.

The circuit incorporating these changes and the resulting calibration data are shown in Figures 3.6 and 3.7. V_{ss} was increased to 6.2 volts for this experiment in an effort to increase output swing but returned to 5.0 volts in the final implementation.

The standard approach for thermal compensation was used, applying the same type of strain gages in the inactive legs as in the strain-sensing legs only mounted to a dummy piece of steel that does not come under stress. This matches resistive values in the bridge, but more importantly the thermal coefficients of the resistive material in the gages. Since the bridge circuit amplifies proportional changes of the elements, a uniform temperature change in all elements will generate no change in the output. The dummy is made of steel to match the thermal coefficient of expan-

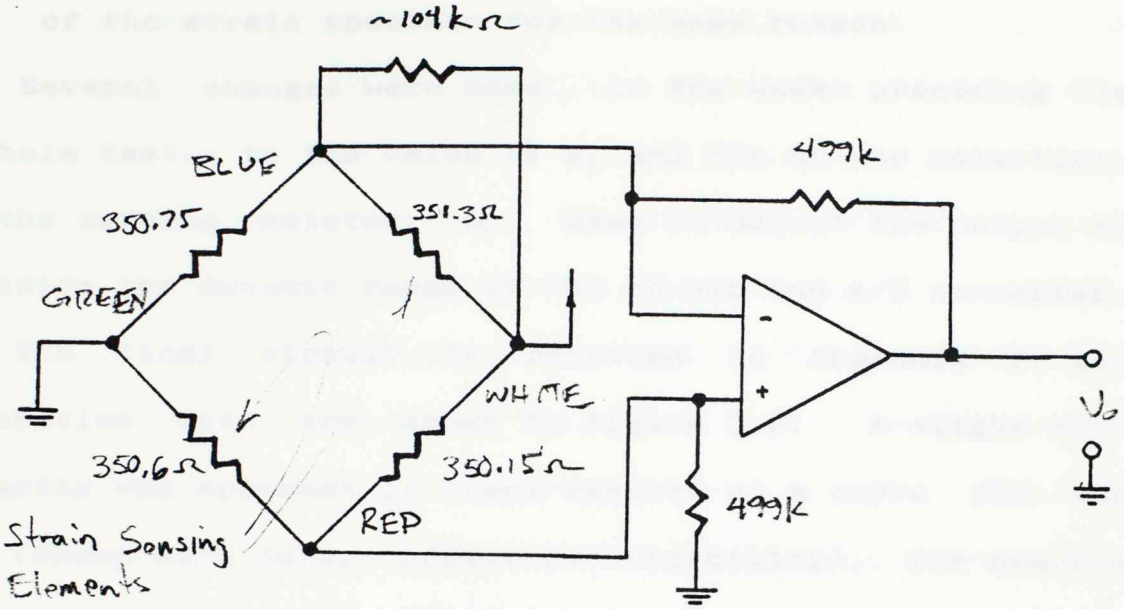

Figure 3.6 Dual Strain Sensing Element Configuration

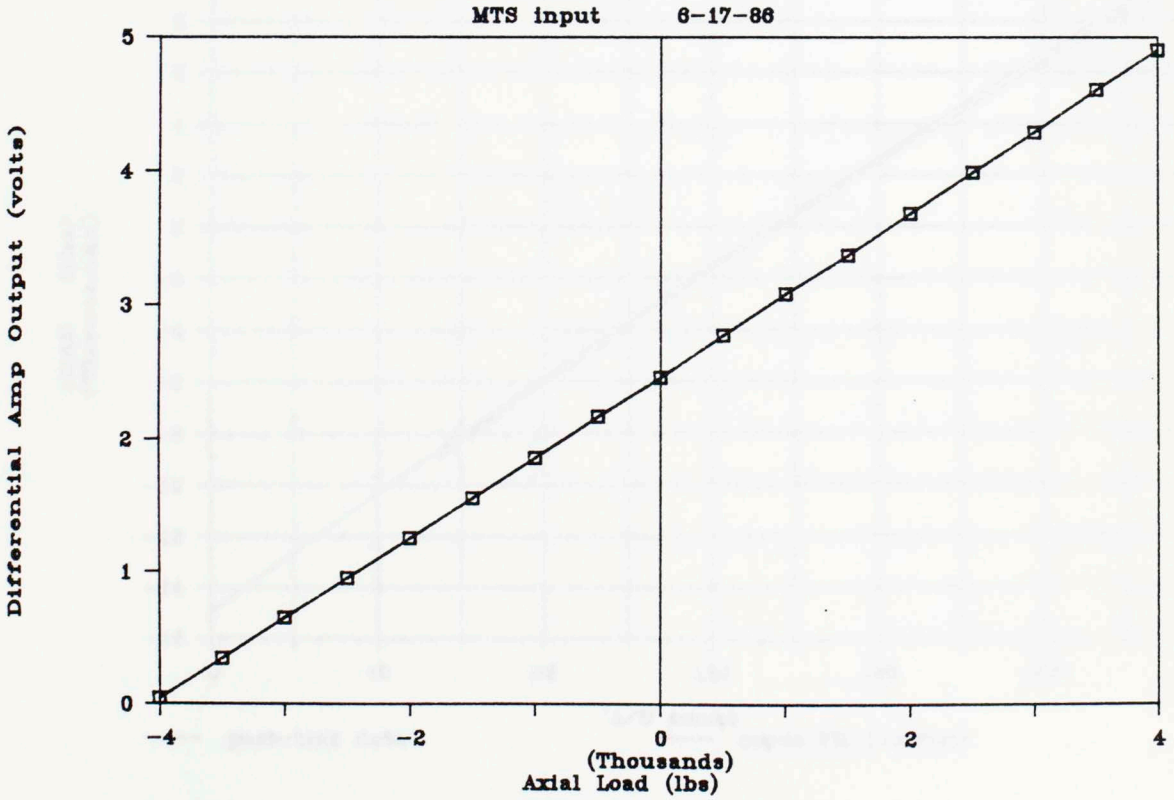

Figure 3.7 Dual Strain Sensing Element Data

sion of the strain specimen for the same reason.

Several changes were made, in the weeks preceding the downhole test, to the value of R_f and the op-amp selection, and the zeroing resistor, R_z, used to adjust the output to be inside the dynamic range of the op-amp and A/D converter.

The final circuit is provided in Appendix F and calibration data are shown in Figure 3.8. A slight non-linearity was apparant in these results so a curve fit was made (shown with data, offset for visibility), for precise interpretation of the downhole results. Assuming a quad-

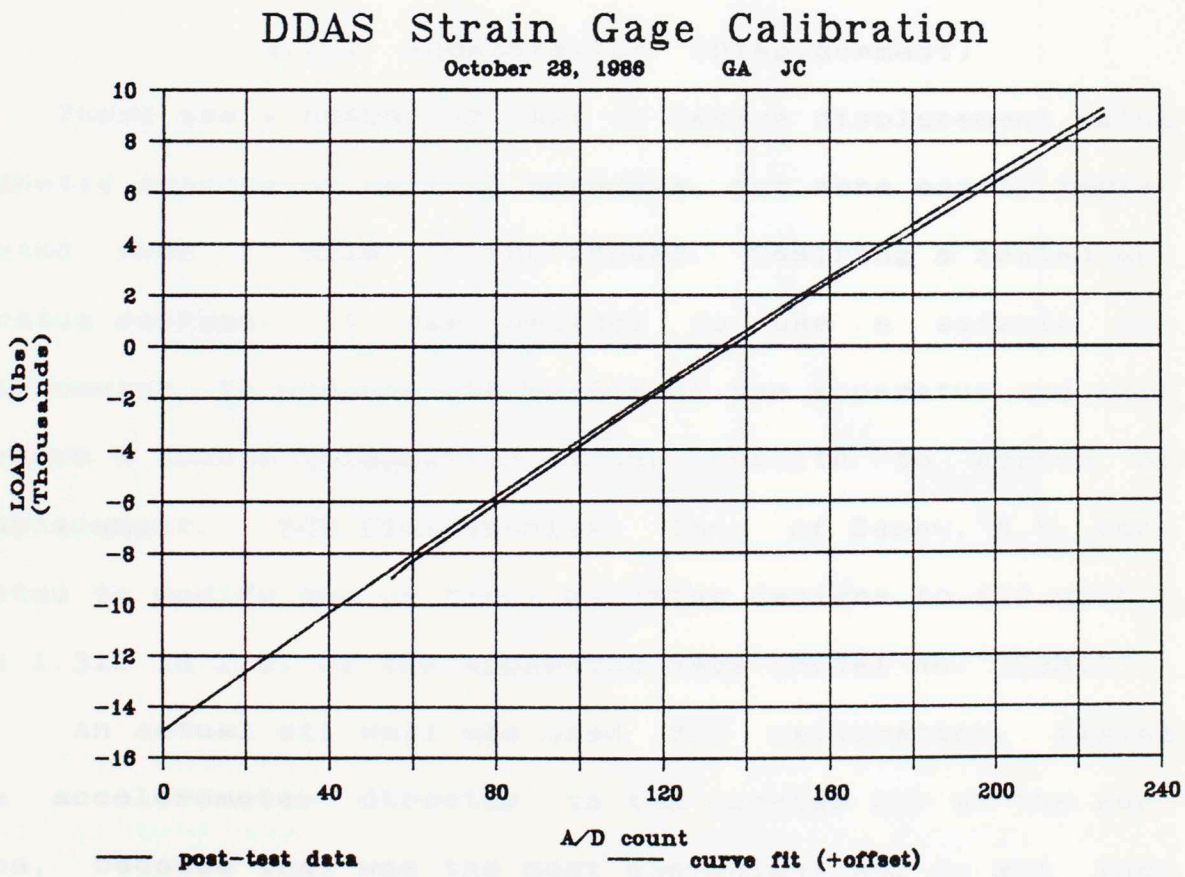

Figure 3.8 Calibration Data, Final Circuit Configuration

ratic relationship, the curve was fit, using tools available in Lotus 123, ver. 2, by creating a column reflecting the local slope of the data (on a point-to-point basis), performing a linear regression of this vs load, and then mathematically integrating the straight line result to produce the shown curve fit. Load is plotted vs A/D count because that is the form in which the data is stored. The 8-bit A/D used produces 256 levels of input between 0 and 5 volts, each level representing 19.0 mV of transducer signal. The data and analysis is saved in a Lotus 123 worksheet and stored on Disk 1, under filename FCALA282.WK1.

3.1.2 Acceleration (Displacement)

There are a number of ways to derive displacement using magnetic sensors or optical encoders, but none easily implemented over 1 mile in the ground. Desiring a sealed apparatus package, it was decided to use a seismic accelerometer to measure the motion of the apparatus and then perform a double integration on the results to arrive at displacement. PCB Piezotronics, Inc. of Depew, N.Y. consented to modify one of their existing designs to fit within the 1.312 in I.D. of the apparatus case (Model No. 393M11).

An actual oil well was used for calibration, fixing the accelerometer directly to the carrier bar at the surface, because that was the most convenient way to get such large displacements and low frequencies. Early attempts at

calibration, on Sooner #1 revealed the accelerometer's extreme sensitivity to shock. The signal saturation and following decay shown in each cycle of Figure 3.9 resulted from a mechanical impulse to the sucker rod string about 5 inches into each upstroke. Figure 3.9 also includes the position signal, recovered from a Delta-X displacement potentiometer, for comparison to the position signal derived numerically from the accelerometer data.

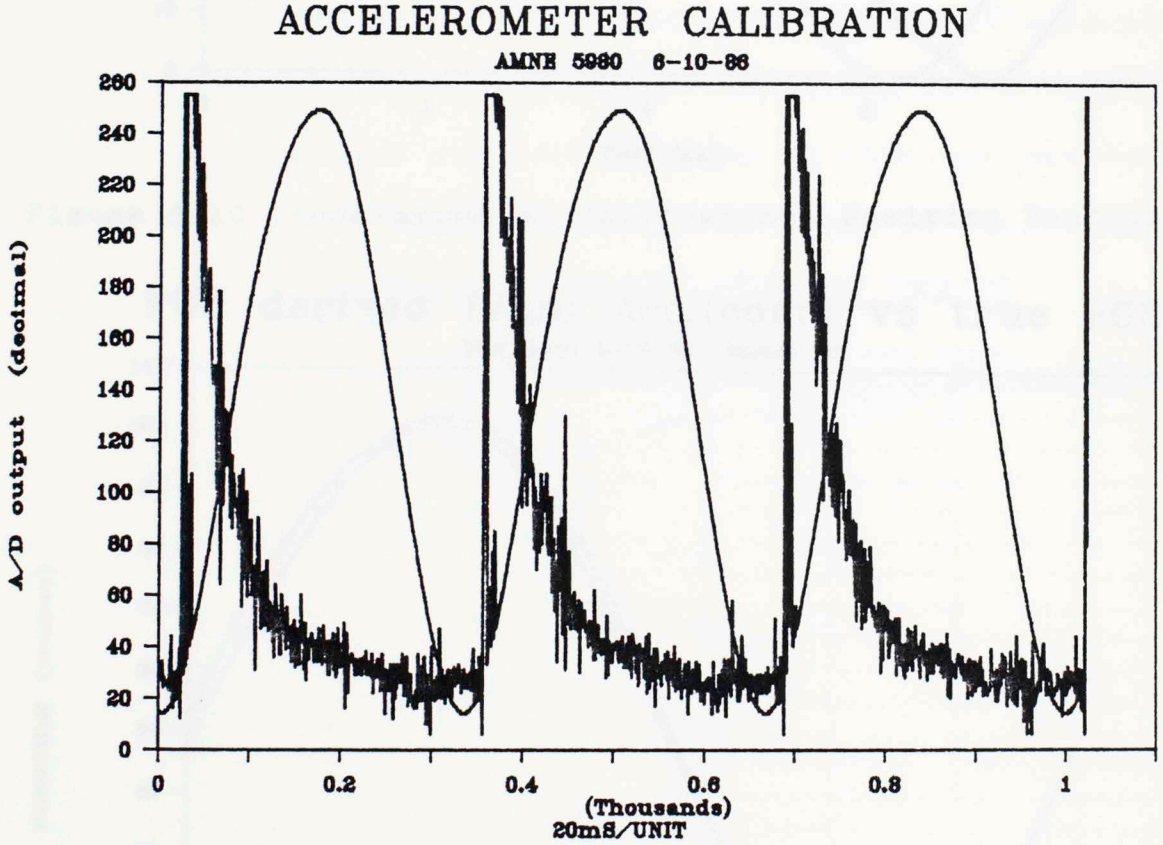

Figure 3.9 Accelerometer Calibration, First Attempt

PCB consented to fix the problem and eventually did. Testing continued with the accelerometer mounted in a spring-damper support. Figures 3.10 and 3.11 depict the results, both graphs containing the same true-position

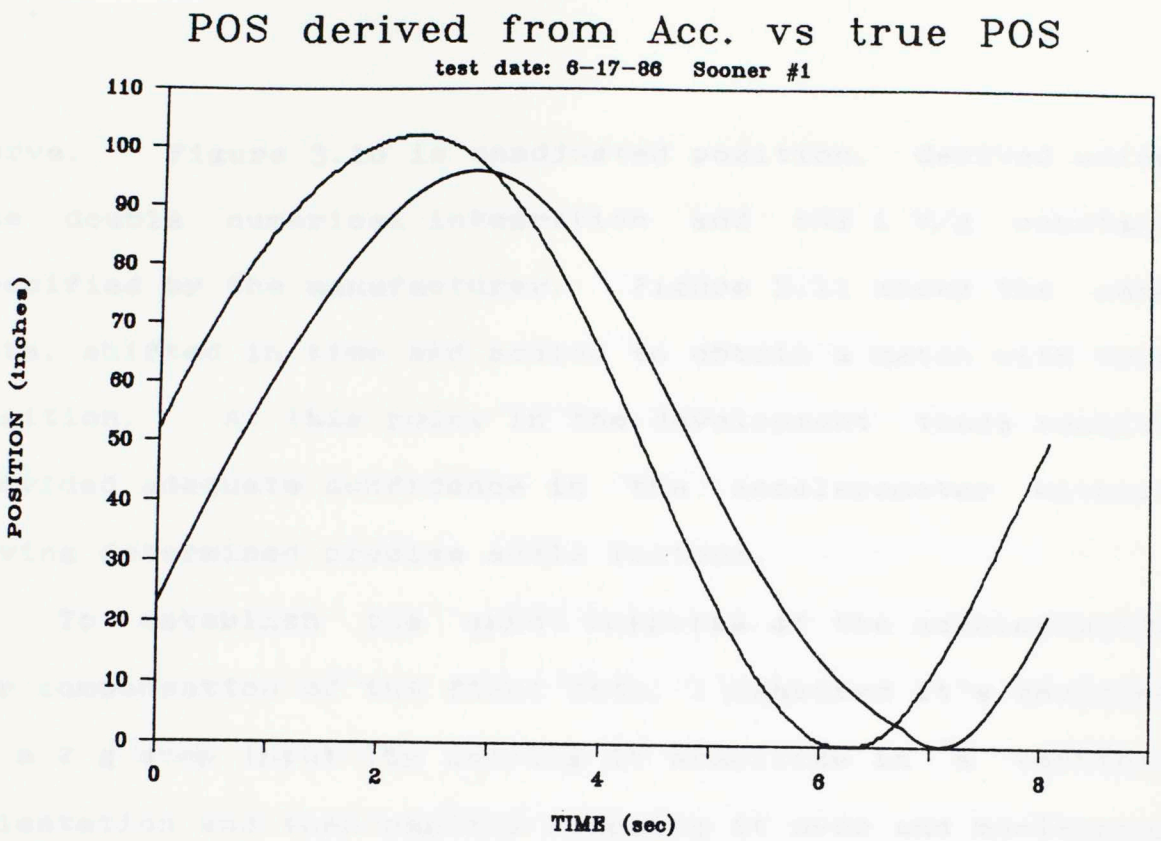

Figure 3.10 Accelerometer Calibration, Position Unadjusted

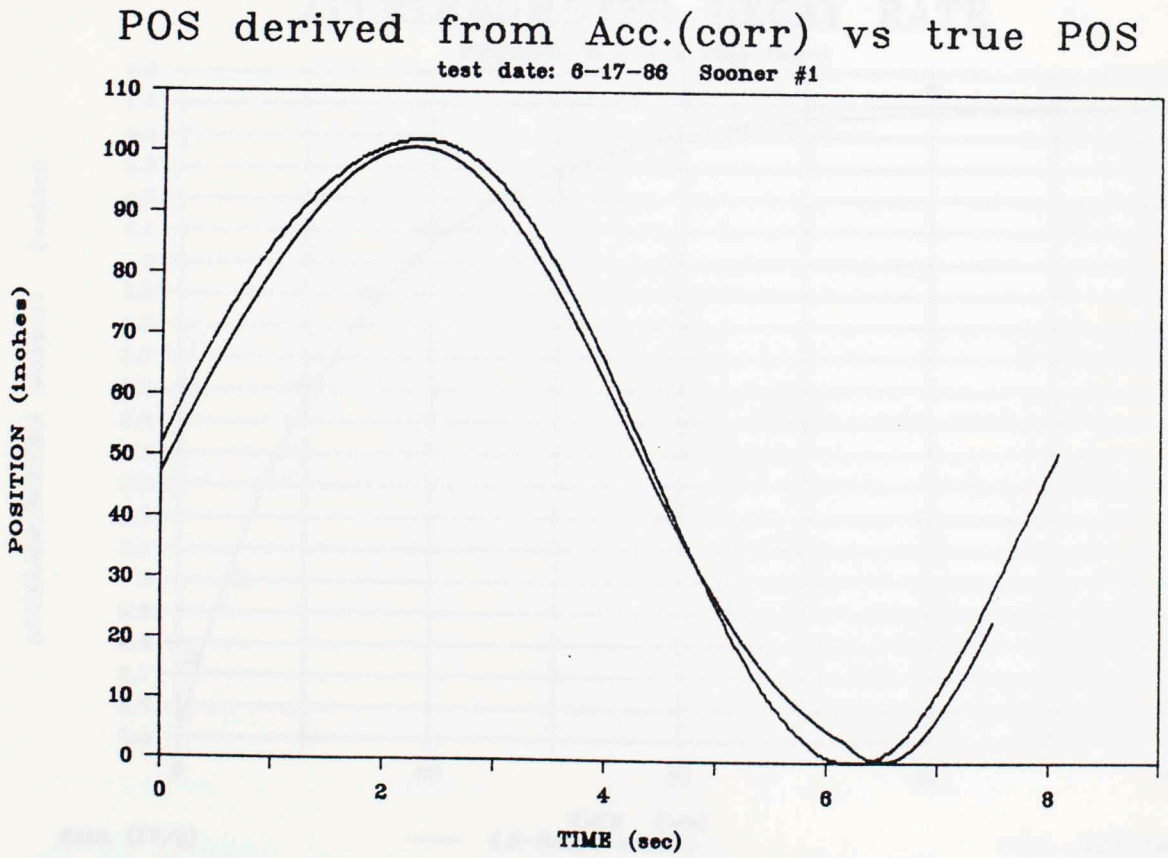

Figure 3.11 Accelerometer Calibration, Position Adjusted

curve. Figure 3.10 is unadjusted position, derived using the double numerical integration and the 1 V/g constant specified by the manufacturer. Figure 3.11 shows the same data, shifted in time and scaled to obtain a match with true position. At this point in the development these results provided adequate confidence in the accelerometer without having determined precise scale factors.

To establish the exact response of the accelerometer for compensation of the final data, I measured it's response to a 2 g step input (by letting it stabilize in a vertical orientation and then rapidly flipping it over and monitoring the output). The response is easily modeled by a single

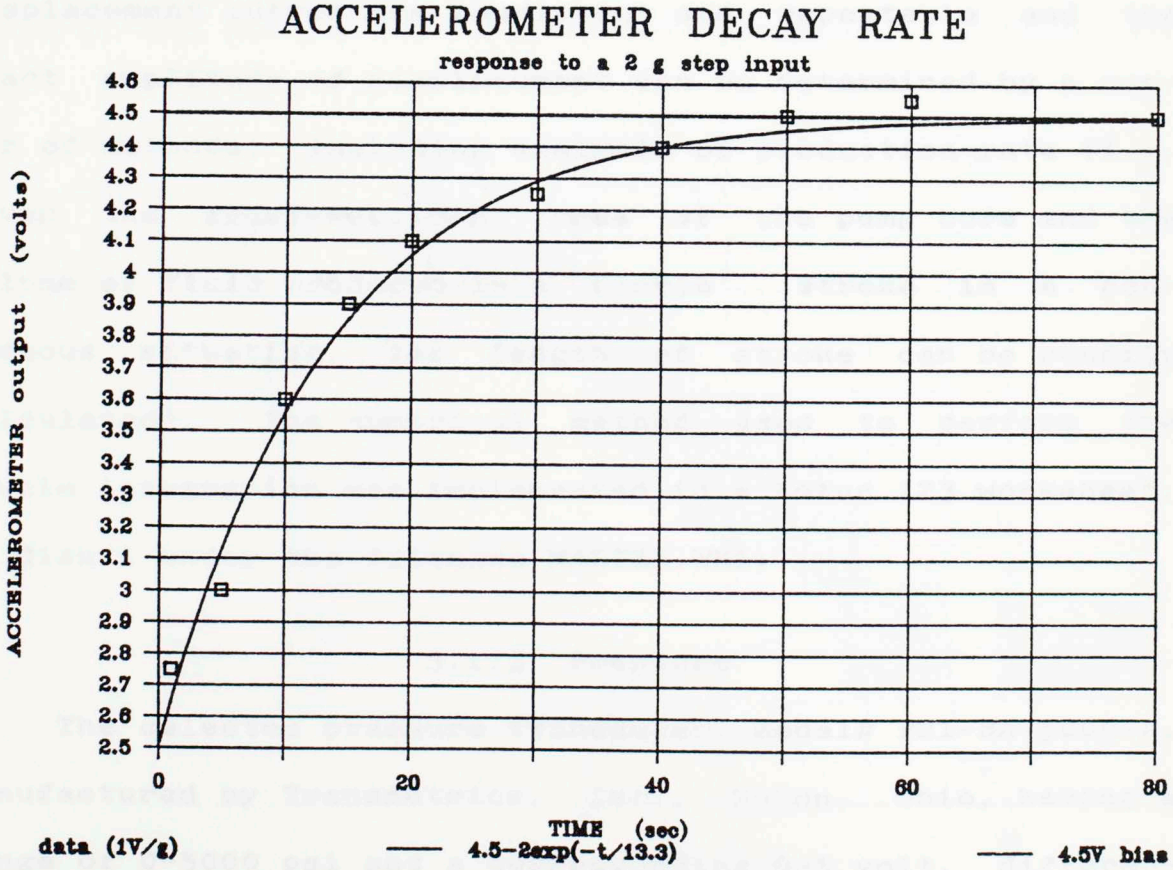

Figure 3.12 Accelerometer Response, Lab-measured

pole filter with a time constant of 13.3 seconds, which would produce roughly 5 degrees of phase lead in the output, at the pumping frequency of 0.125 Hz, and negligable attenuation. This analysis is shown in Figure 3.12. The exact electrical circuit to supply power to and recover signal from the transducer is shown in Appendix F.

A large variation in derived peak-to-peak displacement, from cycle to cycle, was observed in the analysis of the downhole data, which is not completely understood, but fully exhibited in Figures 4.18 through 4.24. This problem detracts from the validity of the displacement data but, in this case, is not completely detrimental. The shape of the displacement curves are consistent and repeatable and the exact amplitude of displacement can be determined by a number of methods, including analysis of production rate (i.e. given the cross-sectional area of the pump bore and the volume of fluid produced in a single stroke in a non-gaseous situation, the length of stroke can be readily calculated). The numerical method used to perform the double integration was implemented in a Lotus 123 worksheet, on disk 1 under the filename MASTER.WK1.

3.1.3 Pressure

The selected pressure transducer, model# P21-BA-5000-A, manufactured by Transmetrics, Inc., Solon, Ohio, having a range of 0-5000 psi and a corresponding 0-5 volt, differen-

tial output.

The calibration of this very rugged, high-precision sensor was initially hampered by trying to implement it as a single ended device, grounding the minus output line and attempting to measure a pressure signal on the plus output. A 4 volt DC signal was measured regardless of the applied pressure. This problem was solved, after consulting with the Application Engineer at Transmetrics, by adding a differential amplification stage before the A/D converter. Calibration data is presented in Figure 3.13. The high level of noise is undesirable and, I believe, introduced by an oscillation in the mentioned differential amplifier which was potted in Epoxe at the base of the transducer connector. I could not

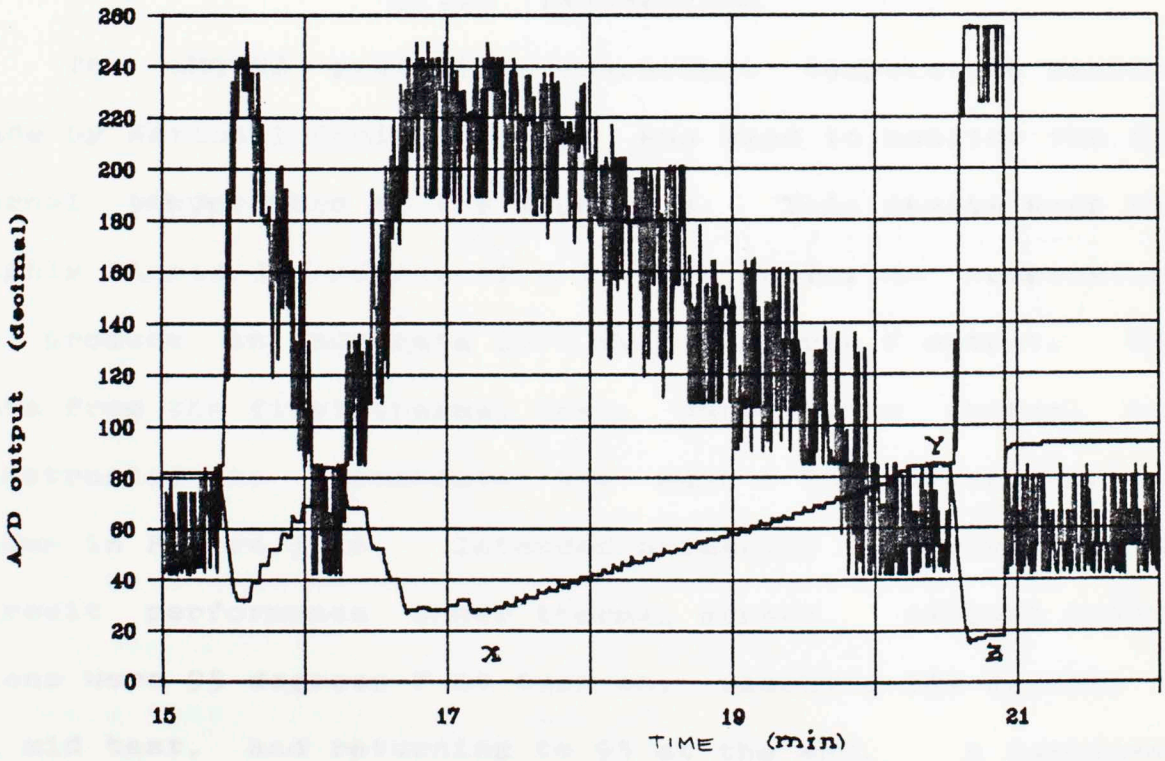

Figure 3.13 Pressure Transducer Calibration

justify the rework required to improve this signal quality, (though, in hindsight, it could have been accomplished with a single-pole filter at the A/D input) since it was of relatively low importance and was adequate for the general needs of the downhole field test.

Also shown in the lower trace of Figure 3.13 is the strain gage sensitivity to external pressure. The information in this graph is interpretted by knowing at point X, pressure was 4000 psi, each step to the right is 100 psi, and the pressure at point Y being atmospheric. At point Z, pressure is 5000 psi. A shift in the load transducer output can be observed, beyond point Z, where the pressure was reduced rapidly from 5000 psi to atmospheric.

3.1.4 Temperature

The LM34CZ precision Fahrenheit temperature sensor, made by National Semiconductor, was used to monitor the internal temperature of the apparatus. This device uses the highly linear dependence of a transistor V_{be} on temperature to produce an accurate 10.0 mV per degree F output. The data from the first thermal test, done in the thermal box constructed to accomodate the near 6 foot apparatus, is shown in Figure 3.14. Intended primarily to verify digital circuit performance under thermal stress. Ambient conditions were 95 degrees F at turn-on, reaching 165 degrees F in mid test, and returning to 95 at the end. A compensa-

tion term of 25 degrees must be subtracted to account for the heat added by power dissipation in the electrical cir-

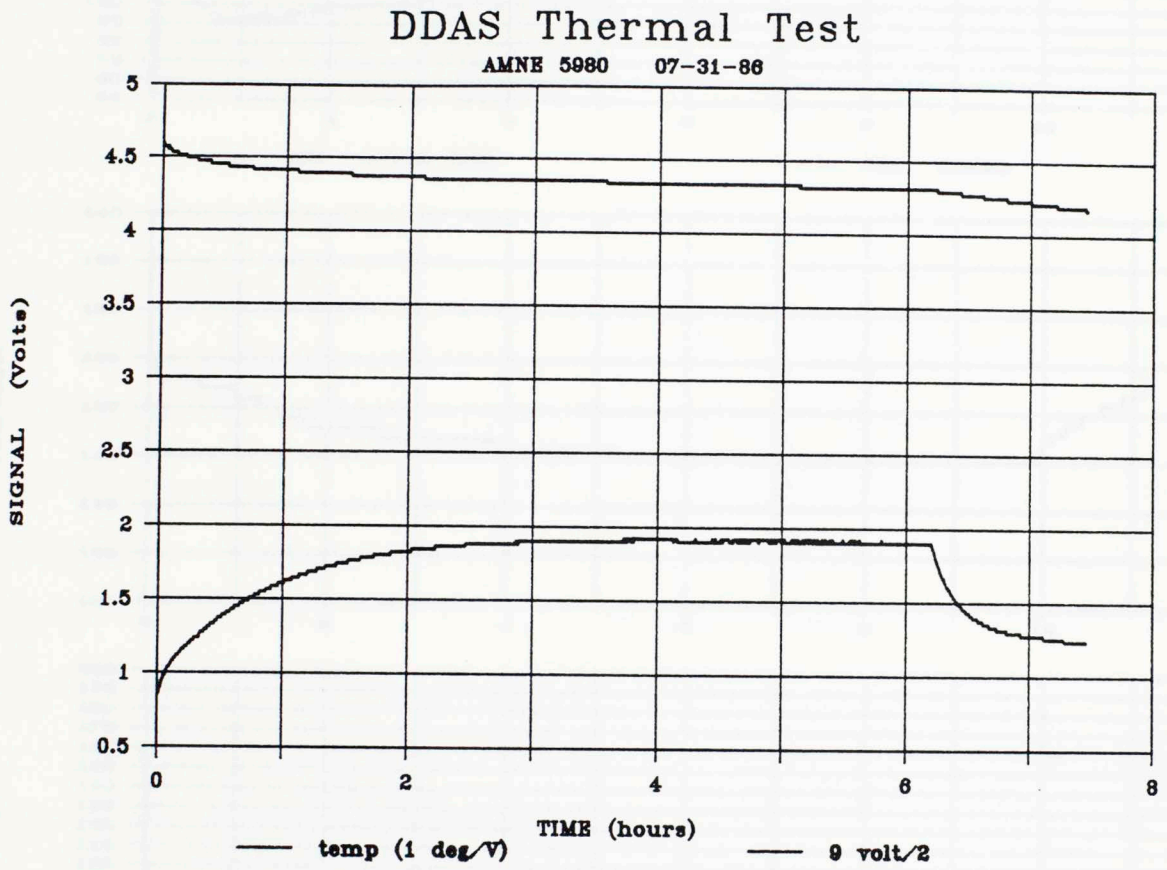

Figure 3.14 Temperature Sensor Output

cuits. This number comes from the difference between the measured starting temperature (no circuit dissipation yet) and the final asymptote.

Also shown is the battery pack monitor signal which represents the 9 volt unregulated supply divided by two.

Figure 3.15 shows the effect of temperature on each transducer, sampled during one of four overnight thermal dependence tests that were conducted.

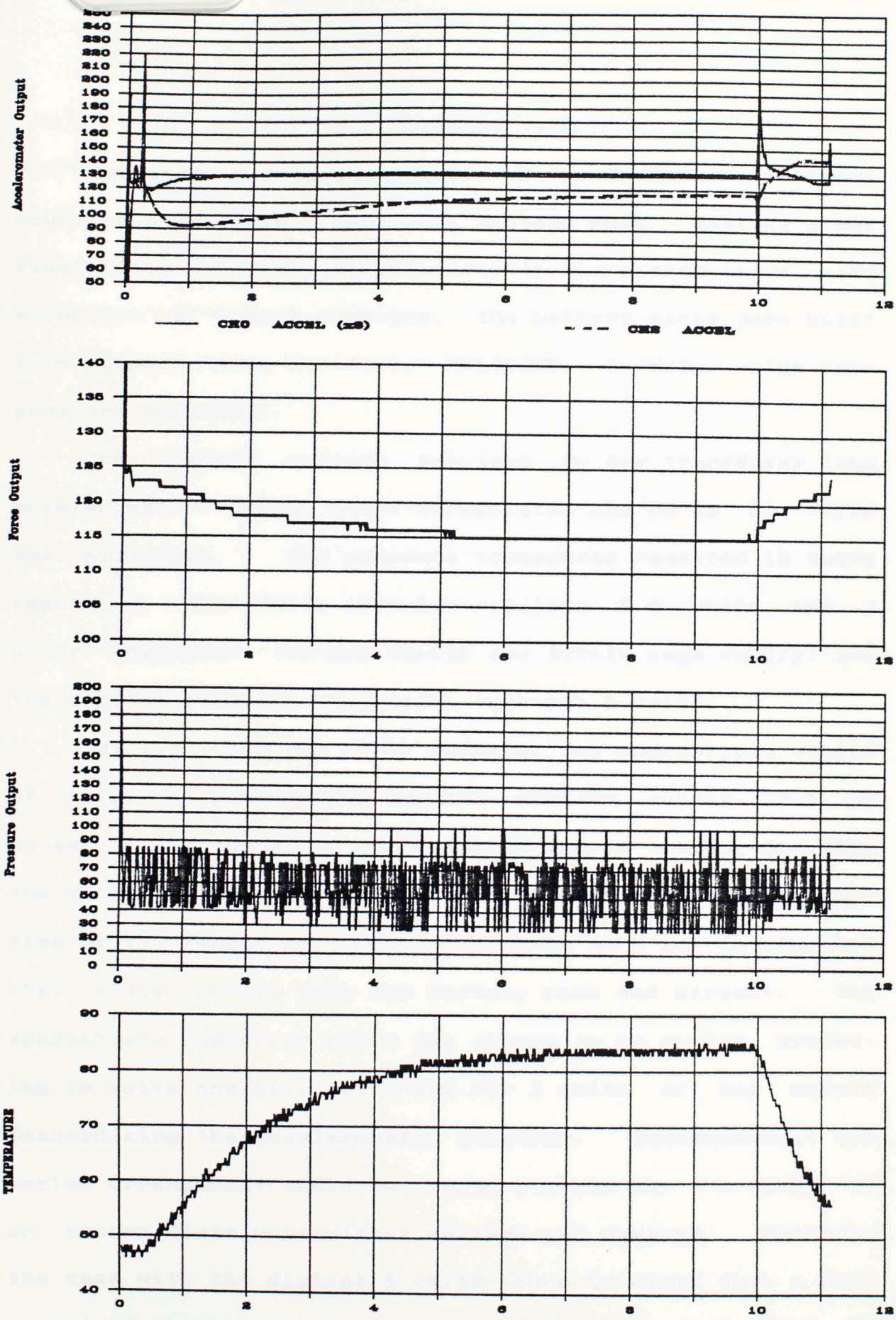

Figure 3.15 Transducer Thermal Dependence

3.2 BATTERY PACK

Certainly key to the success of the downhole experiment would be a reliable, unfailing battery pack. Wanting great flexibility of size, adaptability to the system needs, and selection of output voltages, the battery packs were built from scratch using Duracell, MN1400HT, Zn/MnO_2, high temperature alkalines.

The highest voltage required by any transducer (the accelerometer) was 15 volts unregulated and up to 24 volts was allowable. The pressure transducer required 12 volts regulated, the analog circuits required 8.2 volts and 5 volts regulated (op-amp supply and strain gage supply) and the digital dircuits required a separate 5 volts.

At 1.5 volts per cell, nominal, the appropriate number of cells, to produce the desired maximum output, can be chosen. The number of cells was chosen in conjunction with the known length of the printed circuit board and the selection of the length of tubing (available in 6 in. increments) that would contain both the battery pack and circuit. The appropriate number of cells was chosen to be twelve, producing 18 volts nominal, allowing for 3 volts of sag before jeapordizing the accelerometer function. Conveniently, the series arrangement could be tapped between any two cells if an intermediate unregulated voltage was desired. This was the case with the digital 5 volts since it would draw a fair amount of the total current and regulating it down from 18

volts would produce excessive dissipation in the regulator (power wasted=($V_{unreg.}-V_{reg.}$)*I). Hence, the center of the series, or 9 volts unregulated, was also brought out for the input to the digital 5 volt regulator. This configuration is shown schematically in Appendix F.

The results of a battery life test are shown in Figure 3.16 where the upper trace indicates the presense of a 39 Ohm load across the 18 volts and the lower trace is the measured center-tap voltage, V_{ct}. The rapid decay prompted the pursuit of all CMOS circuitry. The eventual circuit current requirements were much less than this and one battery pack lasted for over 35 hours of preliminary testing in applications similar to the downhole test.

Desiring absolute integrity of the power supply, the cells were soldered in series and covered by several layers of heat shrink tubing (see Appendix C). The pack is retained axially, at both ends, within the plastic inner sleeve by lateral dowel pins.

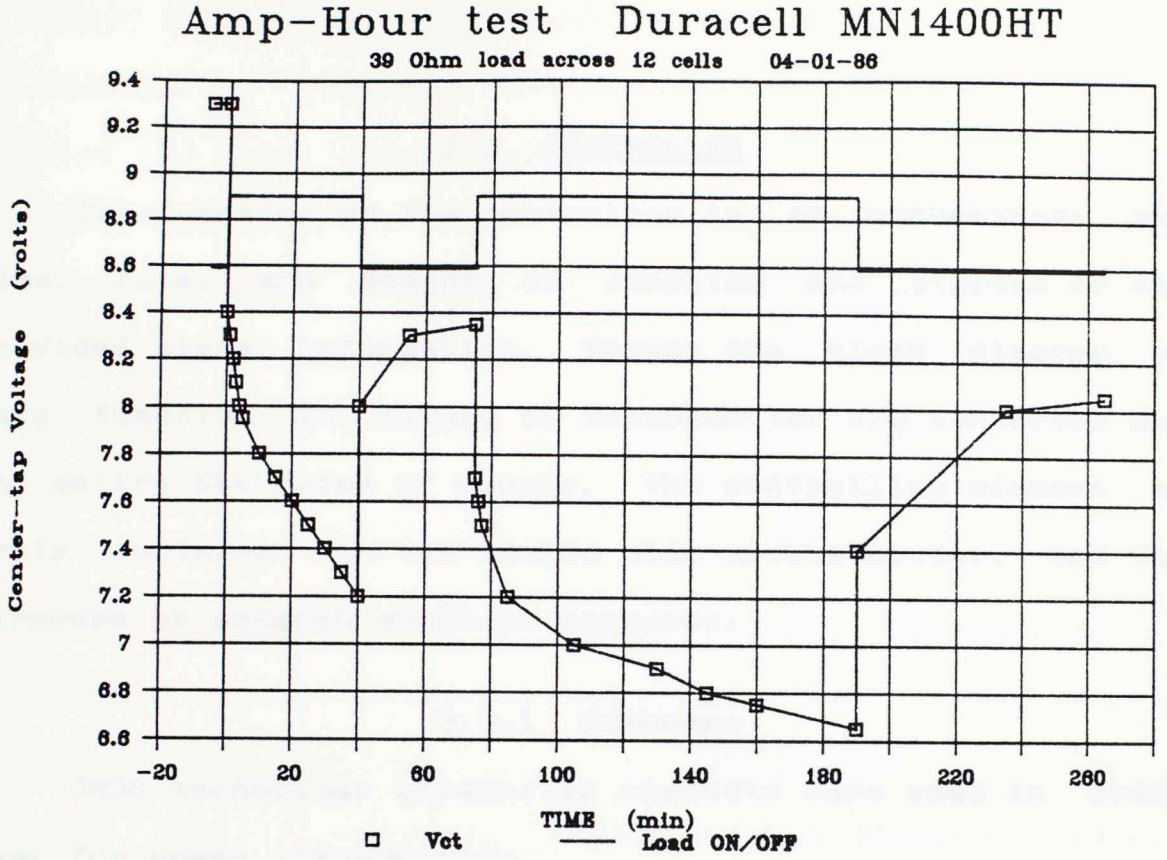

Figure 3.16 Battery life

3.3 CONTROLLER

The function of the controller is to orchestrate the time, rate, and amount of sampling and storage of the provided signal information. Though the block diagram of this function in Figure 18 includes the A/D converter and the entire 64k bytes of memory, the controlling element is truly contained in the single chip microcomputer, and the firmware or program which it executes.

3.3.1 Hardware

CMOS technology integrated circuits were used in every case for power conservation.

Microprocessor Selection of the Intel 8051 family was based on a good match with the system needs, the author's prior experience, and access to the necessary firmware development tools. The specific chip chosen was the 80C31 which has no internal ROM since the architecture was for instruction execution from external program memory. The entire system schematics are provided in Appendix F. The microcomputer/memory interface is standard and similar examples can be found in the Intel Micontroller Handbook.

Memory The logic behind the memory device selection

(28C64) is partially presented in the design specification in Chapter II. Another benefit of using EEPROMs is that, applied in the program memory space, program code can be changed, through the same interface that data is recovered, without an EPROM programmer or having to remove the program memory chip. This technique is known as in-system programming, and is not possible with any other form of silicon memory.

A/D The ADC0808 is a an 8-channel, 8-bit, microprocessor-compatible Analog-to-Digital converter, every stated feature of which is appropriate for this application. 8-channel meaning that 8 different signals can be selected independently, 8-bit A/D meaning it converts an analog signal into one of 256 (2^8) possible discrete levels within a specified range. Convenient features such as address latching, strobe inputs to start conversions and enable internally latched digital outputs onto an 8-bit data bus make it microprocessor compatible.

Printed Circuit Board (PCB) With reasonable confidence in the digital design, I started the printed circuit board layout providing a breadboard area for the analog interface circuits which were not yet complete. The width of the board(s) (1.10 inches) was determined by the inner diameter of the plastic sleeve designed to contain and protect the

circuits and battery pack from the steel tubing wall. Laying out all the electrical components within the narrow width produced a length in excess of 23 inches, which is not a practical length for this narrow a board. This prompted the decision for a two-board design. After shuffling shapes around on paper, a natural partition emerged with the seven data storage chips on one board and the rest of the circuit on the other.

The artwork was generated with the aid of a PC-based, program for double-layer printed circuit board drafting, which, when compared to hand layout with tape or ink, is like comparing the word processor that this thesis was written on to a 1930's vintage typwriter. The 8 feet long, cut-and-pasted originals (see Appendix F), which Triangle A&E, Oklahoma City, reduced to the full-scale positives still took over 60 hours to make.

Three sets of boards were fabricated by Frontier Engineering, Oklahoma City. The first used in preliminary accelerometer calibration and general design debug, the second, built and refined to a level of quality sufficient for the final application, and the third used for experimentation with soldering and connector application. Problems with board quality in the later stages of development prompted the ordering of back-up boards from a second vendor, Protoquick, Dallas which were of similar cost but much higher quality (mil-spec fiberglass substrates, and reflow

soldered runs) but were not needed.

The final printed circuit board assembly is shown in Appendix F.

3.3.2 Firmware

Background The terms firmware and software both describe a form of computer program. Firmware differs from software in that it generally refers to microcode or the assembly language level of program that resides permanantly with the hardware in some sort of ROM (Read Only Memory). In this case the firmware resides in the program memory EEPROM.

The entire program uses just over 300 bytes of code for 134 instructions, and a table that explicitly defines the sampling session; number of sampling periods, channels to sample and rate of sampling during each period, and memory allocation for all sampled data.

The program resides in shared external memory and program memory space, address 0 to 1FF Hex or 0 to 511 decimal, which is in the program memory chip on the microprocessor board. The entire 64k bytes are commonly addressable as program memory or external memory, due to the hardware configuration (all chips have a common WR strobe and a common RD strobe which is the boolean sum of PSEN and the external memory RD. Unused program memory in the lowest 8k is not useful for data storage since the write cycle of the 28C64 disables the chip for 1 mS, which irrevocably dis-

rupts program execution.

Theory of Operation The flowchart for the downhole data acquisition program is shown in Figure 3.17. Examination of this and the firmware listing in Appendix H, will reveal that the program operates from a table containing key values specifying sampling and data storage locations.

Each line of the table on the second page of the firmware listing completely specifies a single data sampling period of which there were fifteen for the downhole test. Six sampling periods, labeled A through F are of the same mode and duration (CH0 through CH3, 40 Hz, for 1 min). The last 21.6 seconds of information of each of these sampling periods is overwritten with data from the next sampling period. At the given sampling rate and number of channels, 6k bytes are stored in 38.4 seconds. Storing data for the remainder of each minute does no harm and serves to keep the overall sequence on one minute intervals without adding special routines to accomplish this.

The seventh sampling period, labeled G, samples channels 0 and 1 at 20 Hz for six minutes, sacrificing the upper 1984 bytes of memory. This was done because sampling for seven minutes would overflow legal address space and attempt to write to address 0000 (program memory) which would permanantly disrupt program execution. The purpose of this period was to observe settling of pumping conditions during

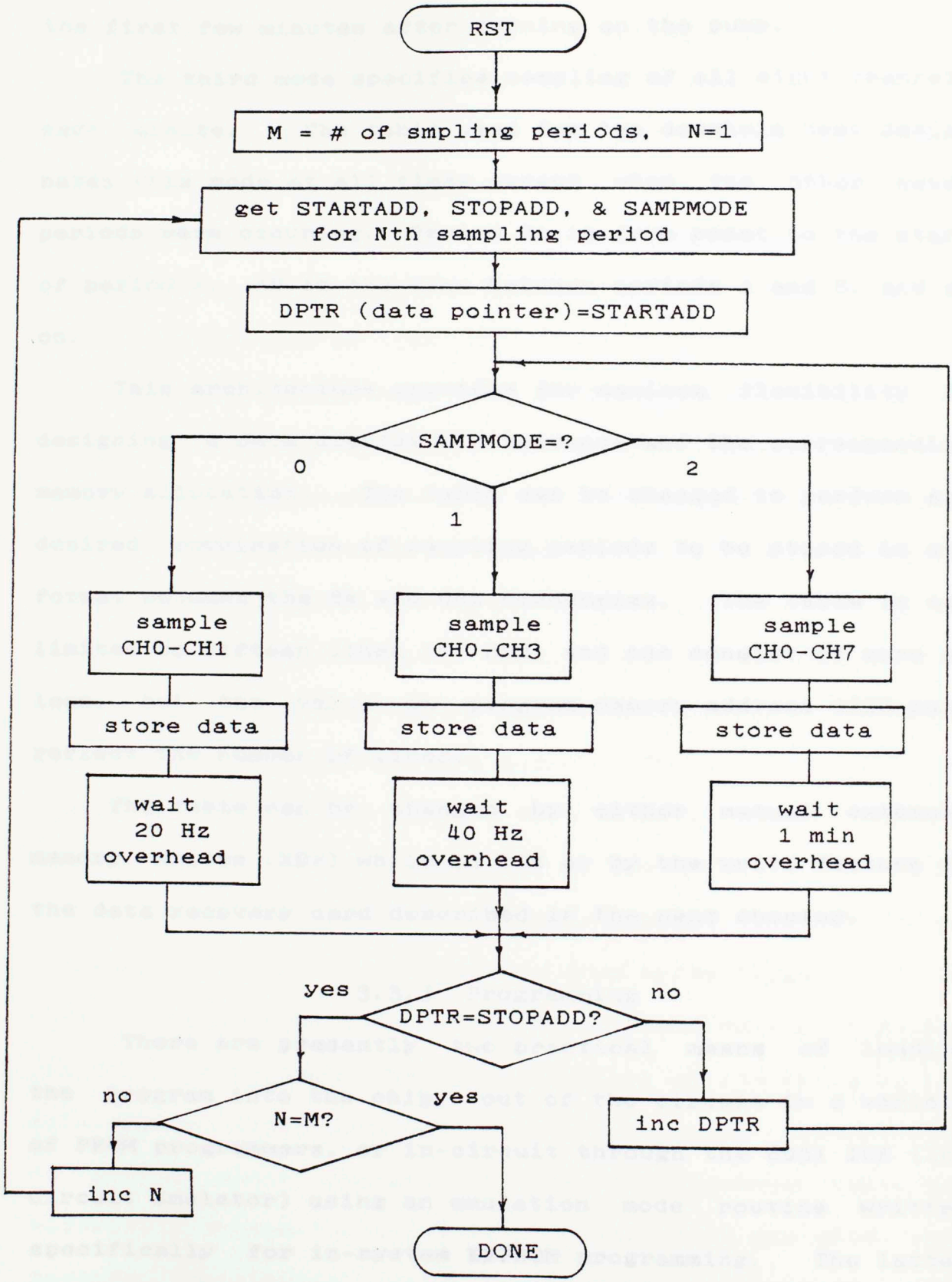

Figure 3.17 Controller Flowchart

the first few minutes after turning on the pump.

The third mode specifies sampling of all eight channels each minute. The table used for the downhole test designates this mode at all times except when the other seven periods were occuring. Period OA is from reset to the start of period A, AB is the time between periods A and B, and so on.

This architecture provides for maximum flexibility in designing a data acquisition sequence and the corresponding memory allocation. The table can be changed to perform any desired combination of sampling periods to be stored in any format between the 8k and 64k boundaries. The table is not limited to fifteen lines (0F Hex) and can consist of more or less, but the value in program memory address 033H must reflect the number of lines.

The table can be changed by either manual external memory writes (XBY) while in ICE or by the write feature of the data recovery card described in the next chapter.

3.3.3 Programming

There are presently two practical means of loading the program into the chip; out of the circuit in a variety of PROM programmers, or in-circuit through the 8051 ICE (In-Circuit Emulator) using an emulation mode routine written specifically for in-system EEPROM programming. The latter method (to be described shortly) was used for this project,

being more convenient and taking advantage of the in-system programmability feature unique to this device.

An ICE is simply a keyboard driven firmware development tool with a control cable that has a pinout identical to, and fully emulates the function of the microprocessor. The program in the ICE can be programmed to start and stop at any point and can be readily altered to aid in the firmware debug process. Once a program is debugged and fully functional it is generally stored on floppy disk for input to a separate PROM programming machine. Wishing to avoid this extra step and to take advantage of the in-system programmability of the 28C64, I wrote a short routine (found at the end of the firmware listing) that, under ICE control, copies the debugged program from ICE memory into the program memory space of the data acquisition board. There it can be executed by ICE (told to execute from external memory) or by a microprocessor in the normal mode of operation.

The BASIC program that runs the data recovery board (Appendix E) could be modified to also write large blocks of data (ie. a program from disk). Though used mainly, in this project, to recovery the large segments of stored data, the data recover board does have single byte write capabilities to enable minor changes to the sample pointer table and especially to the two bytes in addresses 080H and 081H that specify the initial delay in the sampling sequence. The data recovery system is detailed in Appendix D.

CHAPTER IV

RESULTS

4.1 Field Test

The downhole test was conducted on August 28, 1986. The producing oil well used was Chevron F.S.D.U. T55A - 12, located in Carter county near Ardmore, Oklahoma. The weather was excellent with temperatures in the low to mid 80's and clear skies the entire day. Present from the University of Oklahoma were students Carl Adams, Jesus Chacin, and myself and our advisor, Dr. John Purcupile of the AMNE department.

The workover crew had the entire sucker rod string out of the ground when we arrived at 10:00 a.m. The circuits were activated at precisely 10:15 a.m. in an office area and, after completing the hand assembly (see Appendix C), we delivered it to the well site. The crew tightened the apparatus with pipe wrenches (and 4 feet long extensions), which were then also used to attach the top of the apparatus to the bottom of the first sucker rod which, at that point, was laying out on the ground. Then, hoisted into position above the well opening, the bottom of the apparatus was wrenched onto the top of the pump section which was already in the hole, and then everything was lowered into the hole.

Fluid was added to bring the level to the surface, the surface pumping unit was completed and the (add the pump description here) was turned on at approximately 12:10 p.m.

Seven high-frequency sampling periods were specified in the controller program of one minute duration each (except the last period which was 6 minutes) commencing precisely 210 minutes after resetting the microprocessor at the surface, and ocurring at ten minute intervals (start-to-start). These sampling periods are labeled A through G. Samples of all parameters were made each minute throughout the test. Pumping ceased at approximately 3:25 p.m., the apparatus was brought back to the surface, removed from the string, cleaned with diesel fuel and opened for data recovery and to hopefully verify a successful test.

The first sign of good health was that the LED was still blinking on the minute (within 1 second which is very good considering the timing loops were developed empirically and not by absolute calculation) which indicated the controller had done, and was continuing to do its job and that if the transducers were still alive, the data was probably stored successully. Next the critical voltages were measured with the DMM and all channels into the A/D were observed to be responding as designed. However, the bias point on the load output had shifted from 2.0 volts to 1.2 volts, raising the question in my mind that part of the AC component may have been clipped at the bottom (0.0 volts),

especially if greater downward shifts had occurred at elevated temperatures downhole. Another cause for concern in the early observation was bared conductors in the accelerometer power and signal wires which were adjacent each other in a three-leaded ribbon cable. The insulation was apparantly pinched or rubbed away by contact with the plastic sleeve, but the wires were not touching nor was there any sign of arcing that might have occurred had the power supply line contacted the steel case which was at ground potential.

My personal moment of triumph was minutes later when the first data was recovered, for sampling period A, through the data recovery board which displays the columns of data on the monitor as it stores it onto a disk file. All memory locations had been written with zeroes prior to the test, and I could see legitimate data values being displayed in the respective columns. Real relief for the others present did not come until minutes after this when this data file was imported into a Lotus 123 worksheet and displayed graphically, both Jesus Chacin and Bill Foley recognizing certain features in the load trace that they had seen before in their models.

4.2 Recovered Data

Later, raw data from all sampling periods was recovered from the controller memory and stored in files, via the data recovery board, with .PRN extensions on floppy disk, copies of which accompany this thesis. PIC files were generated in Lotus 123 for all downhole data and those graphs are provided in this chapter. The conversion for A/D output is always 19.0 mV per count here. The load data and accelerometer data were further reduced and graphed in actual units to compose the axes of downhole dynagraph cards.

Due to their size, quantity and sequence, all graphs are grouped together at the end of this chapter, with explanations grouped in the preceding text.

Figures 4.1 through 4.6 show the raw data from the six, 4-channel, 40 Hz sampling periods labeled A through F. Channels 1, 2 and 3 (load, acceleration and pressure) are dislayed together in each case, conveniantly and naturally spacing themselves in non-overlapping ranges. Channel 0 has been omitted since it is a multiple of channel 2 and only clutters the graph. The zebra effect on load in part of Figure 4.5 and all of Figure 4.6 is due to a flaw in the controller memory permanantly containing zeroes in every 32nd address. This probably happened while exceeding the recommended operating temperature in preliminary testing.

The conversion factors for these traces are:

CH0: AMPLIFIED ACCELERATION = .0065 (CT) [g's]

CH1: LOAD = .05xxx $(CT)^2$ + 118.5 (CT) + 2600 [lb]

CH2: ACCELERATION = 0.0195 (CT) [g's]

CH3: PRESSURE = 19.0 (CT) - 850 [psi]

CH4: TEMPERATURE = 1.90 (CT) [degrees F]

CH5: 5 V_{reg} (/2) = .038 (CT) [volts]

CH6: 9 V_{batt} (/2) = .038 (CT) [volts]

CH7: 18 V_{batt} (/4) = .076 (CT) [volts]

where CT is the A/D CounT or value.

Figures 4.7 and 4.8 are the acceleration (x3), and load (channels 0 and 1) taken at 20 Hz for the six minute sampling period G. The purpose of this test was to observe the transient response of the load signal envelope to start-up. The crew's difficulty in restarting the pump can be observed in the 2.5 to 3.0 minutes before periodicity was achieved.

Figures 4.9 through 4.13 are plots of samples taken of all channels, each minute throughout the test. Zeroes were left in the memory cells when sample periods A through G occurred to reference them in time with the overall test.

In Figure 4.10, the bias level of the load can be seen to drift down with increasing temperature and depth, positive and negative spikes can be seen at the seating and unseating of the pump at 95 and 305 minutes. The negative spike demonstrates the dynamic range of the opamp at its

spec of .030 volts or an A/D count of 2. The mentioned shift in bias level from start to finish can also be observed.

The global story on pressure is clearly observed in Figure 4.12, as is the adding of fluid from the surface between the 80 and 95 minute marks.

The temperature inside the apparatus stabilized at 122 degrees F throughout the pumping and the battery pack exhibited very little depletion during the six hours as can be observed in Figure 4.13. Channel 5 was omitted here and is simply a straight line at 127 through the entire test, as would be expected from a voltage regulator.

Figure 4.14 is a comparisons of measured and mathematically predicted load. Derivation of the predicted load and further analysis of this data are presented in J. Chacin's doctoral dissertation (reference).

4.3 Downhole Dynagraphs

The remaining graphs encompass data reduction required to construct a downhole dynagraph. The shape and amplitude of the load curve is extremely consistent and repeatable and the second cycle of sample periods C, D, and E are shown in Figures 4.16 through 4.18. The cycles are taken from a

---

Diagnostic and Design Techniques, J.E. Chacin, 1986

fixed window relative to the beginning of each sample

period, so the curves are not necessarily in phase from graph to graph. This is irrelevant in making a dynagraph.

For reasons not fully understood the accelerometer-derived displacement did not produce consistent or expected amplitudes as can be seen in Figures 4.18, 4.20, and 4.22. To make the best possible use of this information which clearly has some useful content, the five cycles from each sample period were averaged and normalized to 99 inches (a value established with confidence by other methods, noted on page 22) to produce a composite displacement curve having much less random noise content than any of the original cycles (see Figures 4.19, 4.21, and 4.23). The load traces were shifted 5 degrees to compensate for the phase lead of the accelerometer discussed in chapter 3, and plotted versus the three composite displacement curves to produce the three downhole dynagraphs of Figures 4.24 through 4.26.

As an added step toward making an accurate dohnhole dynagraph card, an average was made of all load and displacement traces of the three dynagraphs (see Figures 4.27 through 4.30) to further reduce the noise content and then the data was replotted to form the final composite dynagraph of Figure 4.31.

The preceding analyses (including the double numerical integration) were done in Lotus 123 worksheet MASTER.WK1.

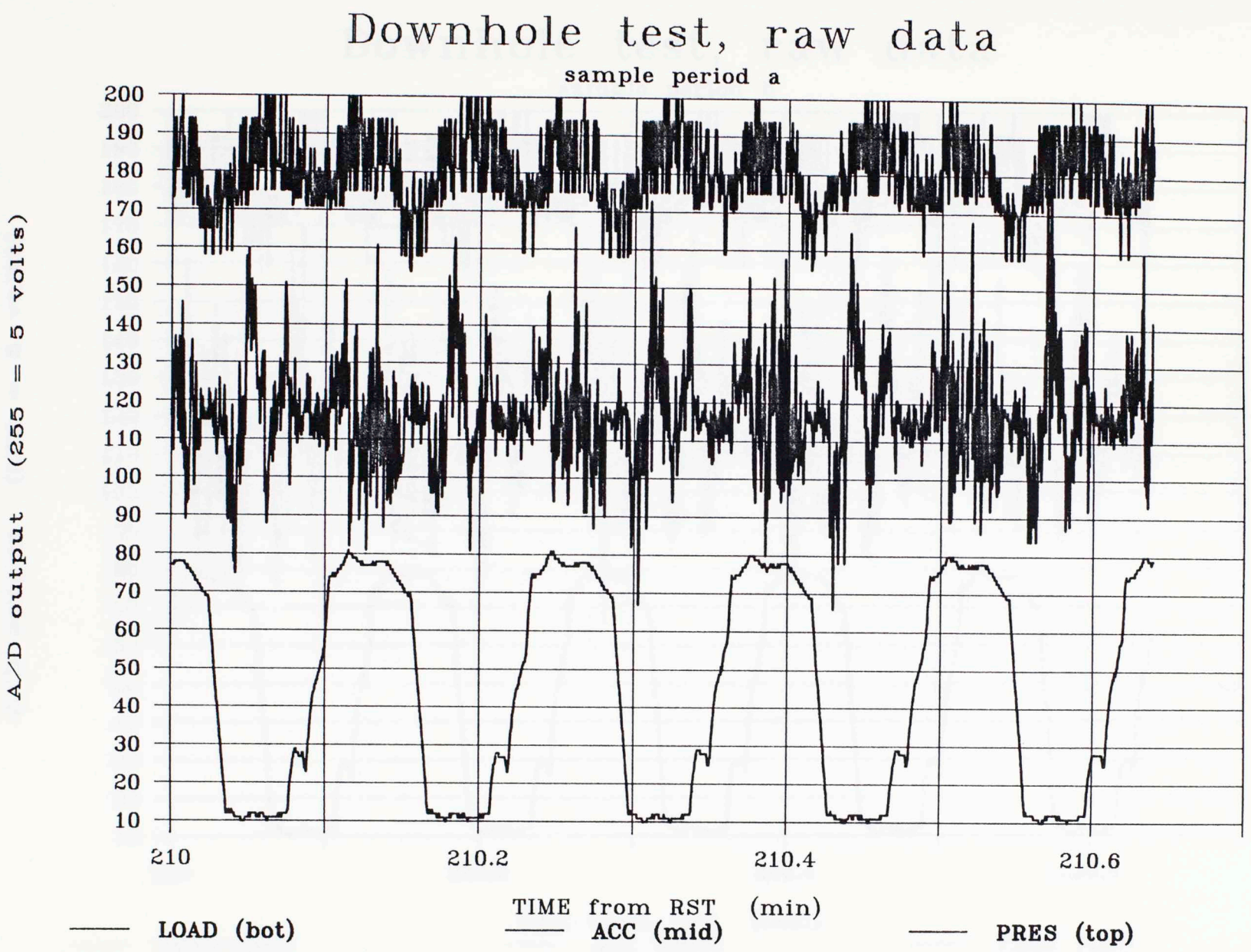

Figure 4.1 Downhole data, sample period A.

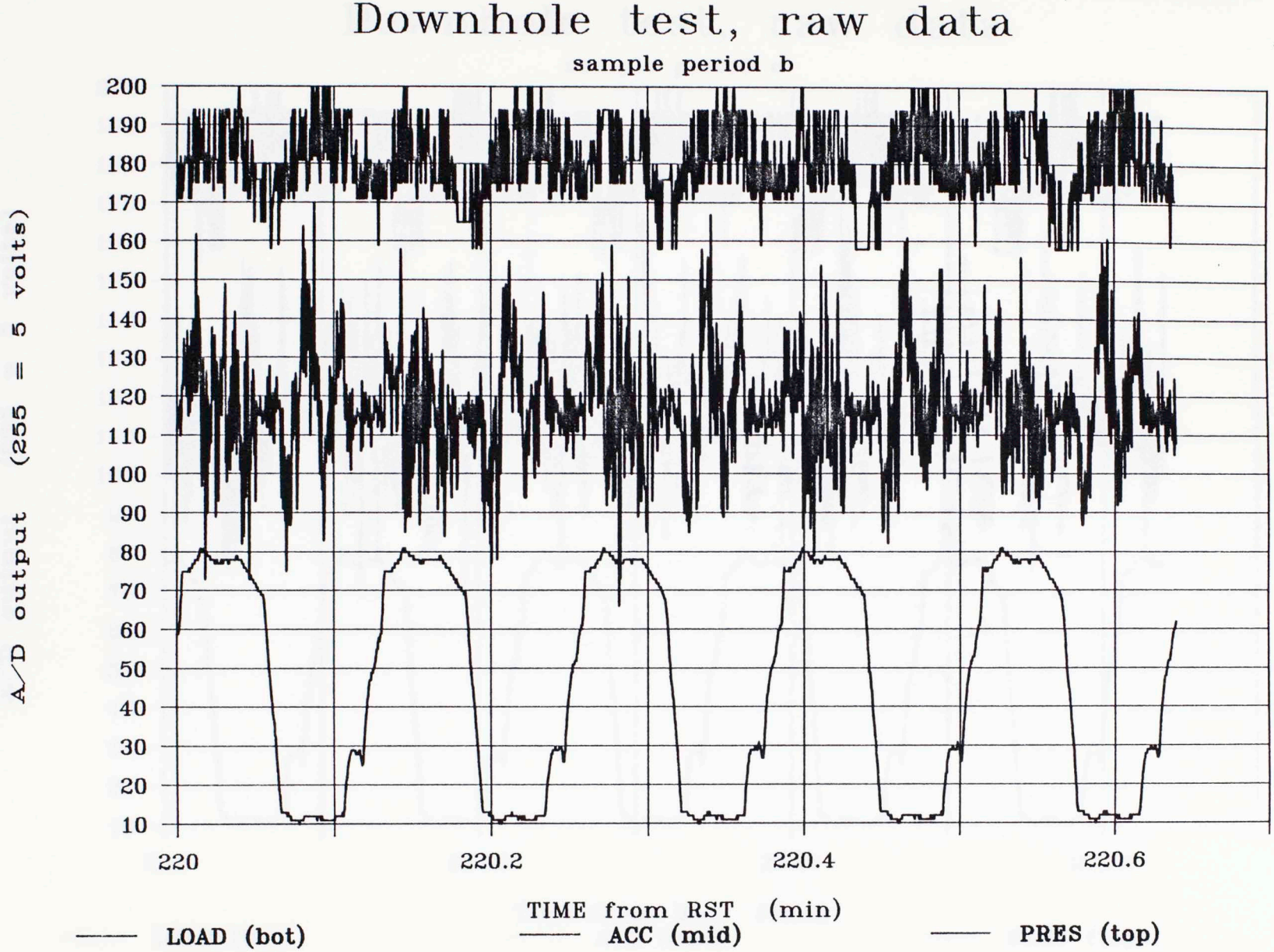

Figure 4.2 Downhole data, sample period B.

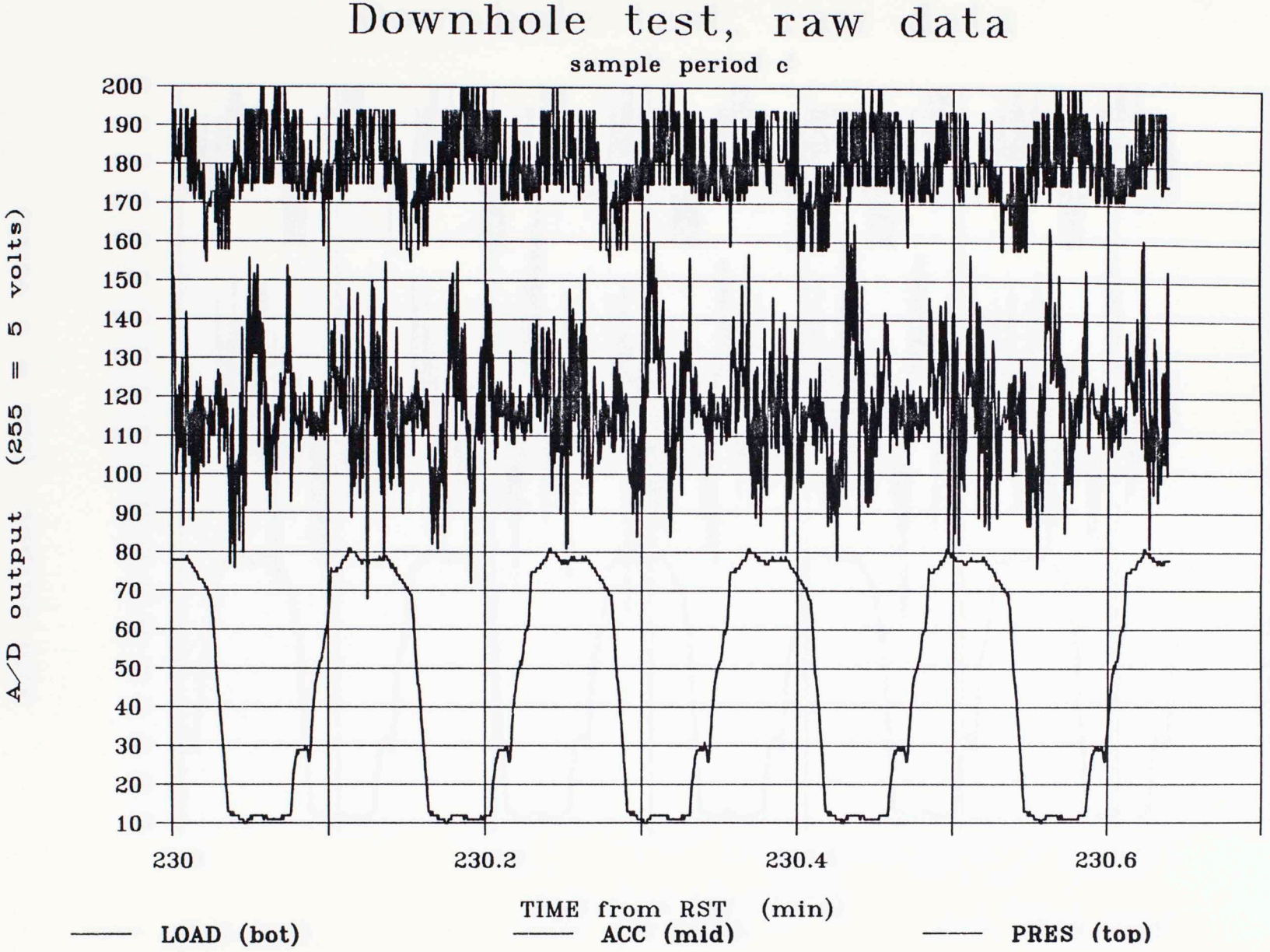

Figure 4.3 Downhole data, sample period C.

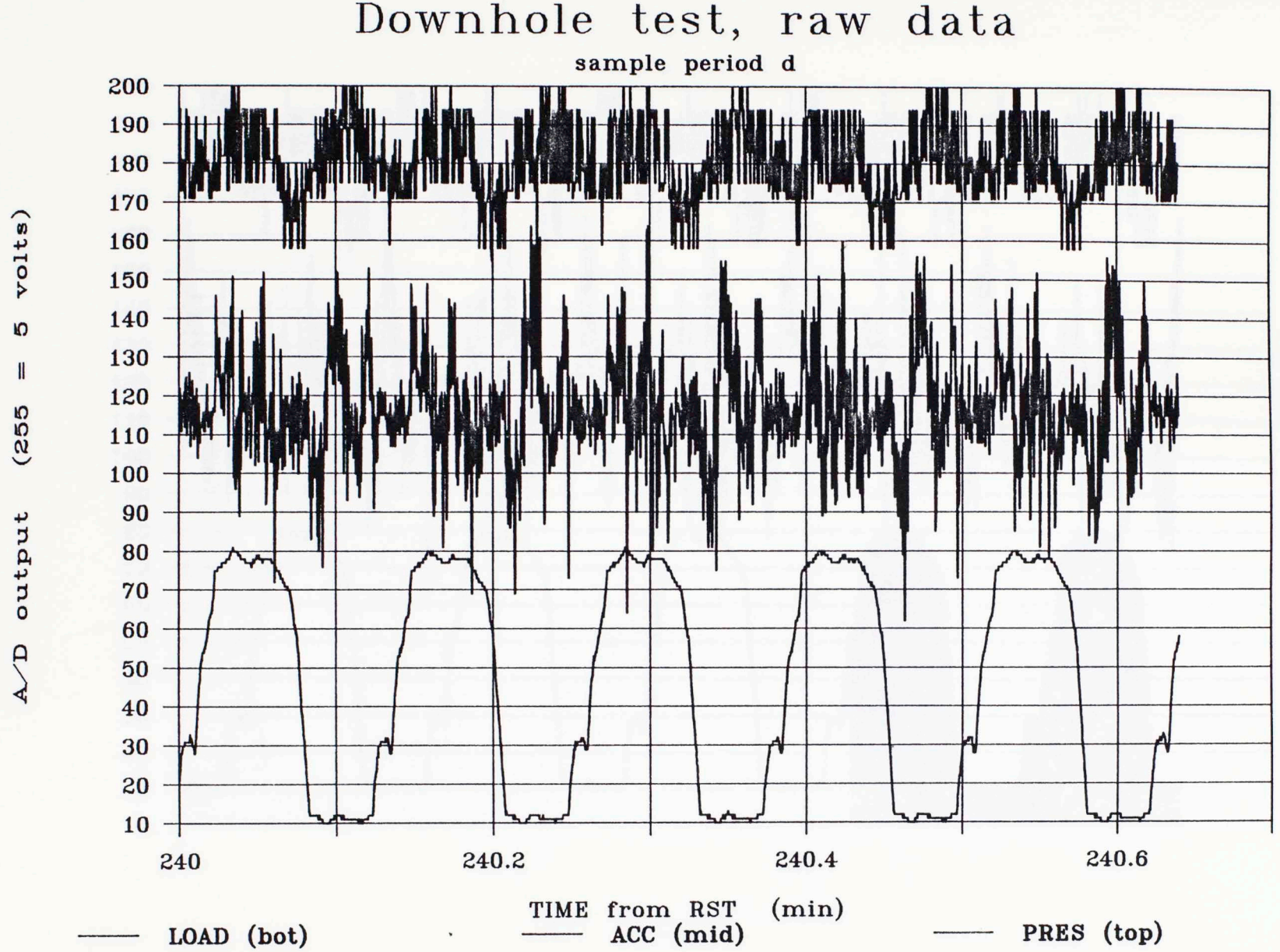

Figure 4.4 Downhole data, sample period D.

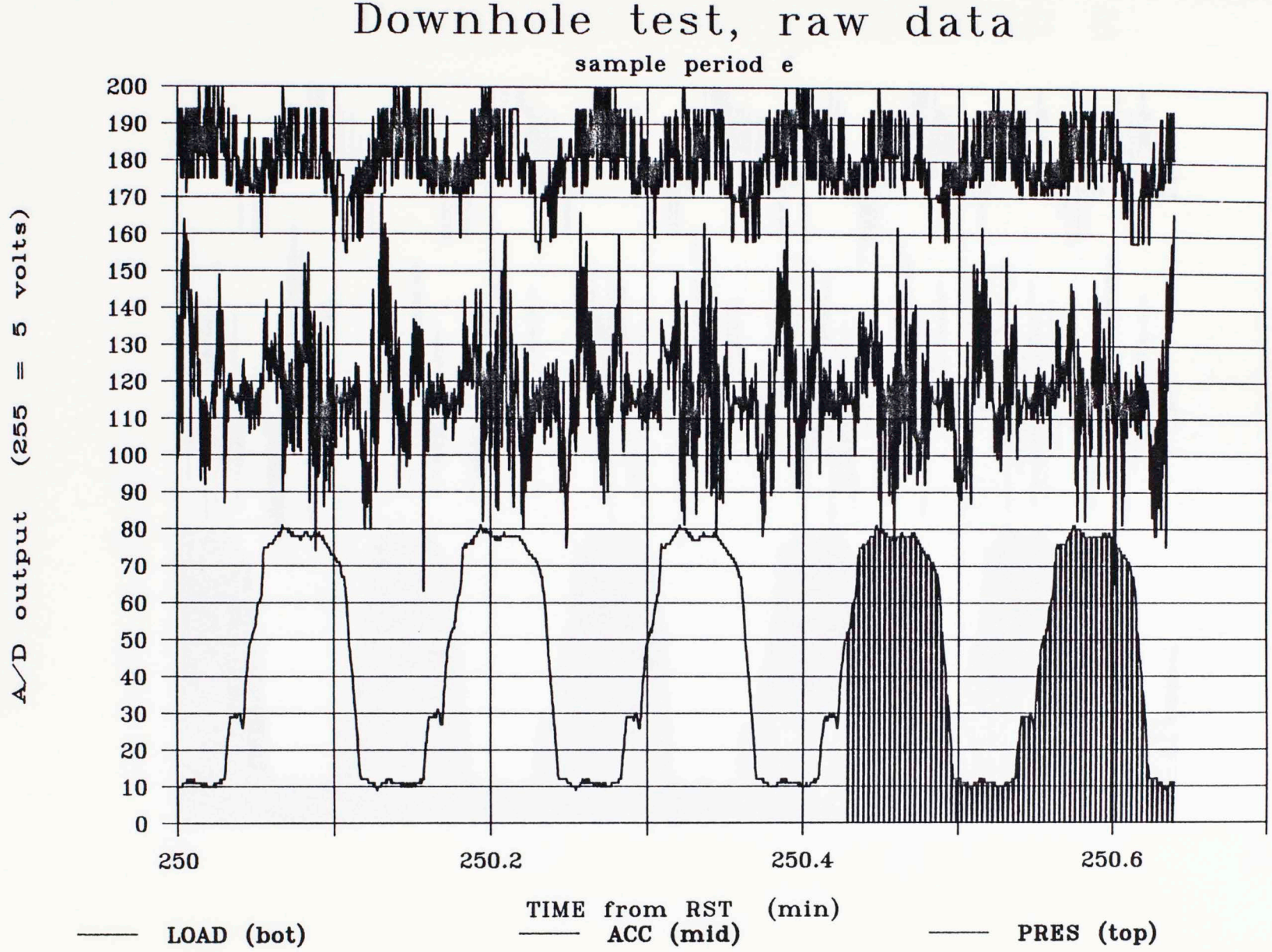

Figure 4.5 Downhole data, sample period E.

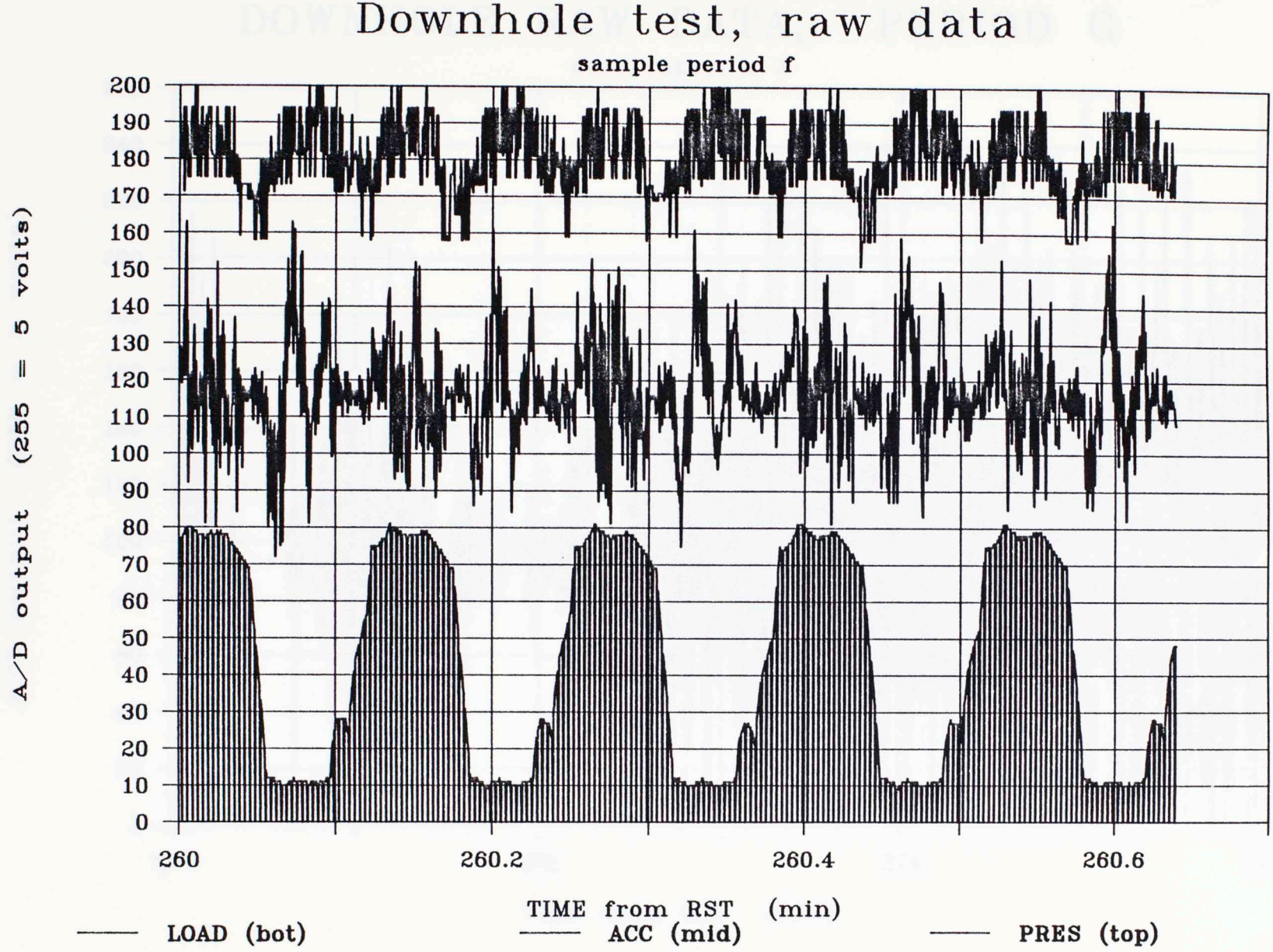

Figure 4.6 Downhole data, sample period F.

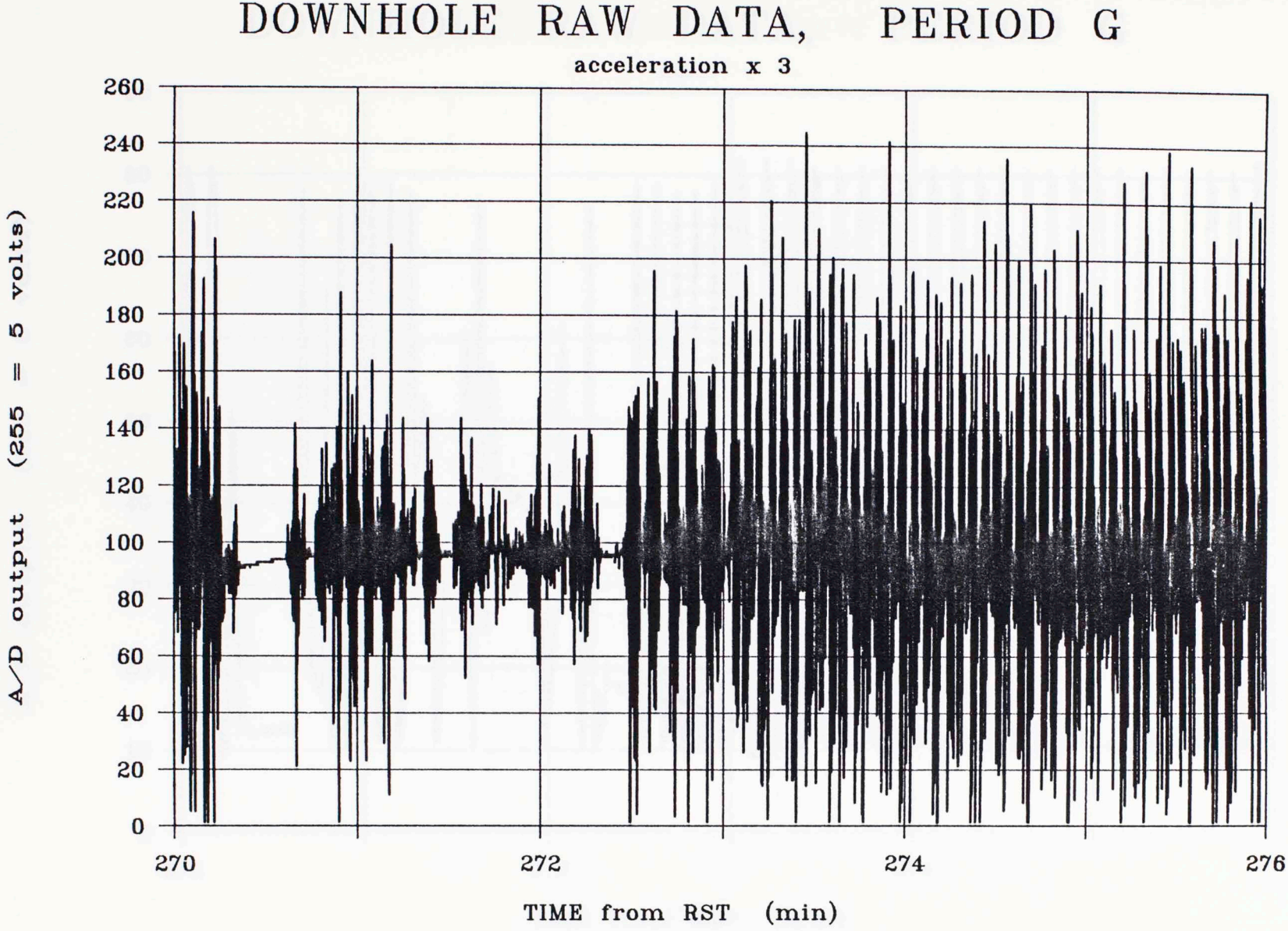

Figure 4.7 Downhole data, sample period G-CH0.

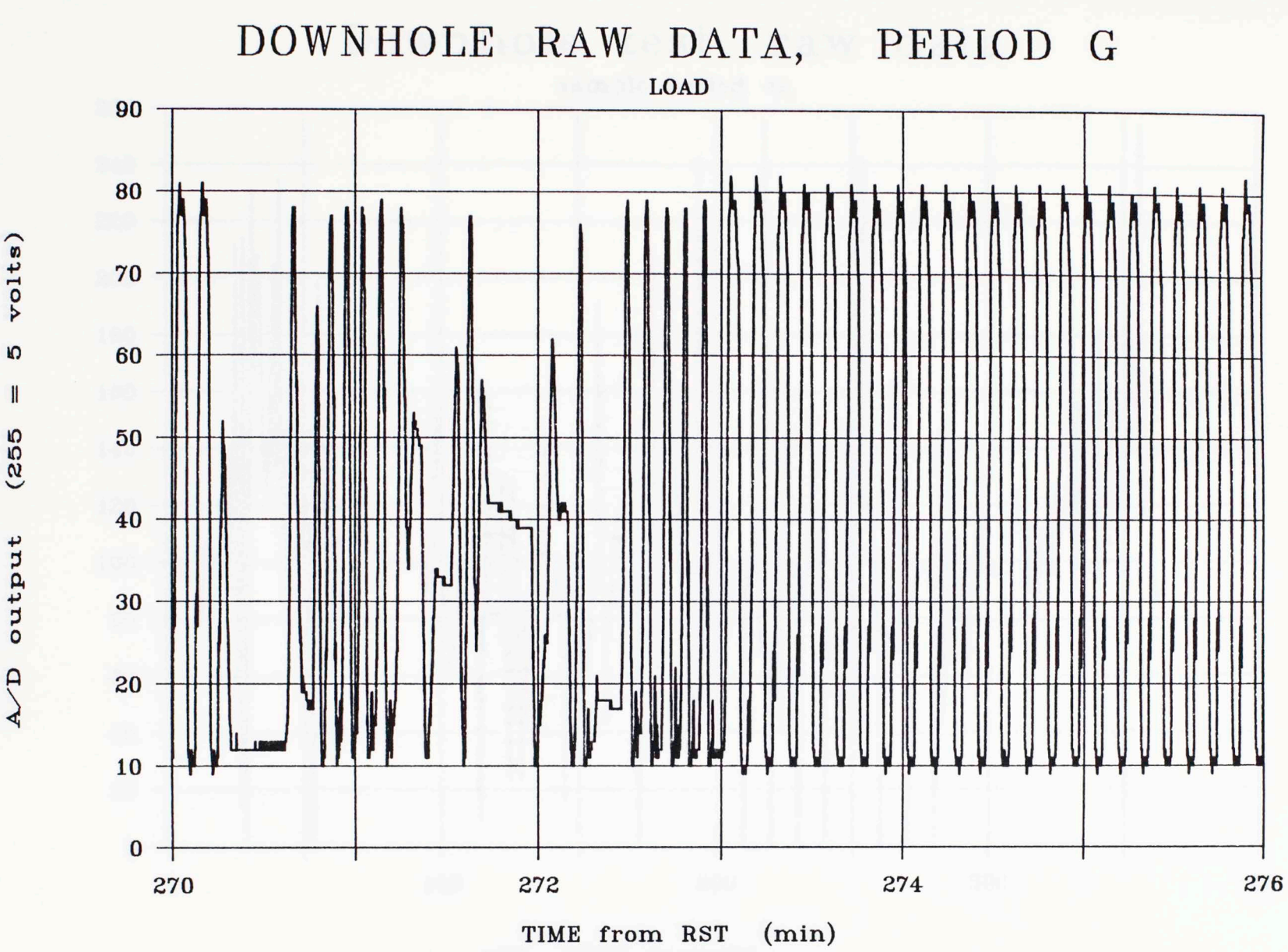

Figure 4.8 Downhole data, sample period G-CH1.

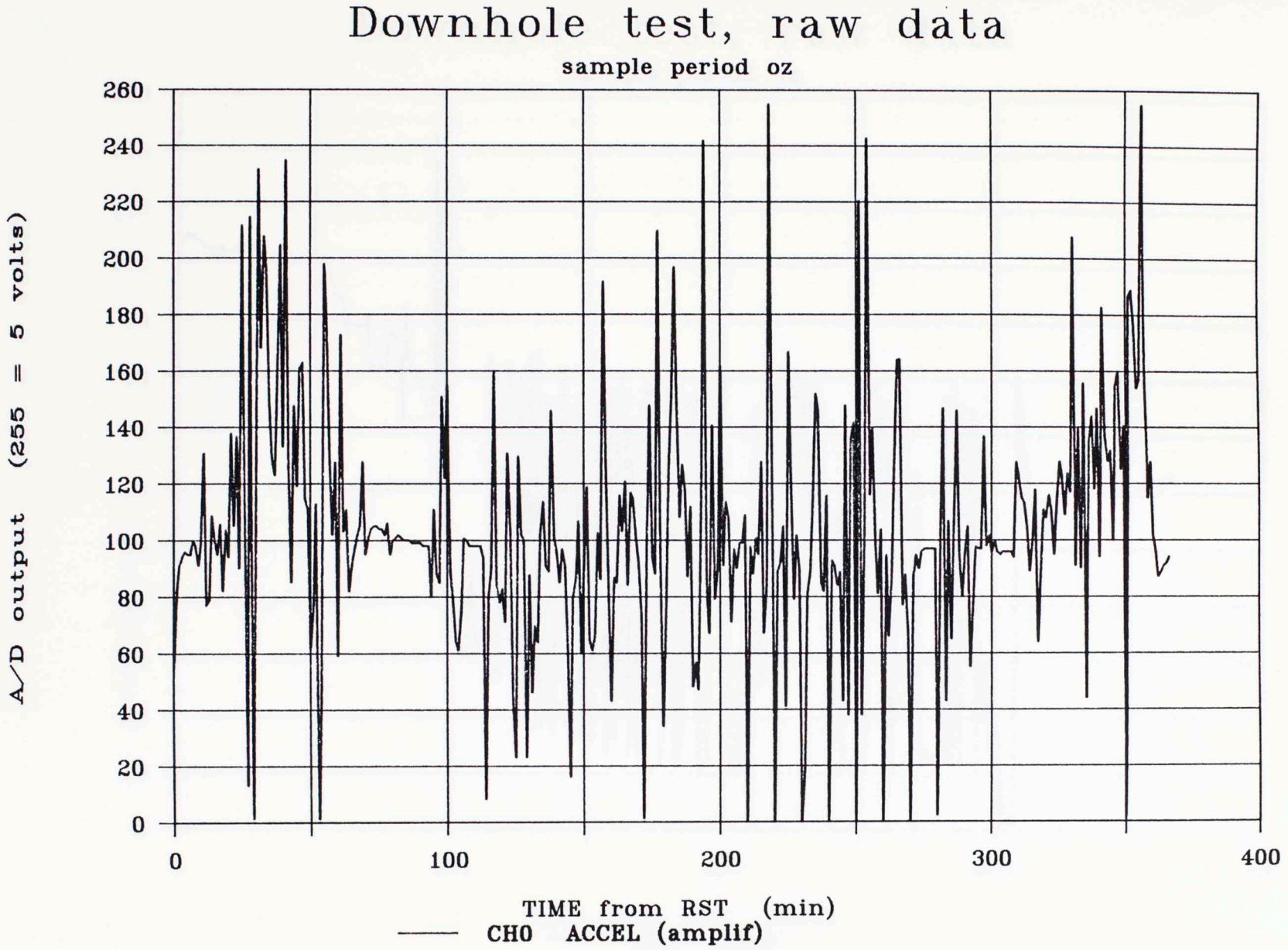

Figure 4.9 Throughout-test samples, CH0, Amplified Accel.

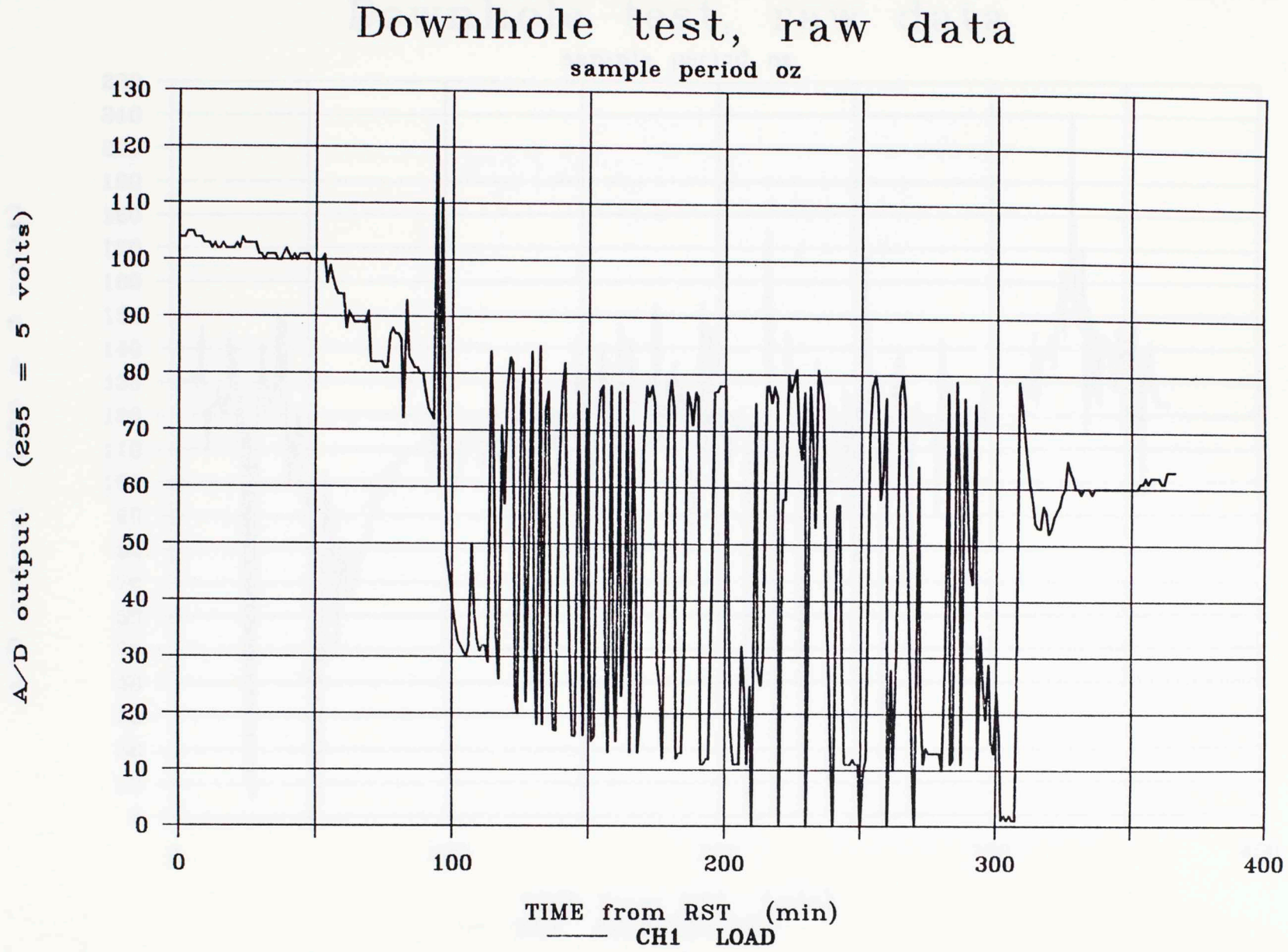

Figure 4.10 Throughout-test samples, CH1, Load

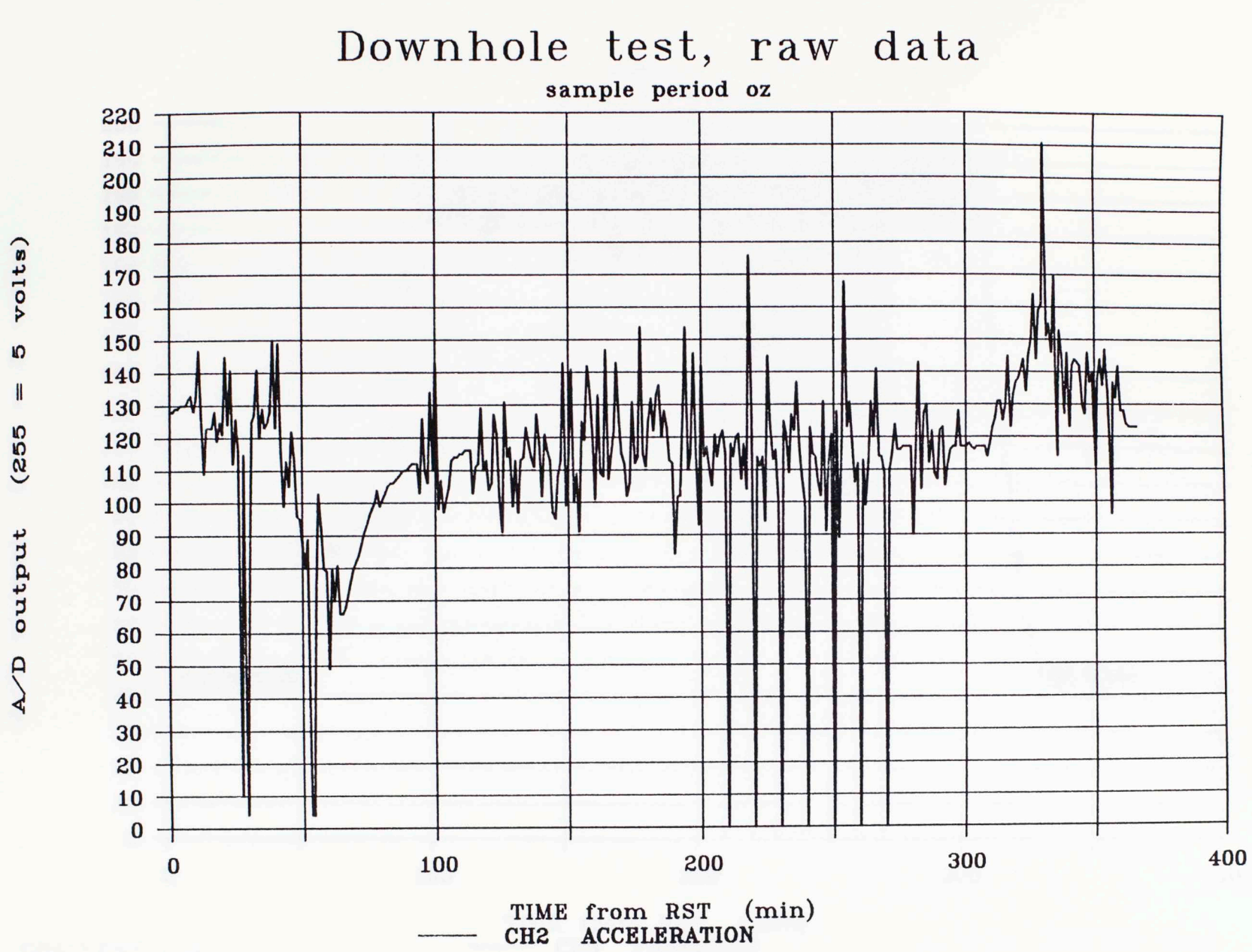

Figure 4.11 Throughout-test samples, CH2, Acceleration

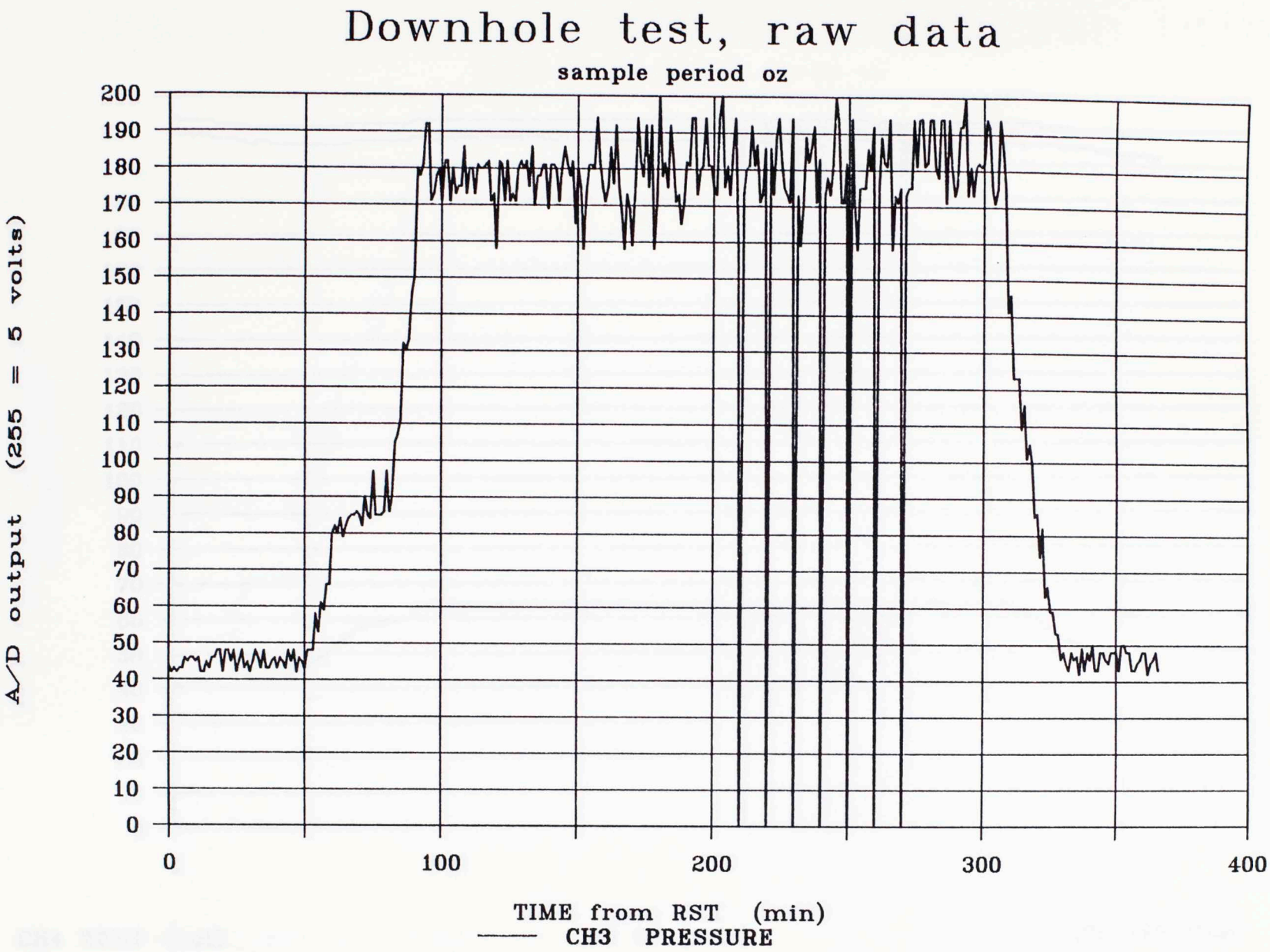

Figure 4.12 Throughout-test samples, CH3, Pressure

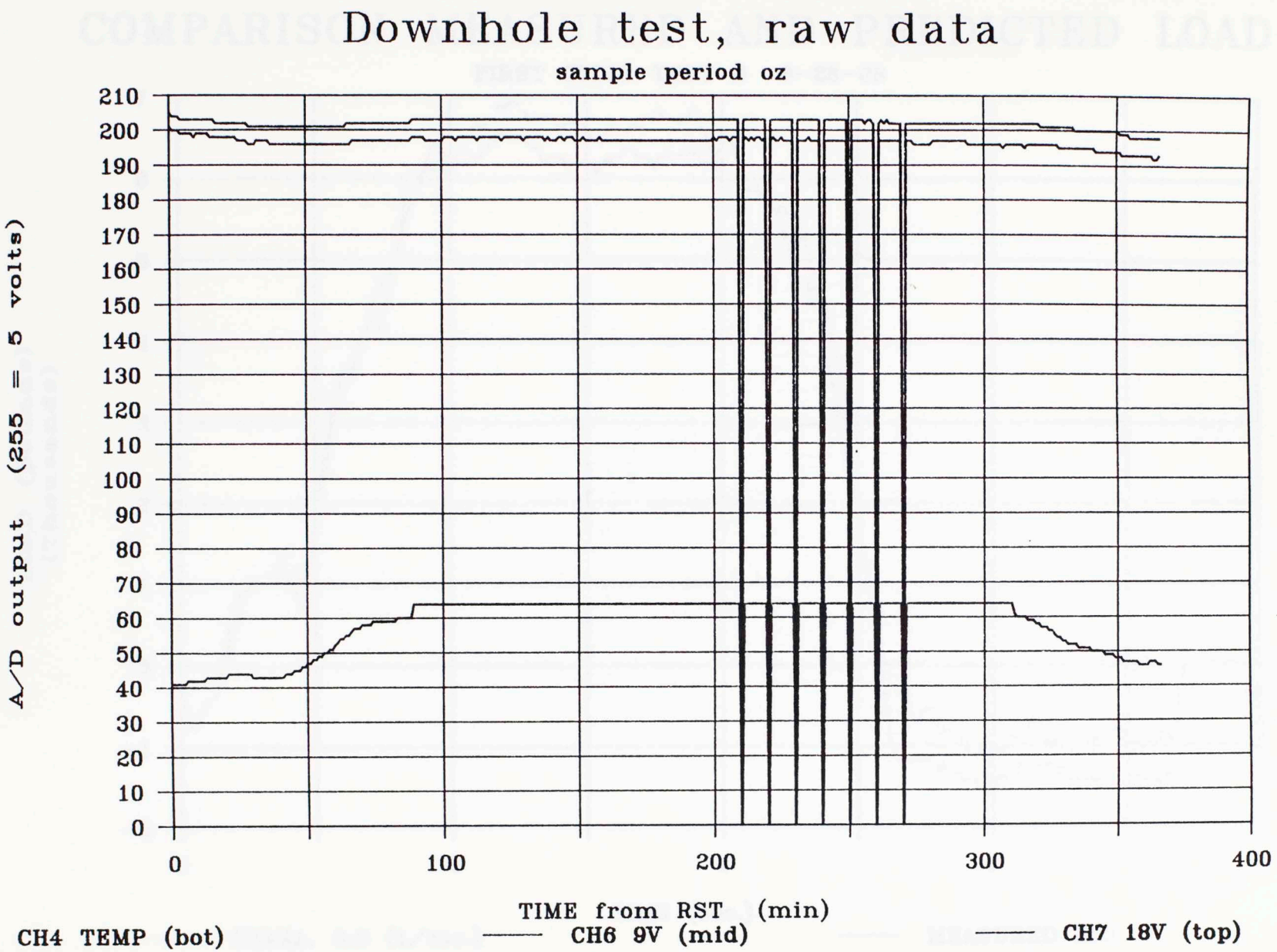

Figure 4.13 Throughout-test samples, CH4-7, Temp. and Volt.

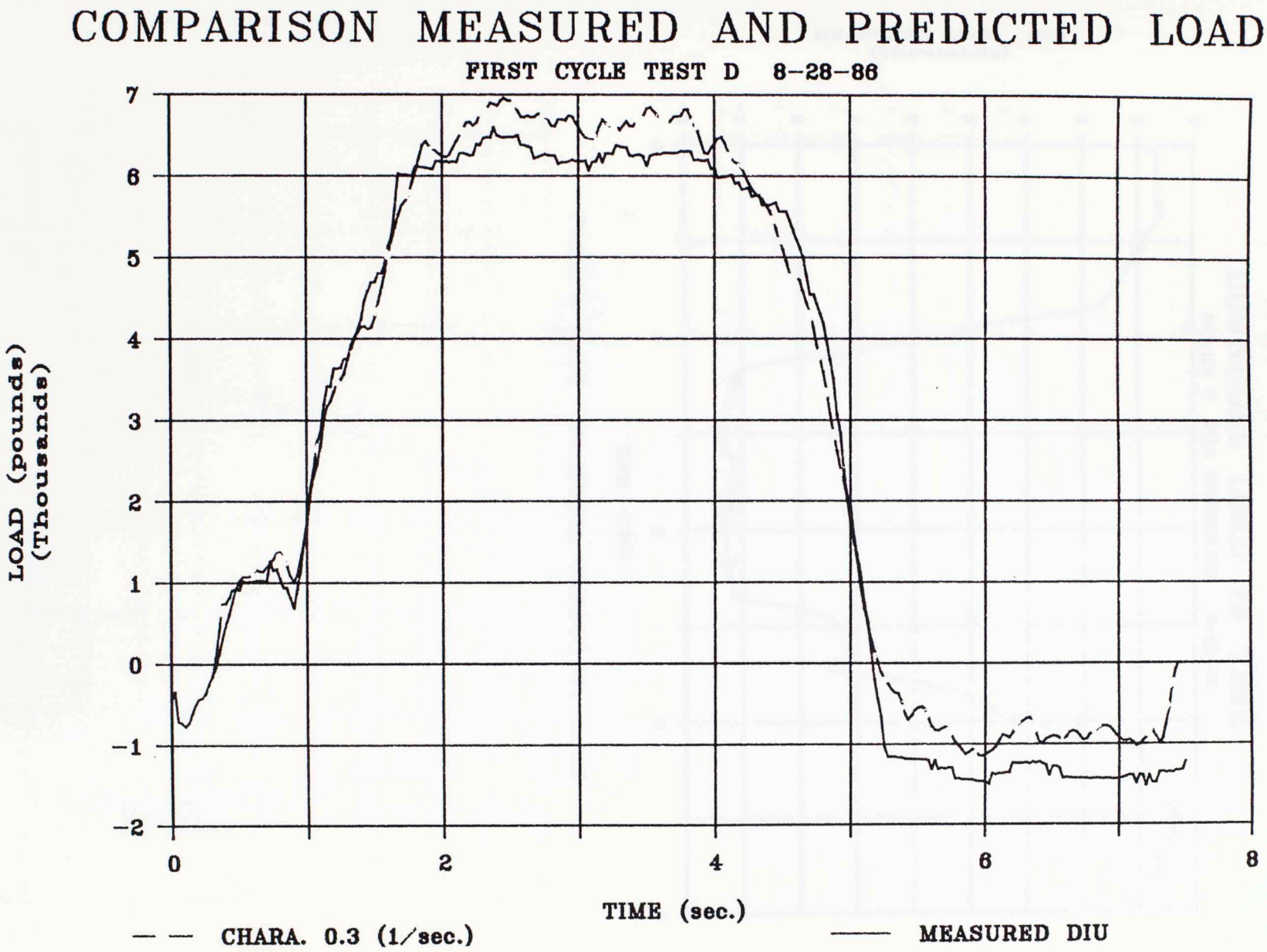

Figure 4.14 Measured and Predicted Load

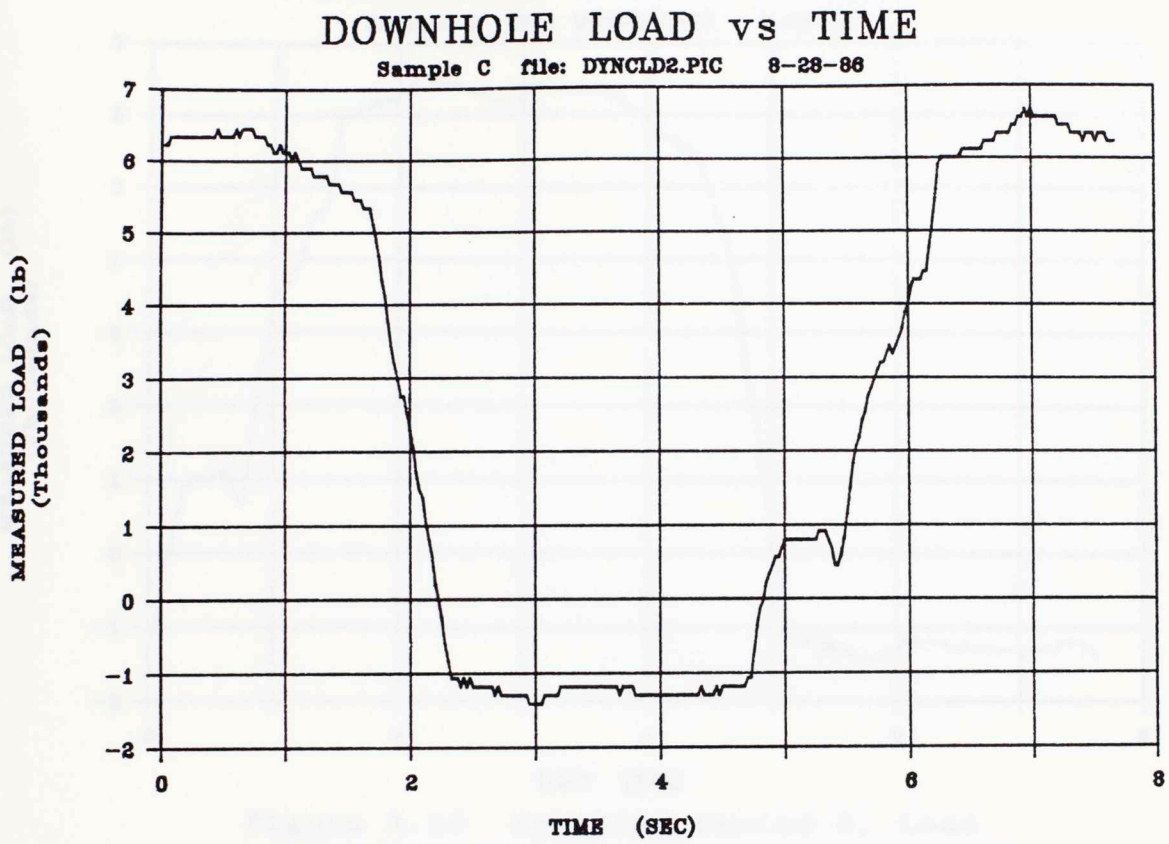

Figure 4.15 Sampling Period C, Load

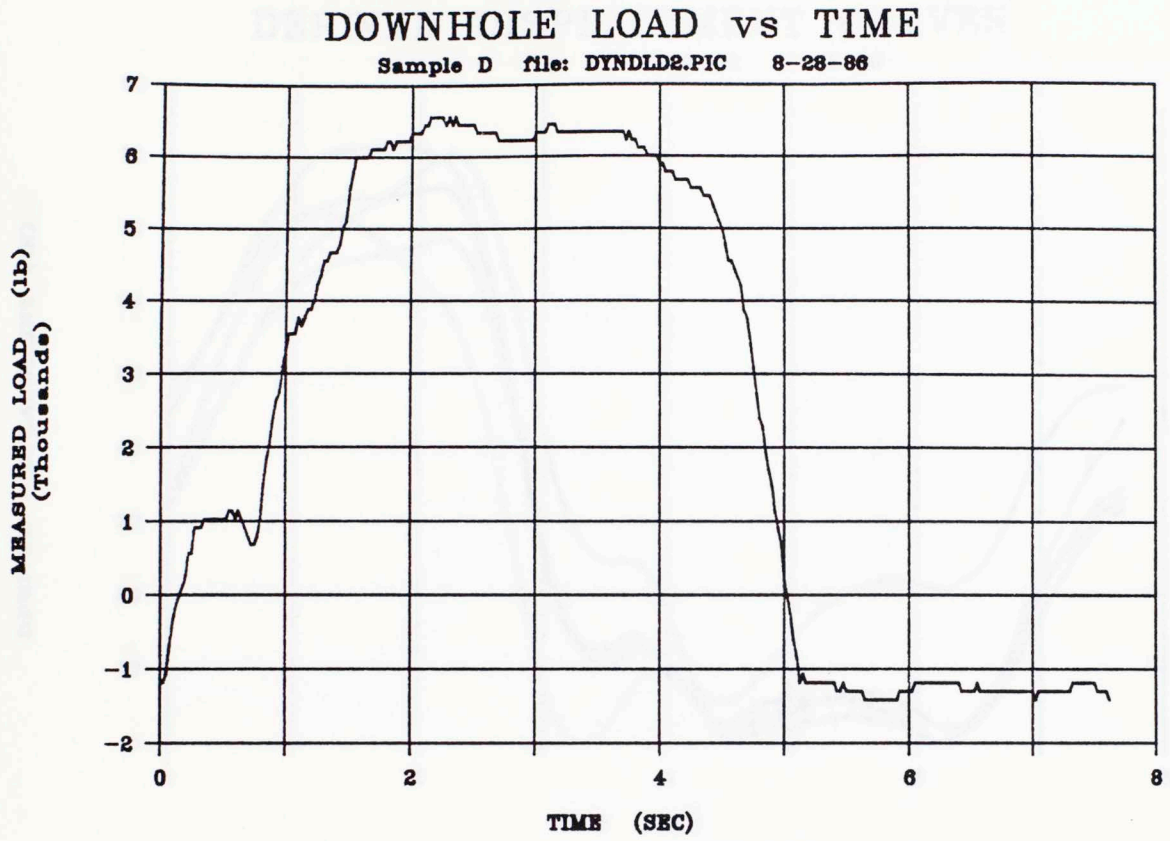

Figure 4.16 Sampling Period D, Load

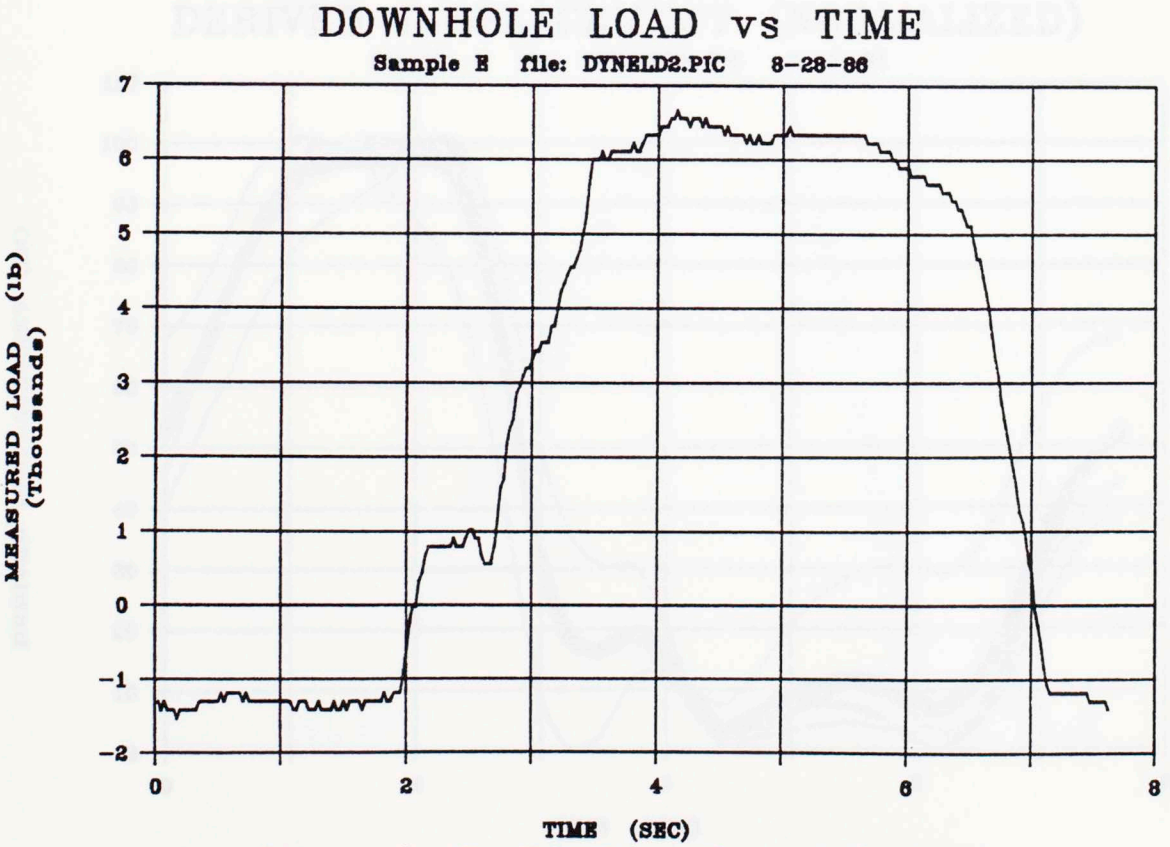

Figure 4.17 Sampling Period E, Load

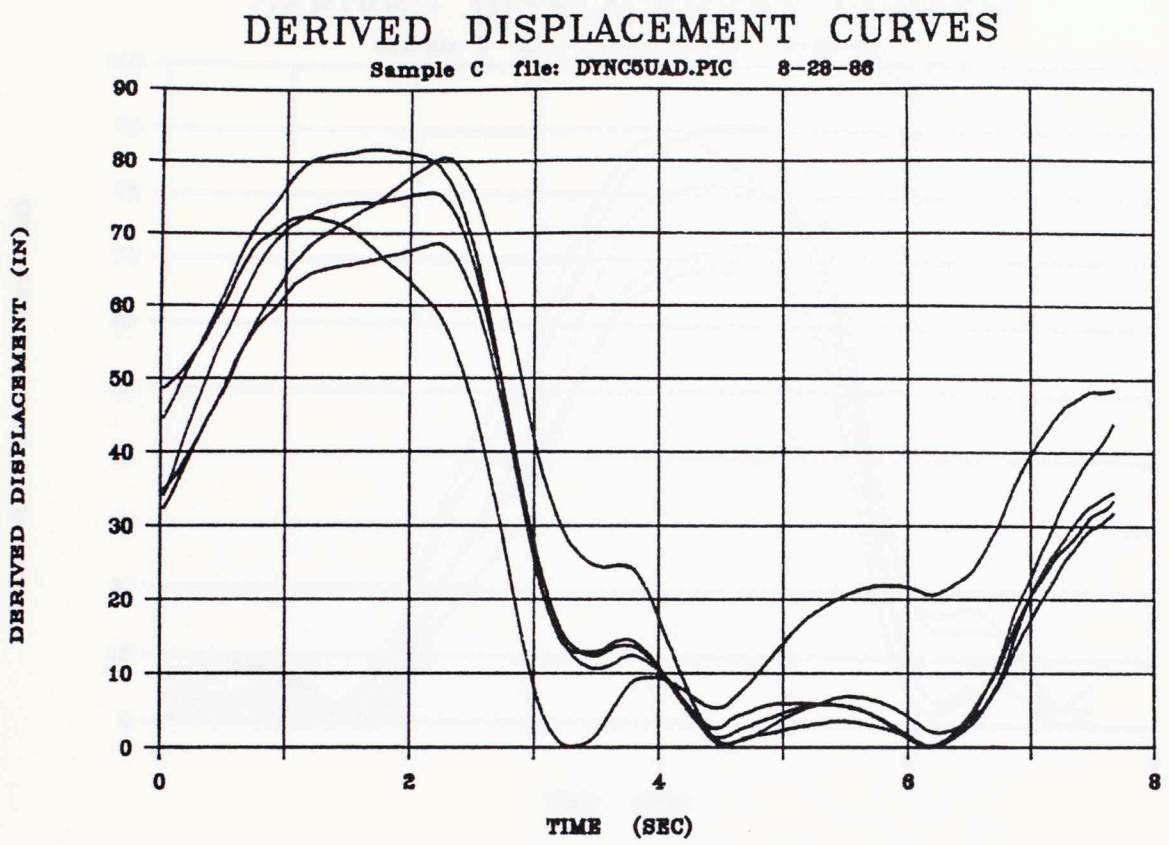

Figure 4.18

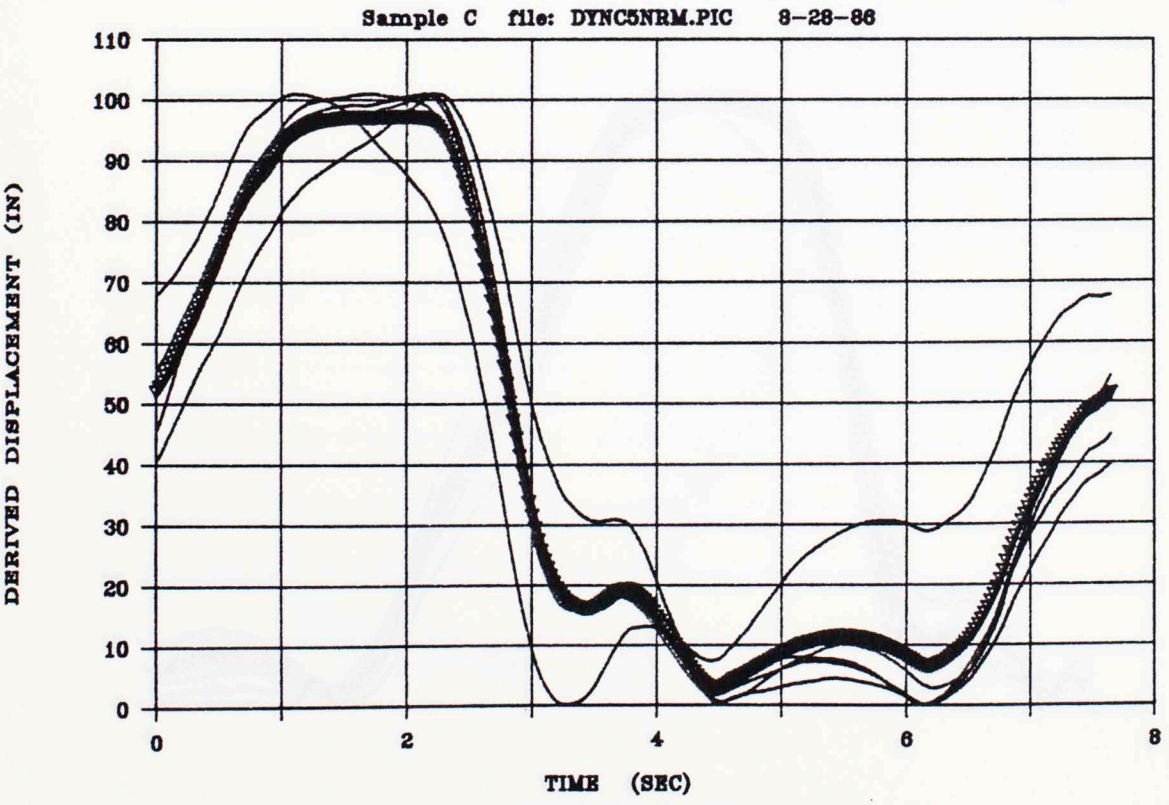

Figure 4.19

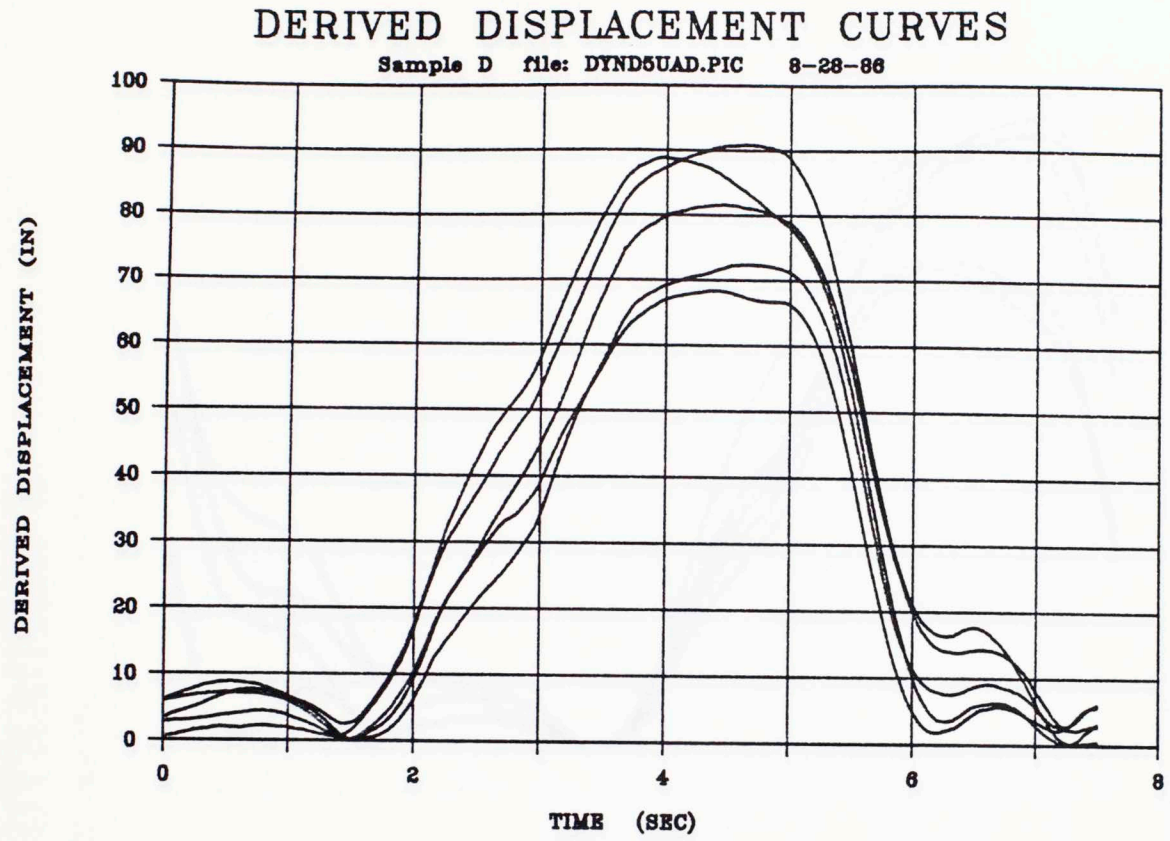

Figure 4.20

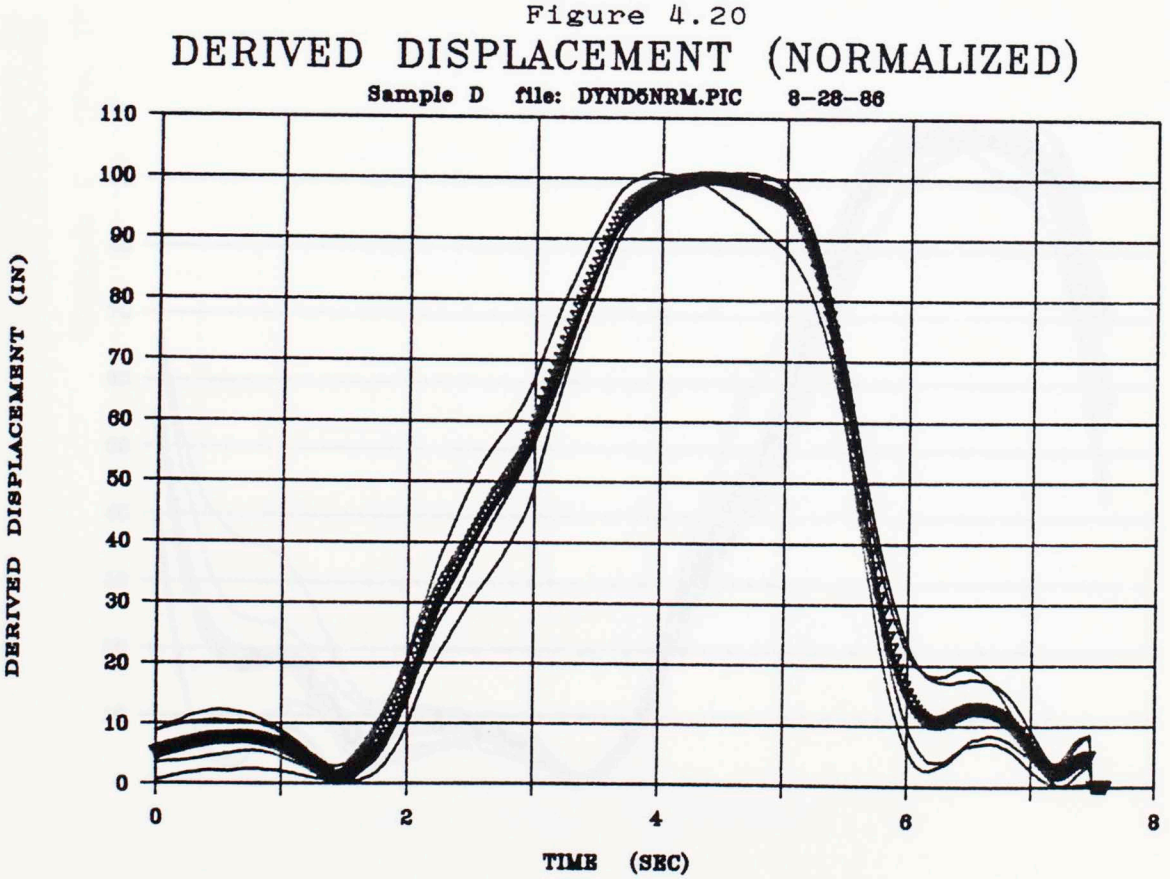

Figure 4.21

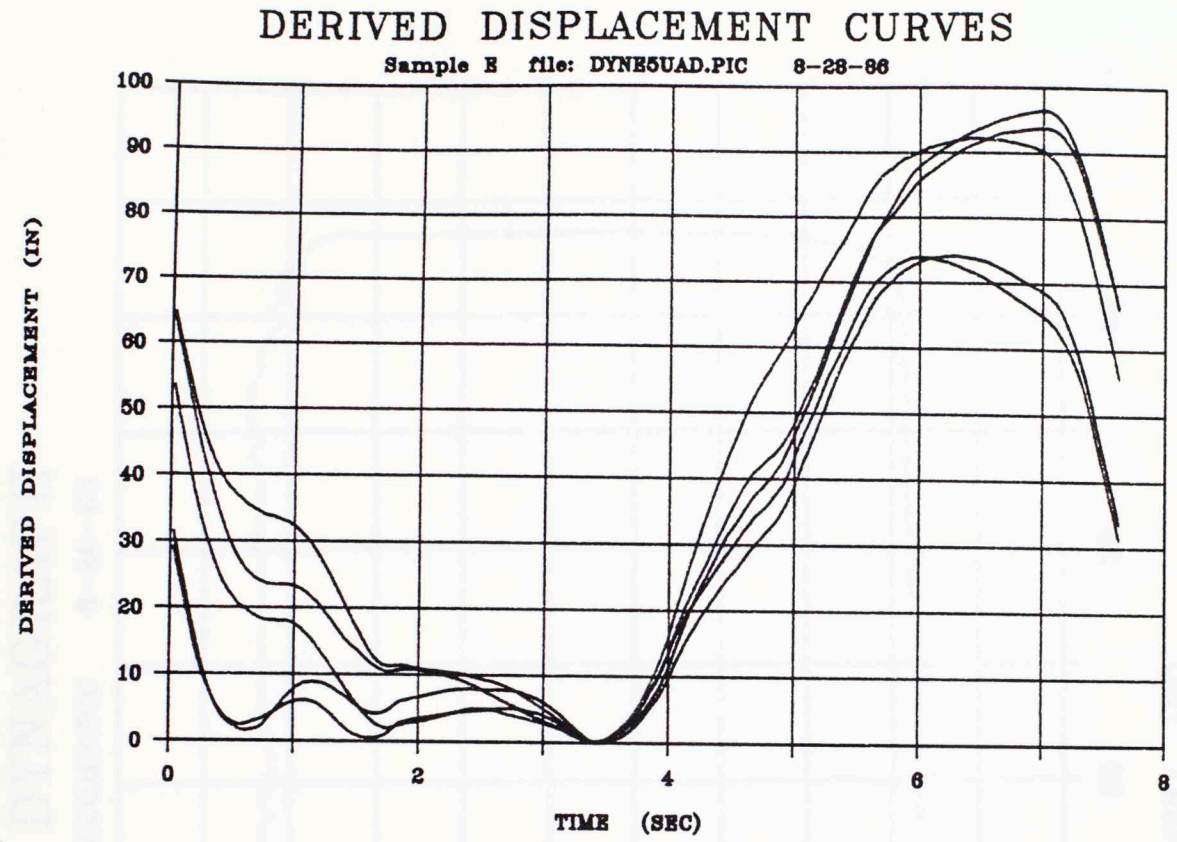

Figure 4.22

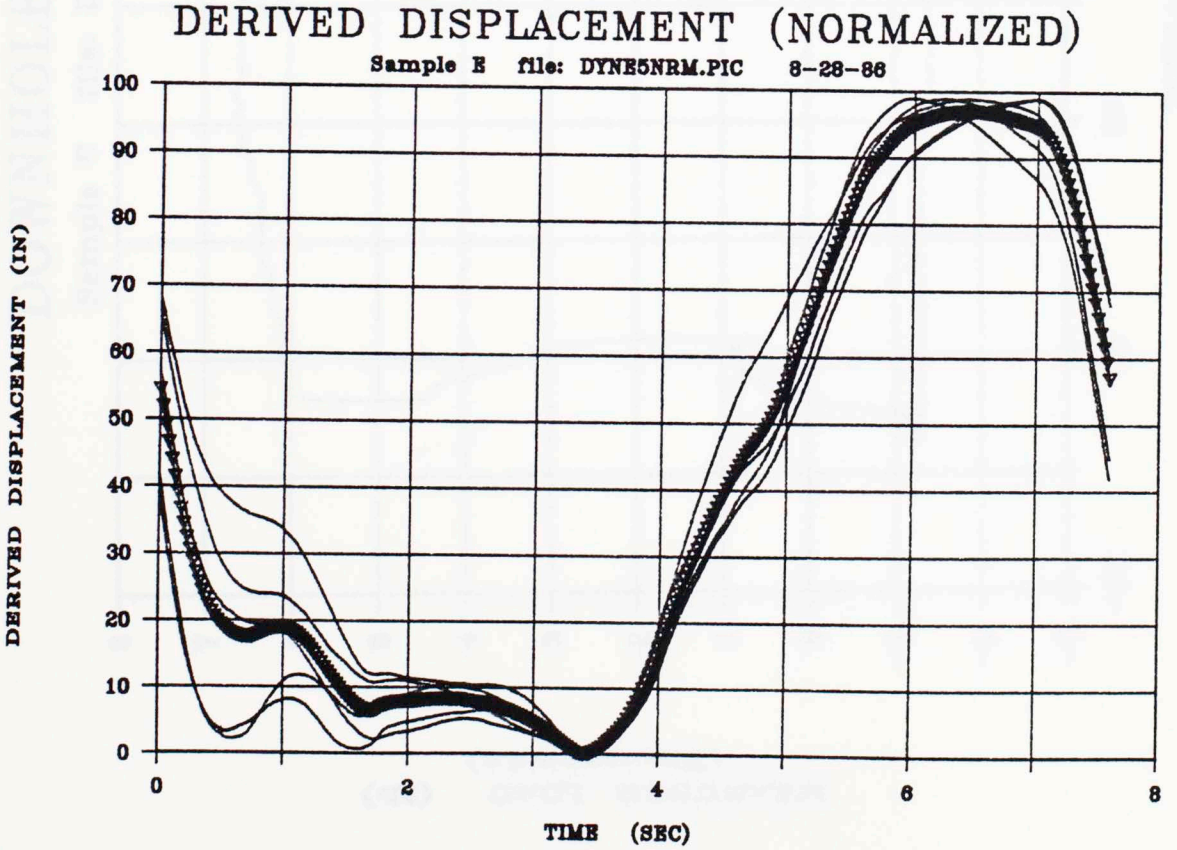

Figure 4.23

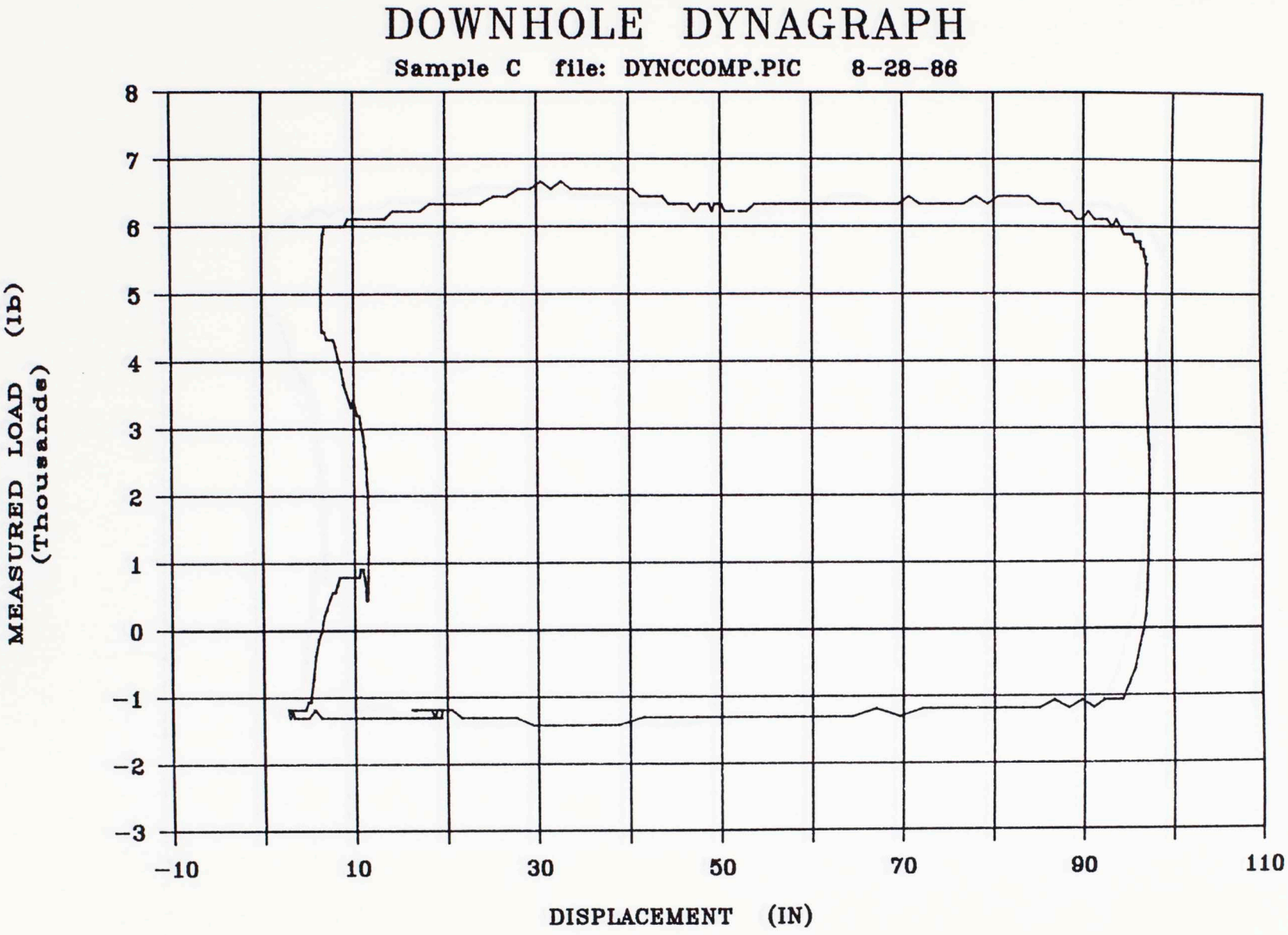

Figure 4.24 Sampling Period C, Downhole Dynagraph

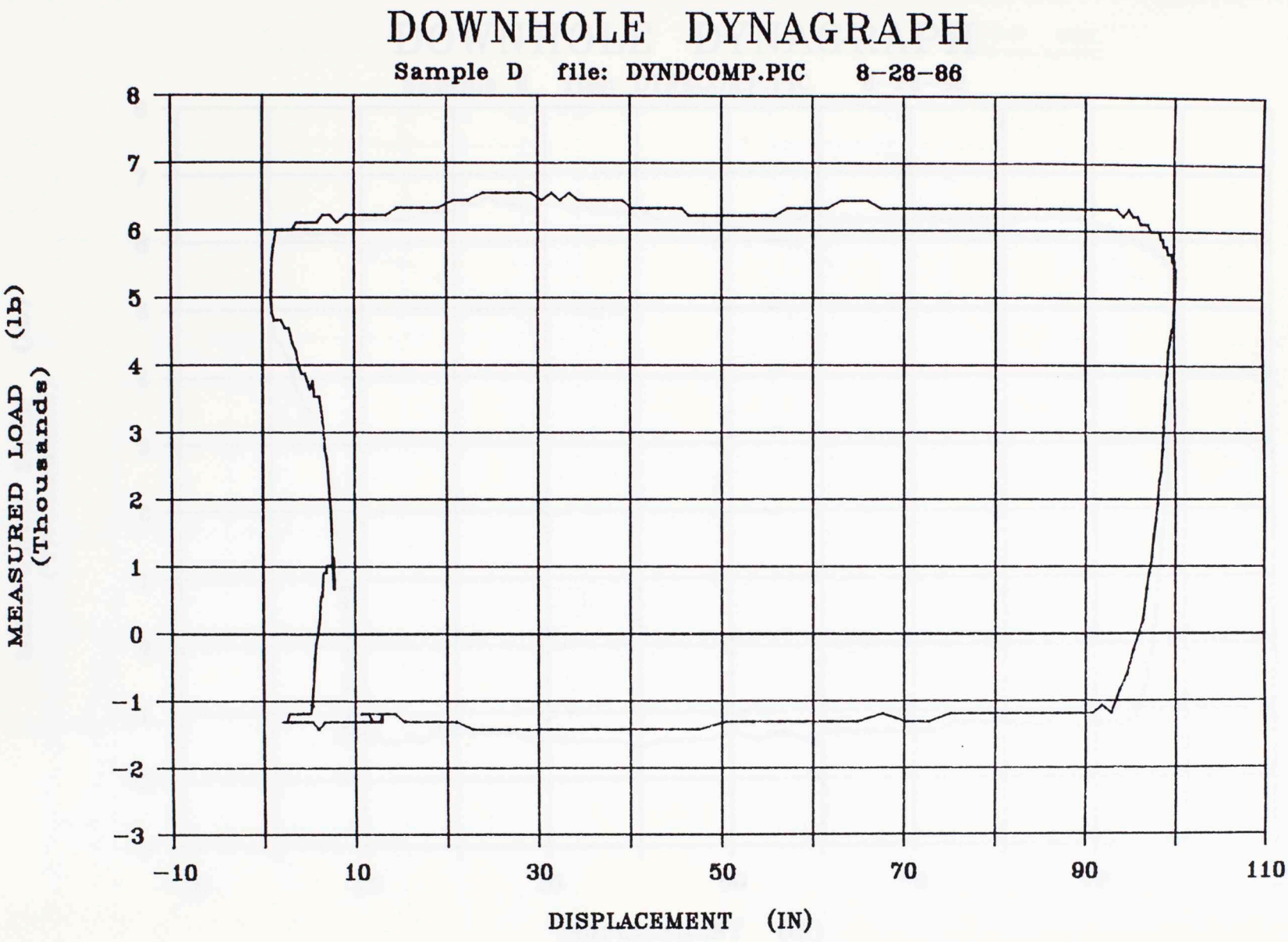

Figure 4.25 Sampling Period D, Downhole Dynagraph

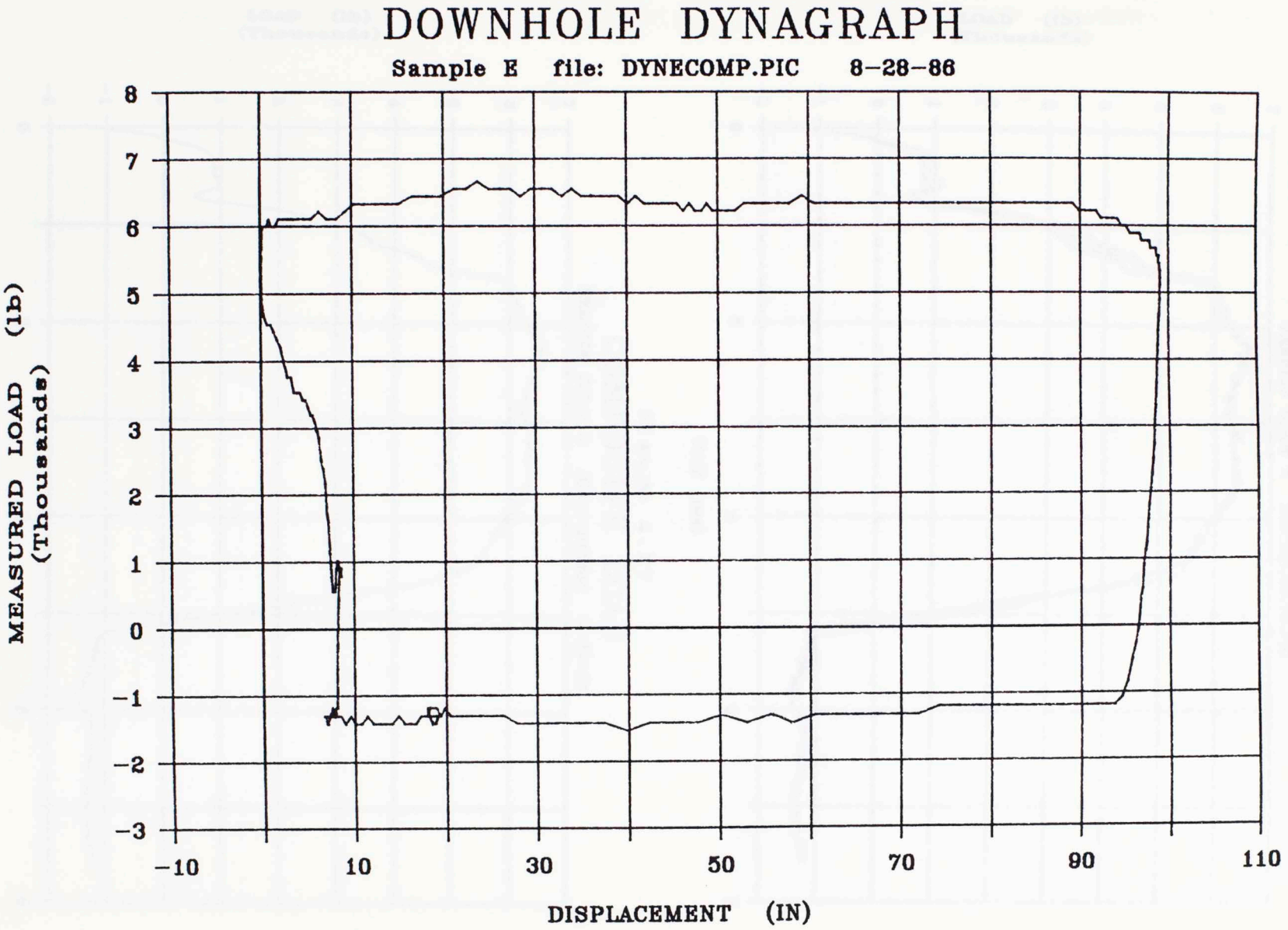

Figure 4.26 Sampling Period E, Downhole Dynagraph

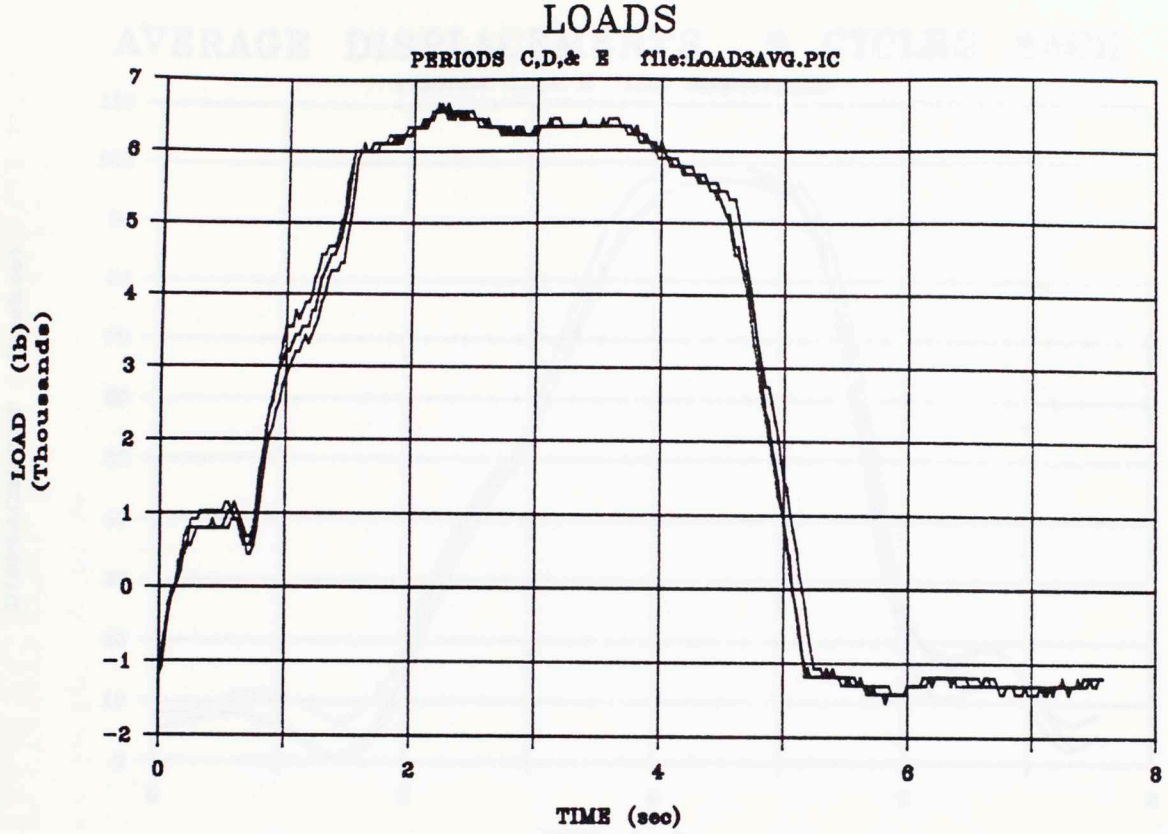

Figure 4.27

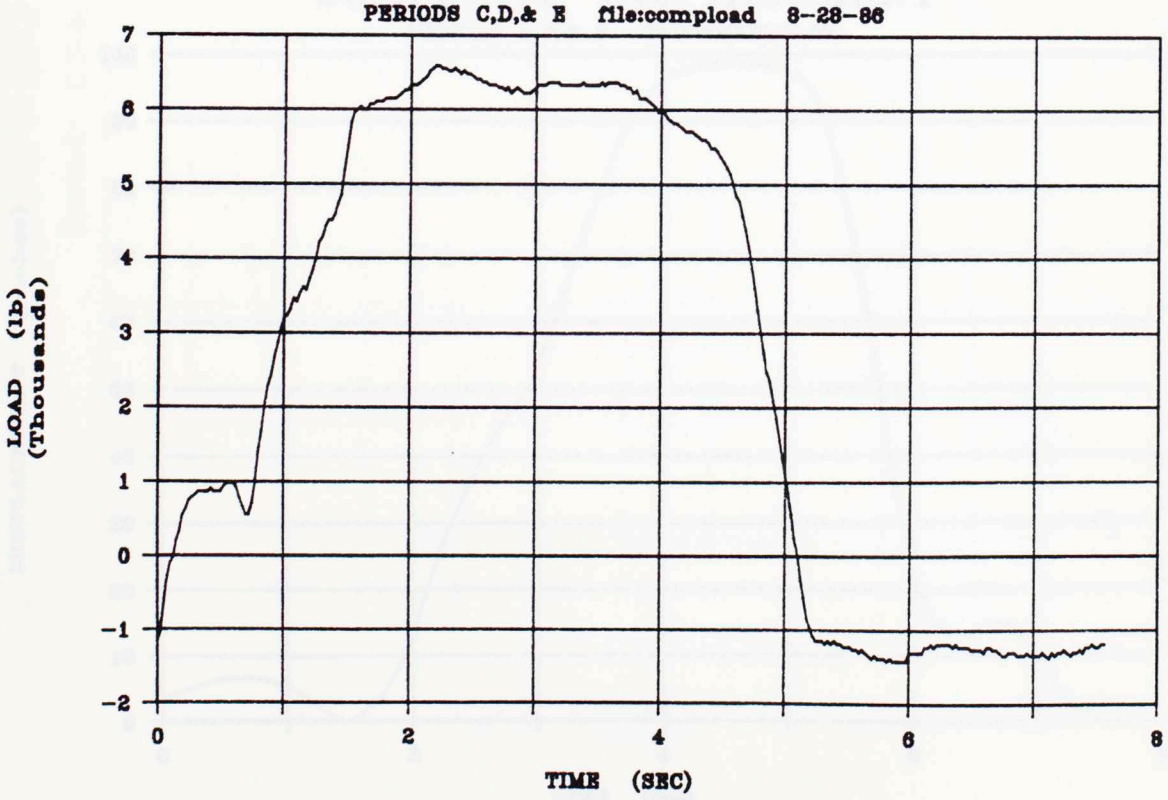

Figure 4.28

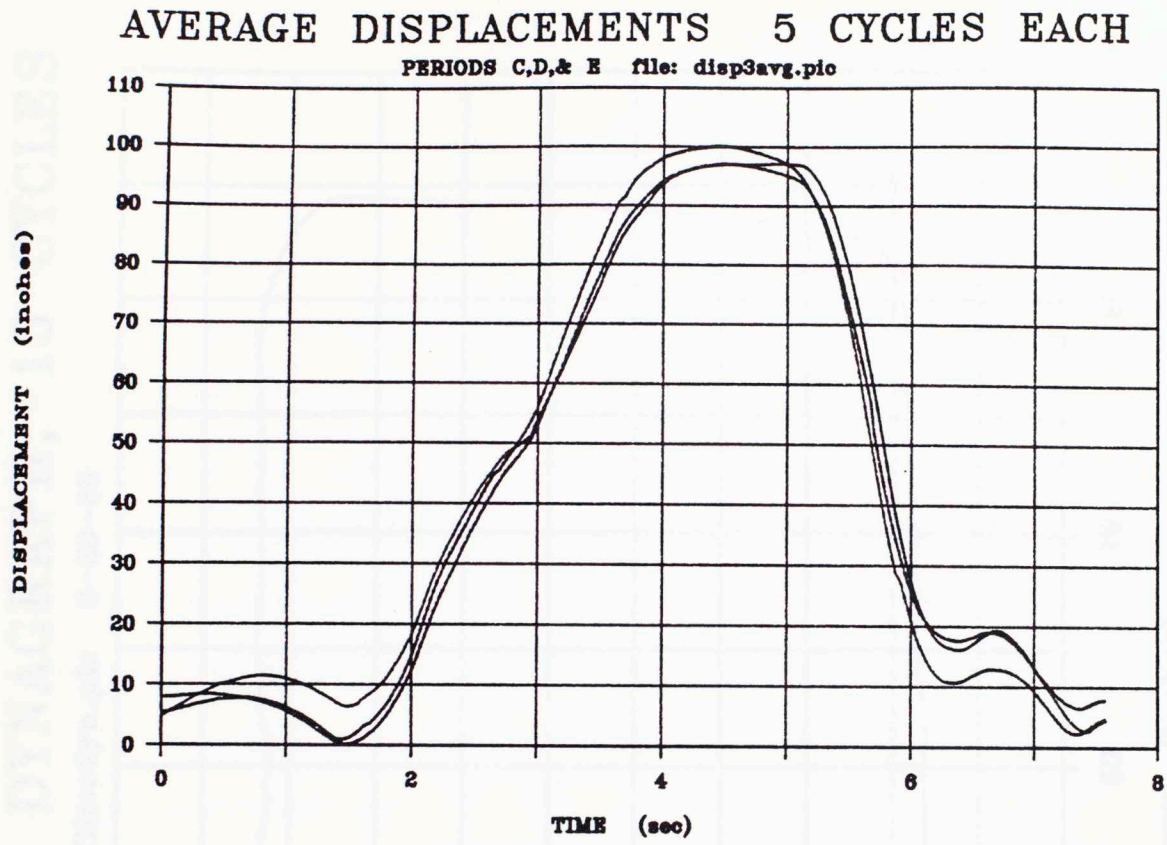

Figure 4.29

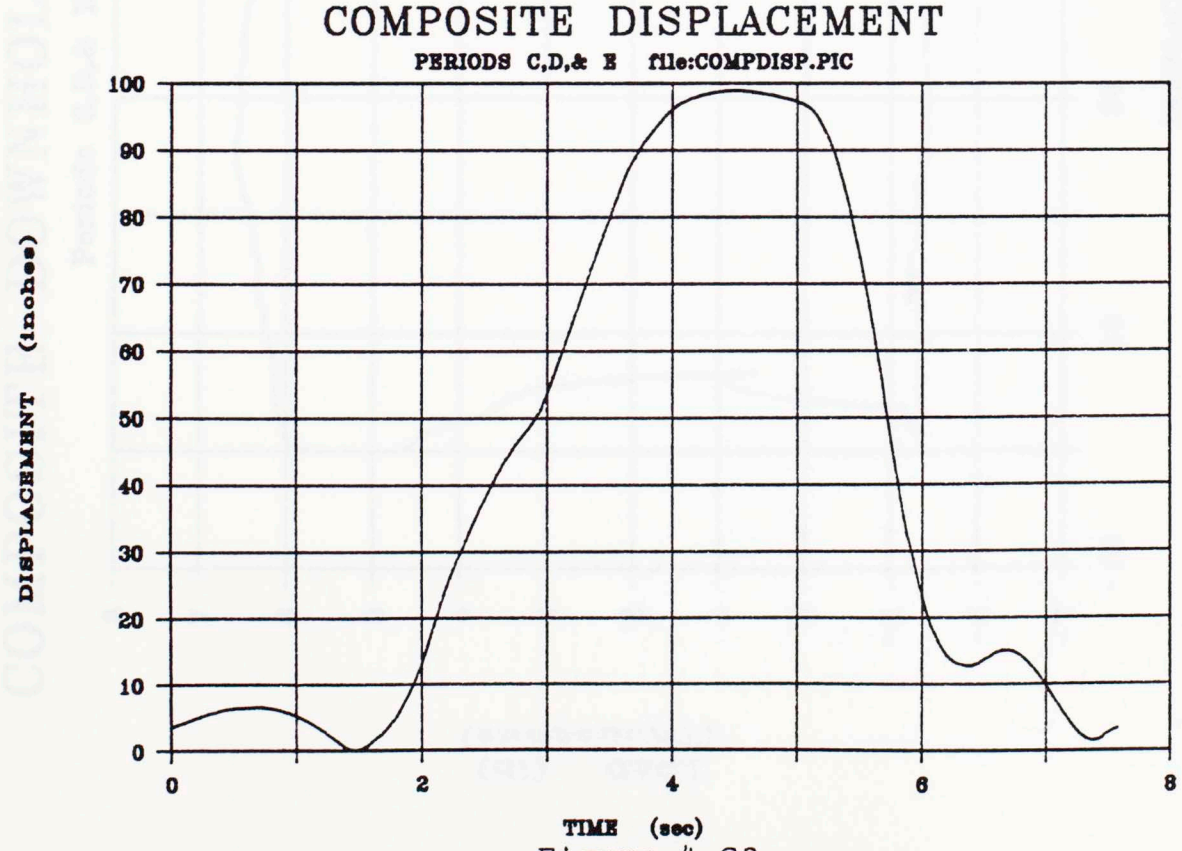

Figure 4.30

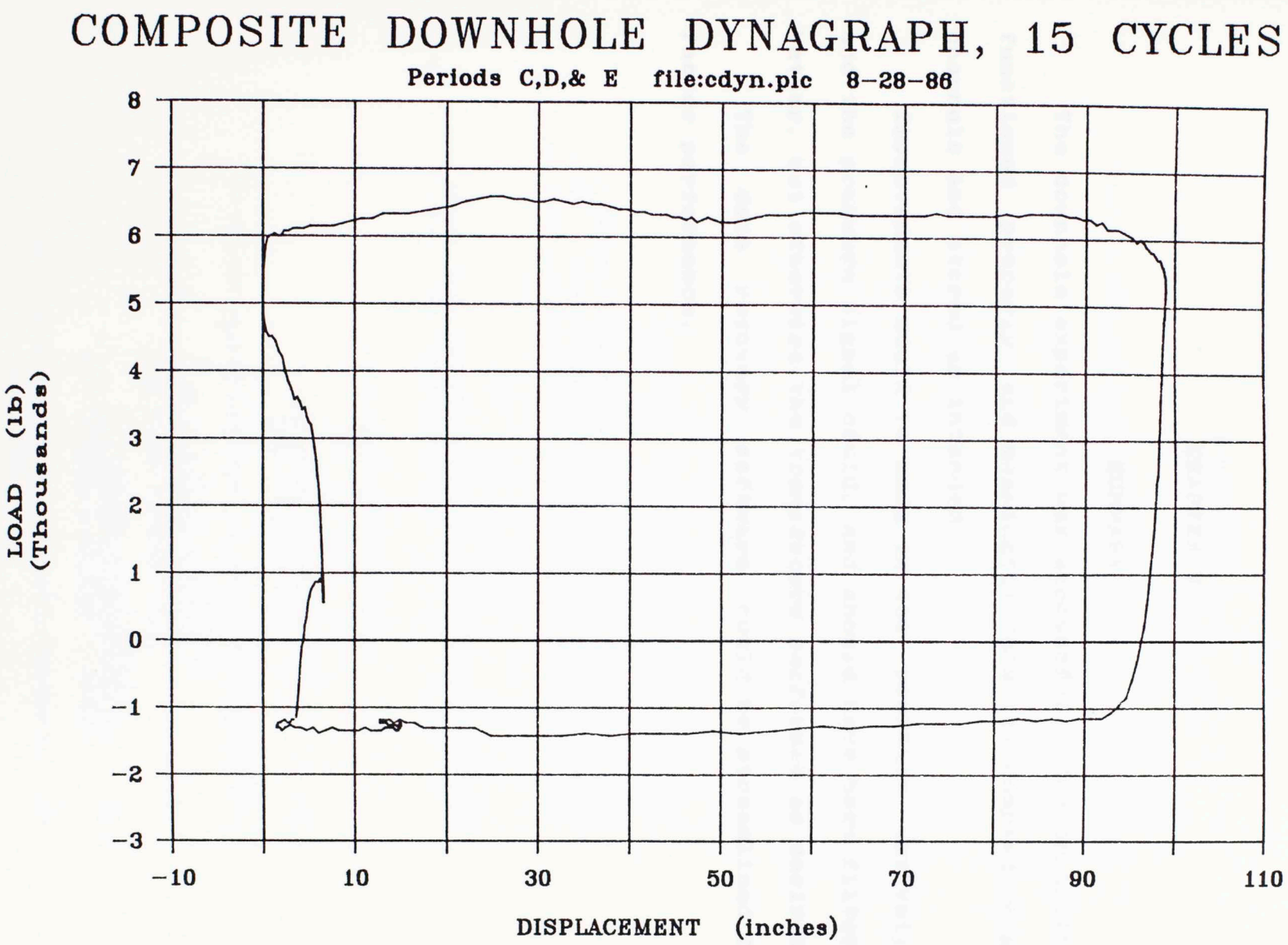

Figure 4.31 Composite Downhole Dynagraph

CHAPTER V

SUMMARY

The downhole experiment was successful. The controller functioned properly and meaningful data was sampled on all channels and stored as intended.

Improvements could be made in the position derivation and the pressure signal could, and should have been filtered better, but otherwise the transducers performed as desired.

The data recovery software could be streamlined for faster performance.

APPENDIX A

WHEATSTONE BRIDGE IN STRAIN GAGE APPLICATION

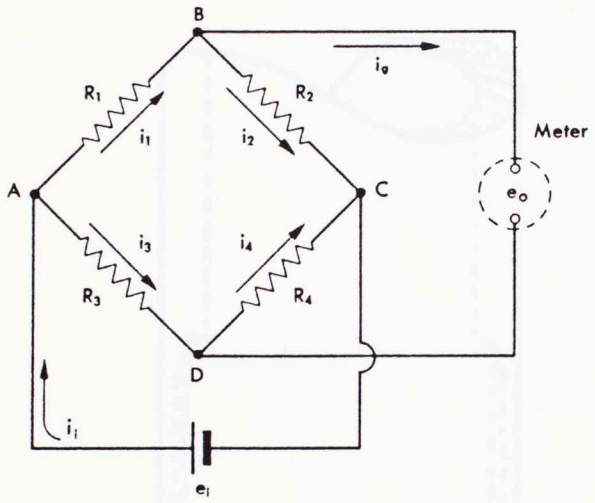

Fig. 7.13 Simple Wheatstone bridge circuit.

a) *The voltage-sensitive Wheatstone bridge.* Let us consider the simplest case first, in which the bridge output is connected directly to a high-impedance device, say an oscilloscope. Referring to Fig. 7.13, we find that

$$e_0 = i_{ABC}R_1 - i_{ADC}R_3,$$

and making use of relations developed in the derivation for null-balance condition and Ohm's law, we may write

$$\begin{aligned} e_g &= e_i\left(\frac{R_1}{R_1 + R_2} - \frac{R_3}{R_3 + R_4}\right) \\ &= e_i\left(\frac{R_1R_4 - R_2R_3}{(R_1 + R_2)(R_3 + R_4)}\right). \end{aligned} \tag{7.42}$$

We will now assume that resistance R_1 changes by an amount ΔR_1, or

$$\begin{aligned} \frac{e_0 + \Delta e_0}{e_i} &= \left[\frac{(R_1 + \Delta R_1)(R_4) - R_2R_3}{(R_1 + \Delta R_1 + R_2)(R_3 + R_4)}\right] \\ &= \left\{\frac{1 + (\Delta R_1/R_1) - (R_2R_3/R_1R_4)}{[1 + (\Delta R_1/R_1) + (R_2/R_1)][1 + (R_3/R_4)]}\right\}. \end{aligned} \tag{7.43}$$

The relation may be simplified by assuming all resistances to be initially equal (in which case $e_0 = 0$). Then

$$\frac{\Delta e_0}{e_i} = \frac{\Delta R_1/R}{4 + 2(\Delta R_1/R)}. \tag{7.44}$$

(ref Mechanical Measurements) Addison Wesley pub.

APPENDIX B

PACKAGING OF APPARATUS

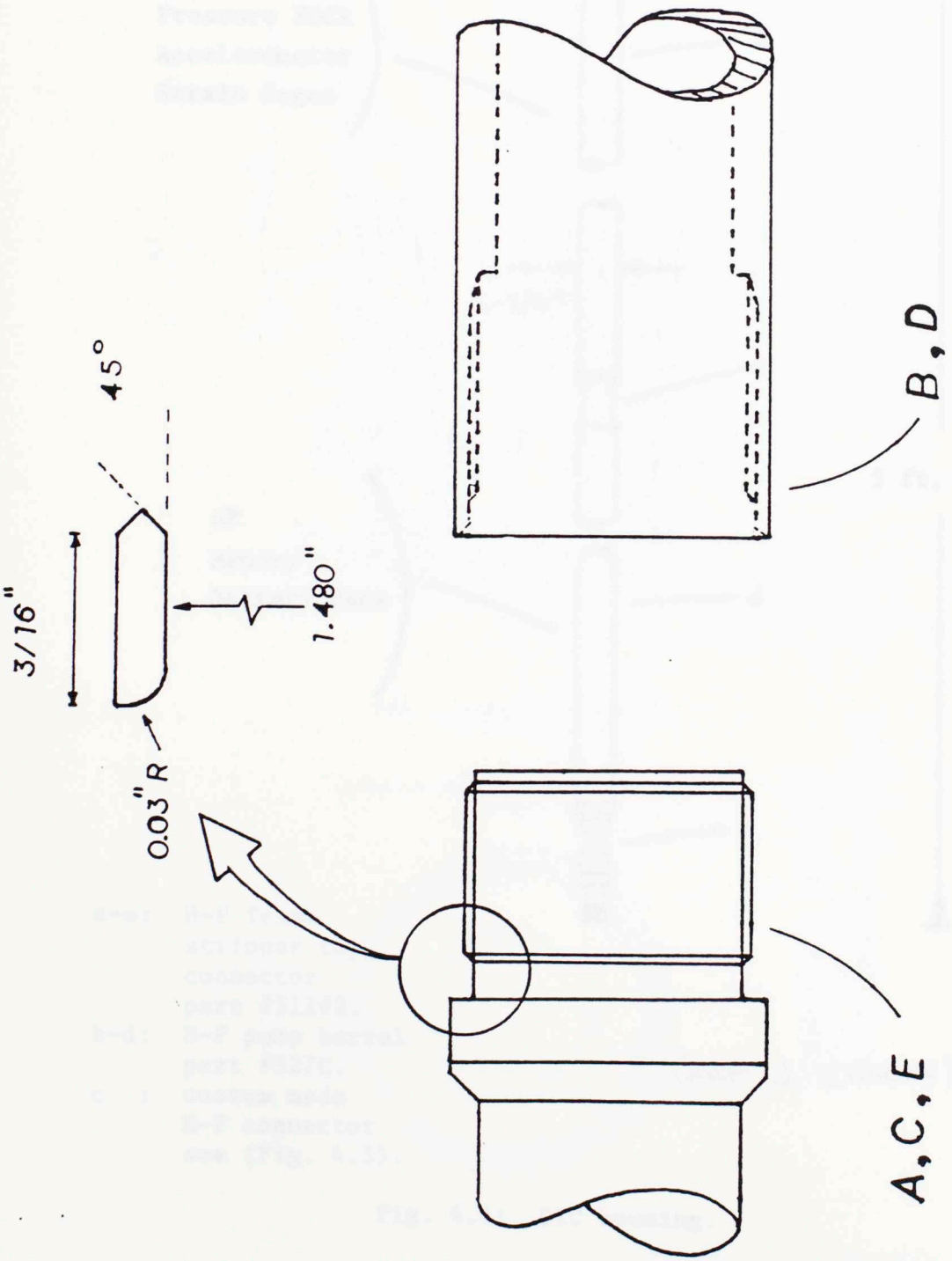

(REF. J. CHACIN)

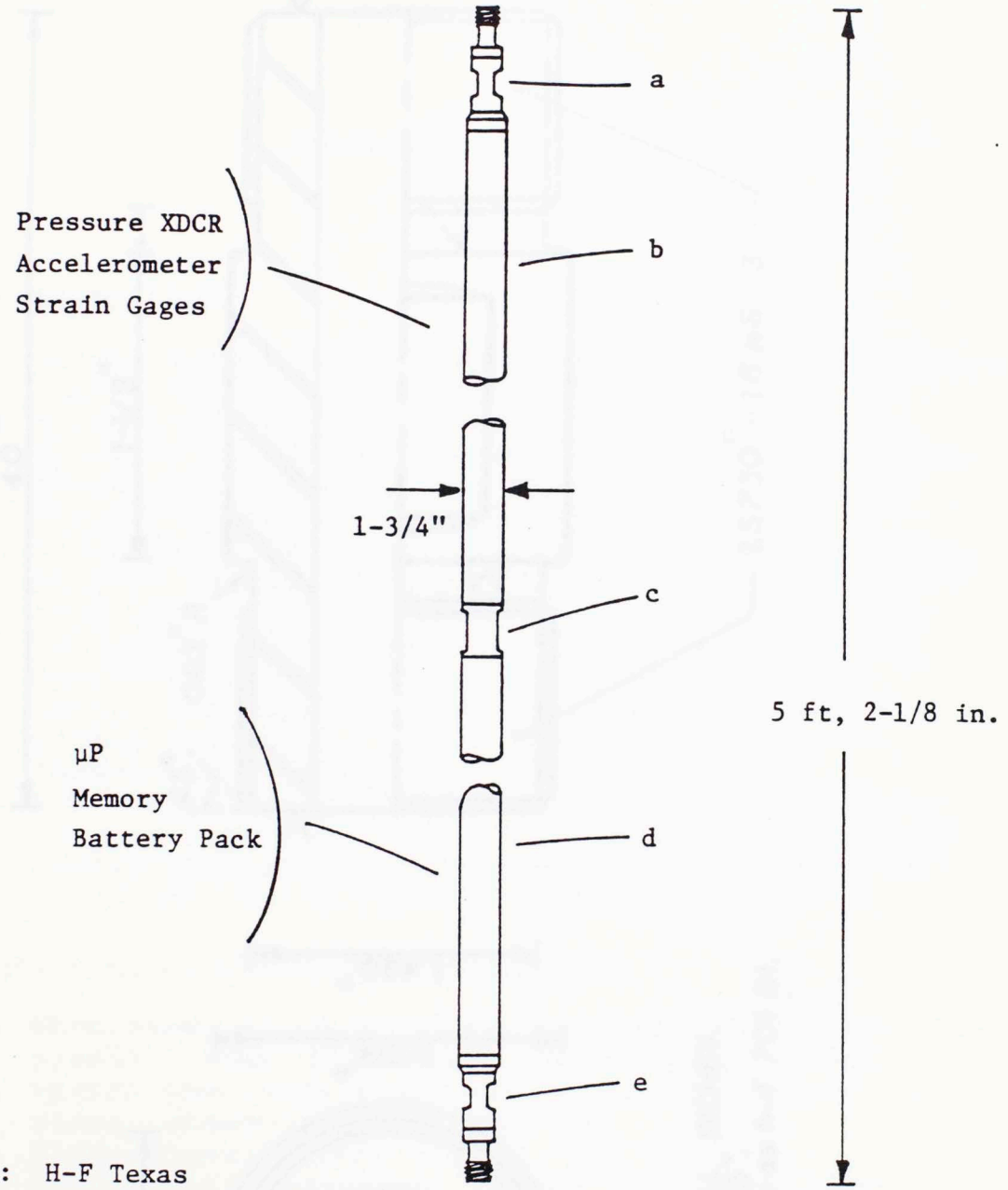

a-e: H-F Texas stripper top connector part #311#2.
b-d: H-F pump barrel part #527C.
c : custom made H-F connector see (Fig. 4.5).

(REF J. CHACIN)

Fig. 4.4: DIU housing.

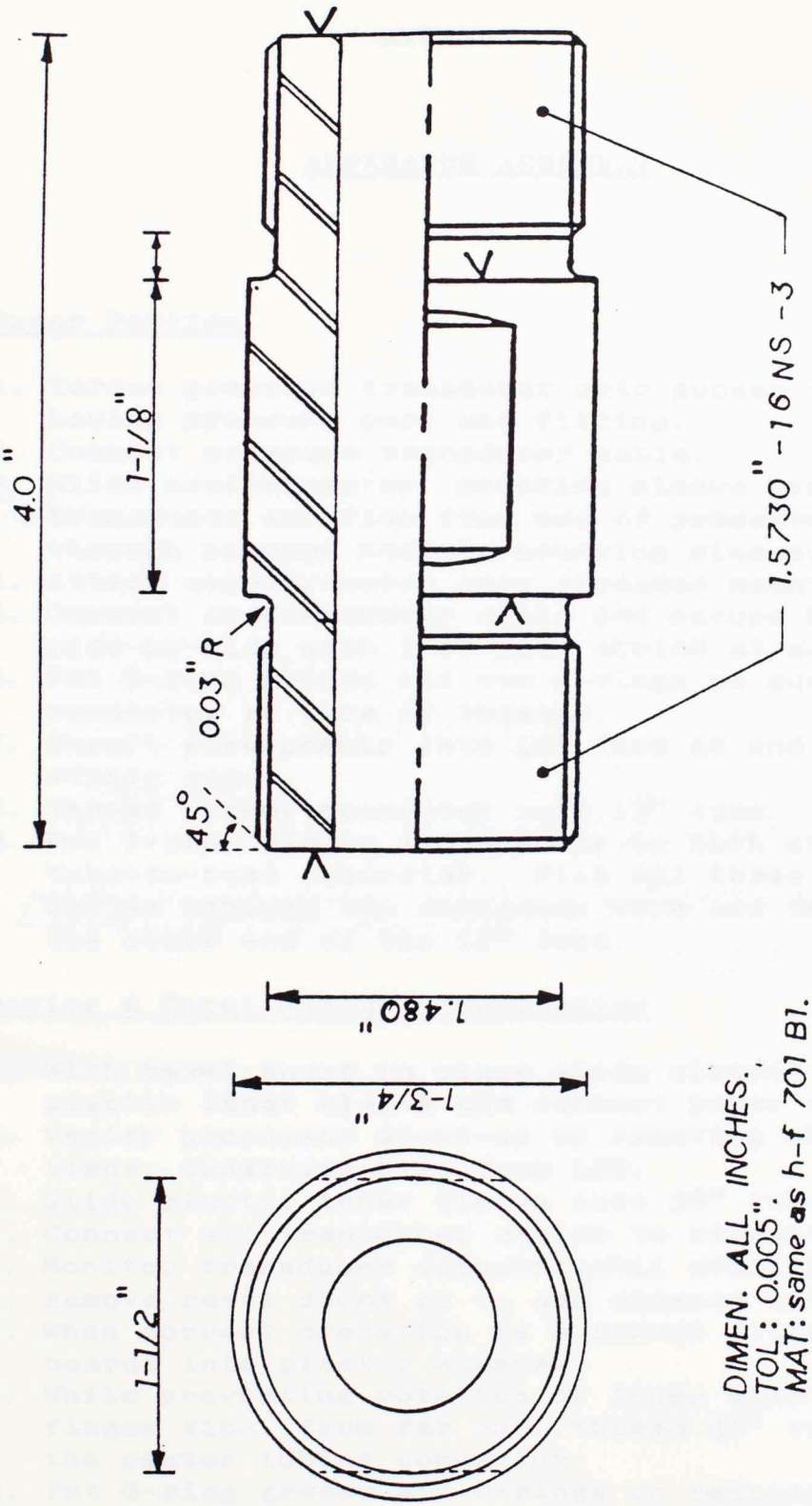

DIMEN. ALL INCHES.
TOL.: 0.005".
MAT: same as h-f 701 B1.

(REF. J. CHACIN)

APPENDIX C

APPARATUS ASSEMBLY

Transducer Portion

1. Torque pressure transducer onto sucker rod connector having pressure port and fitting.
2. Connect pressure transducer cable.
3. Slide accelerometer mounting sleeve over pressure transducer and fish free end of pressure cable through passage hole in mounting sleeve.
4. Attach accelerometer onto threaded mount on sleeve.
5. Connect accelerometer cable and secure both cables side-by-side with 1/4" heat shrink at acc. base.
6. Put O-ring grease and new O-rings on sucker rod connector at base of threads.
7. Insert subassembly into 12" tube at end opposite the strain gages.
8. Thread sucker connector into 12" tube.
9. Put O-ring grease and O-rings on both ends of the tube-to-tube connector. Fish all three transducer cables through the connector bore and thread onto the other end of the 12" tube.

Electronics & Total Assembly Completion

1. With reset shunt in place slide circuit board into plastic inner sleeve and connect power cable.
2. Verify processor start-up by removing shunt a few times, observing blip from LED.
3. Slide plastic inner sleeve into 36" tube.
4. Connect all transducer cables to circuit board.
5. Monitor transducer outputs until stabilized.
6. Remove reset shunt at t_0 and observe LED.
7. When correct operation is observed slide circuit boards into plastic sleeve.
8. While preventing rotation of inner sleeve with finger tips, from far end, thread 36" tube onto the center tubing connector.
9. Put O-ring grease and O-rings on remaining sucker rod connector and thread onto end of 36" tube.

NOTE: Subassembly should be oriented with the pressure port down when mounted into string for correct accel. polarity.

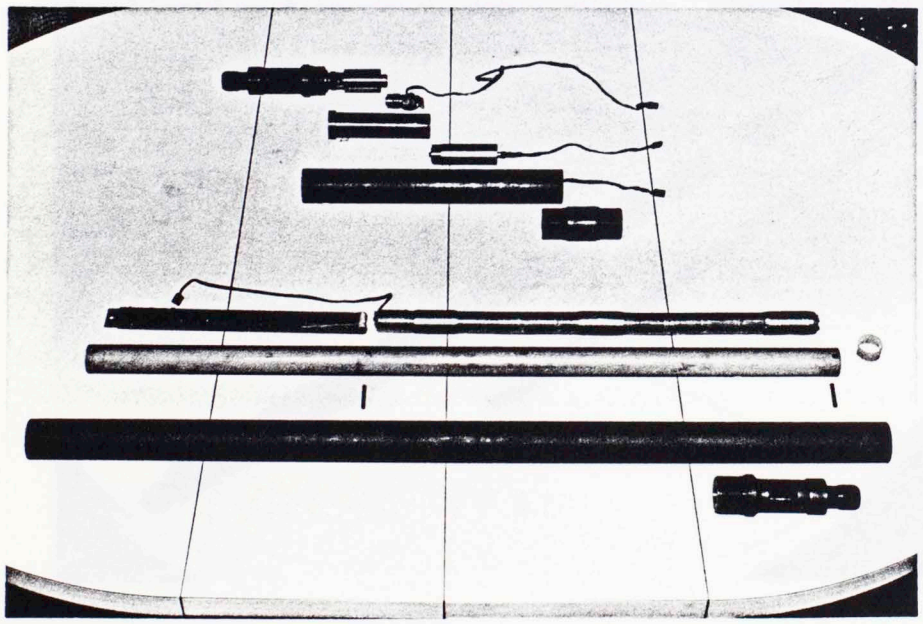

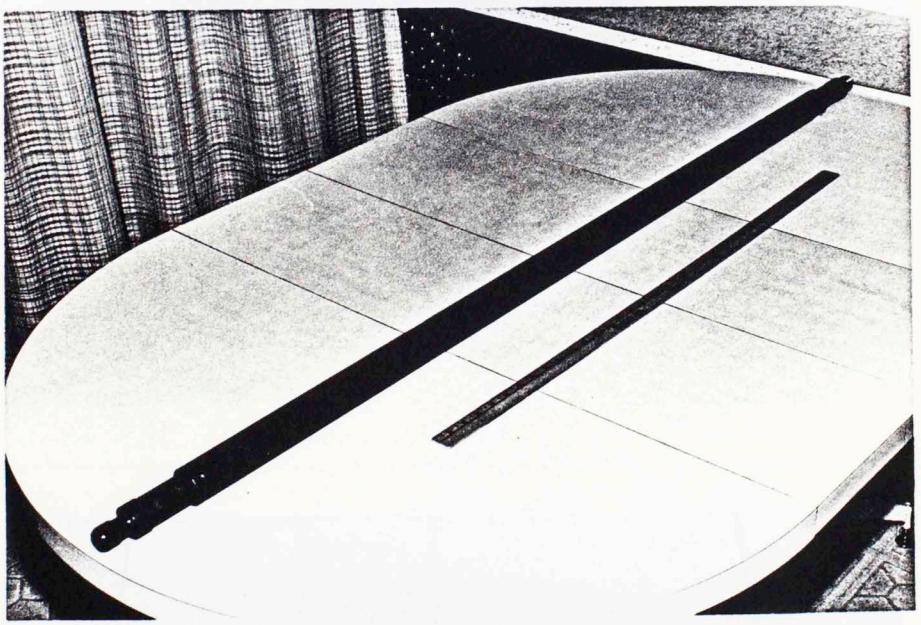

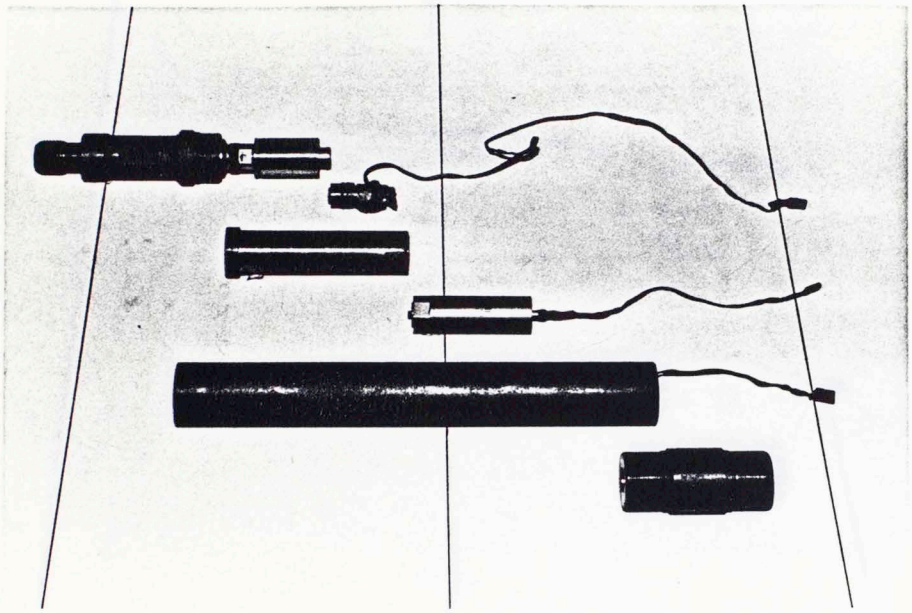

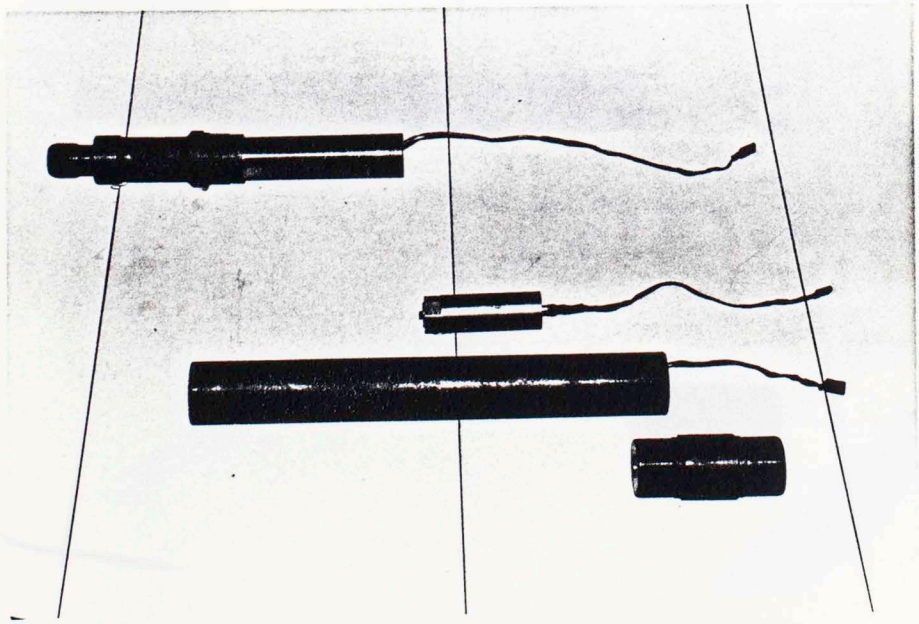

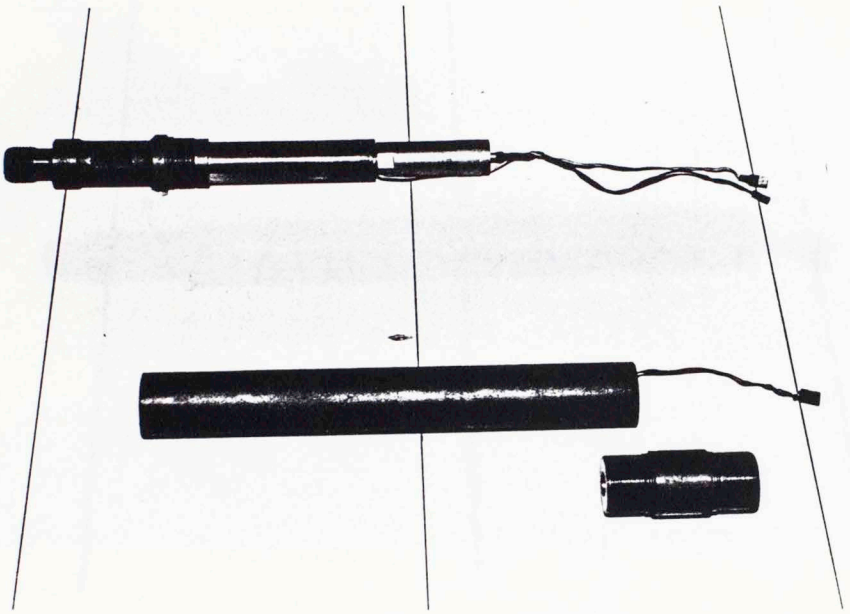

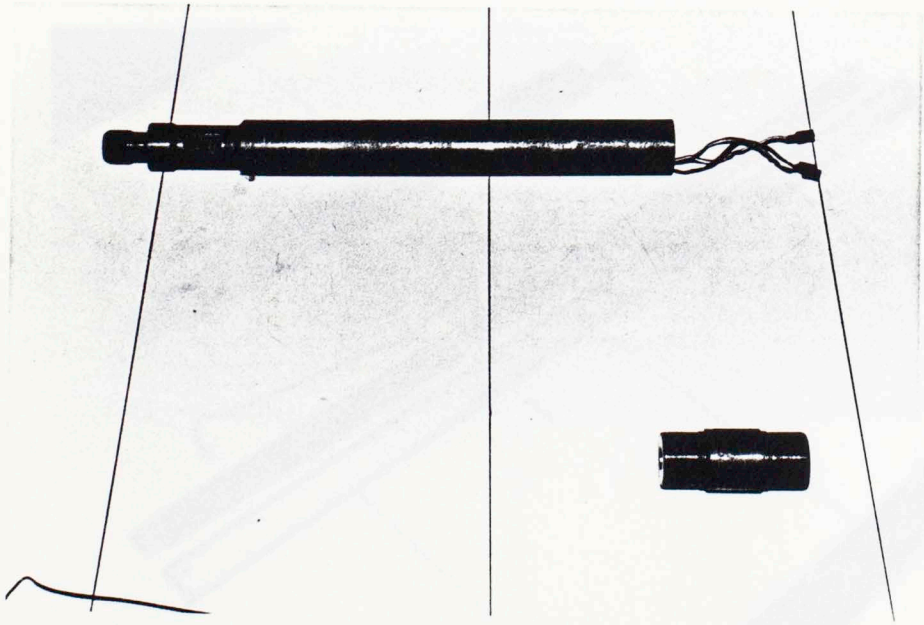

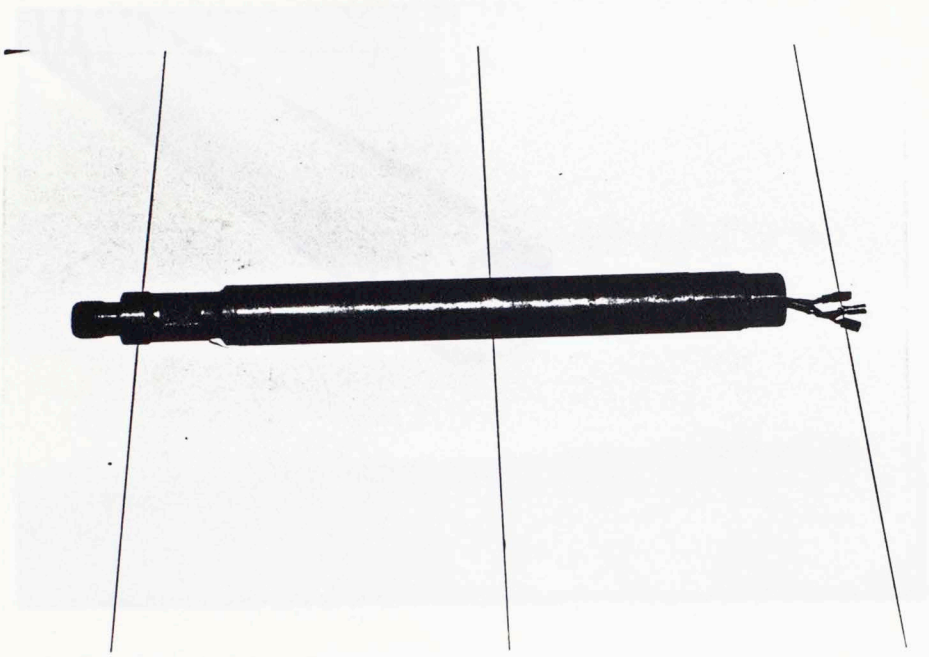

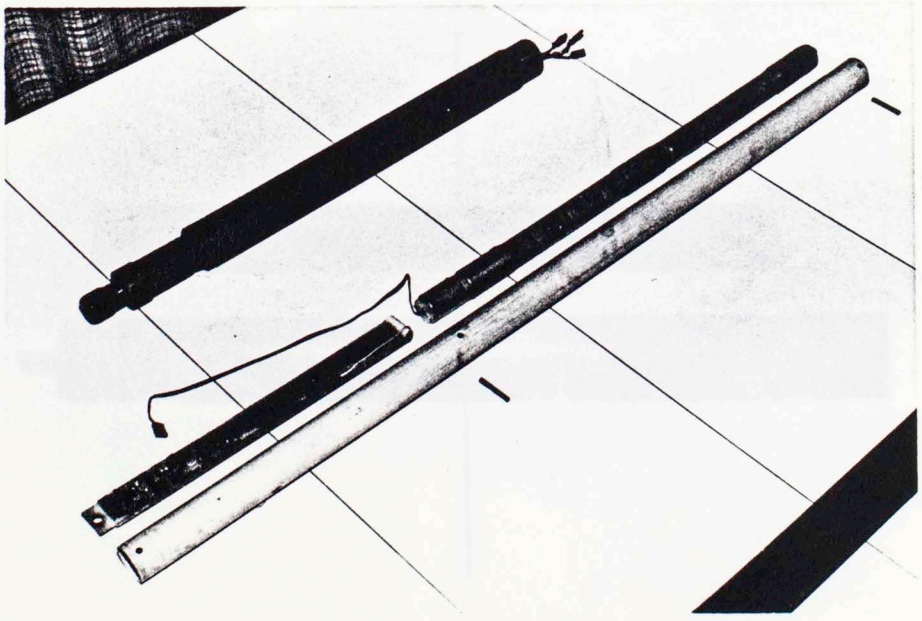

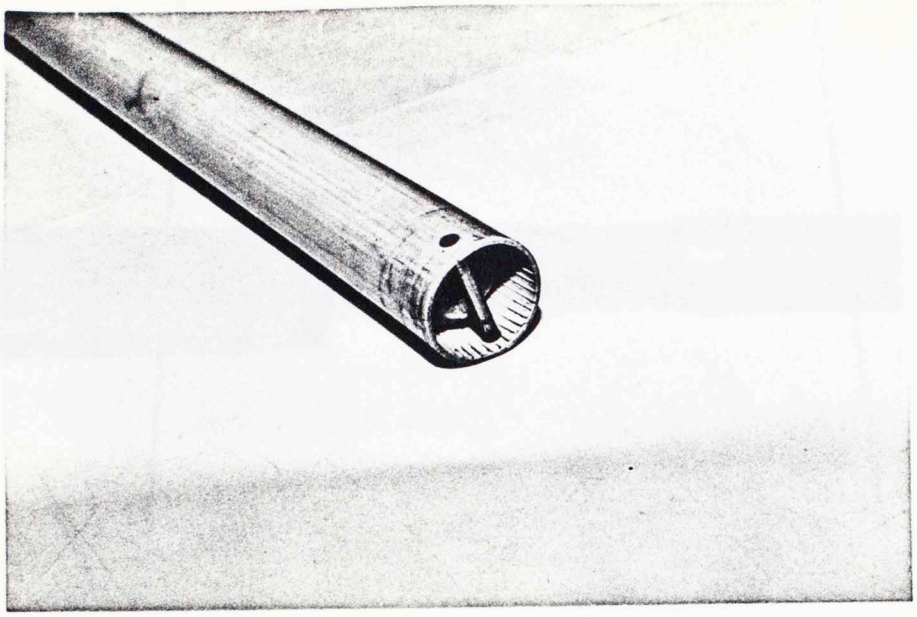

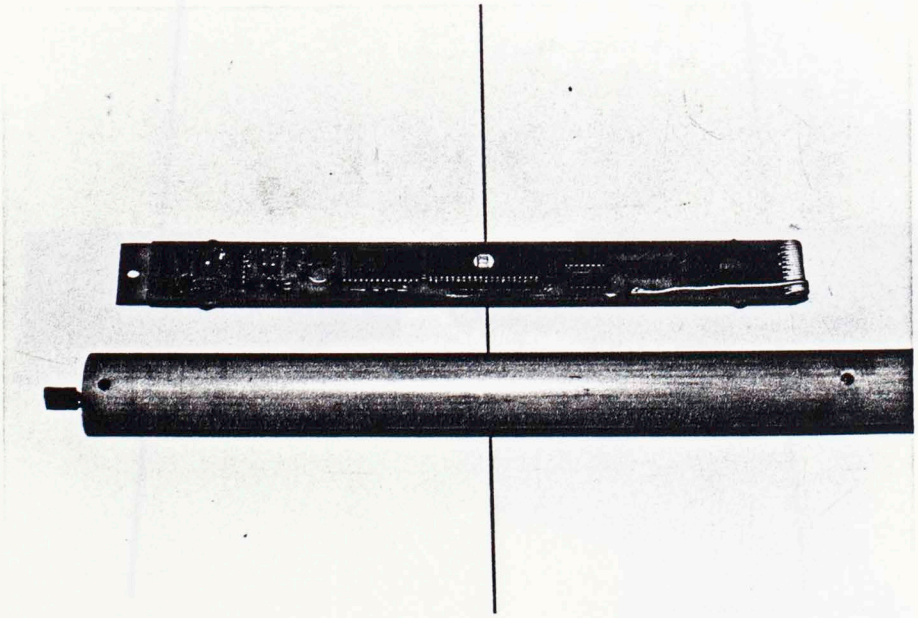

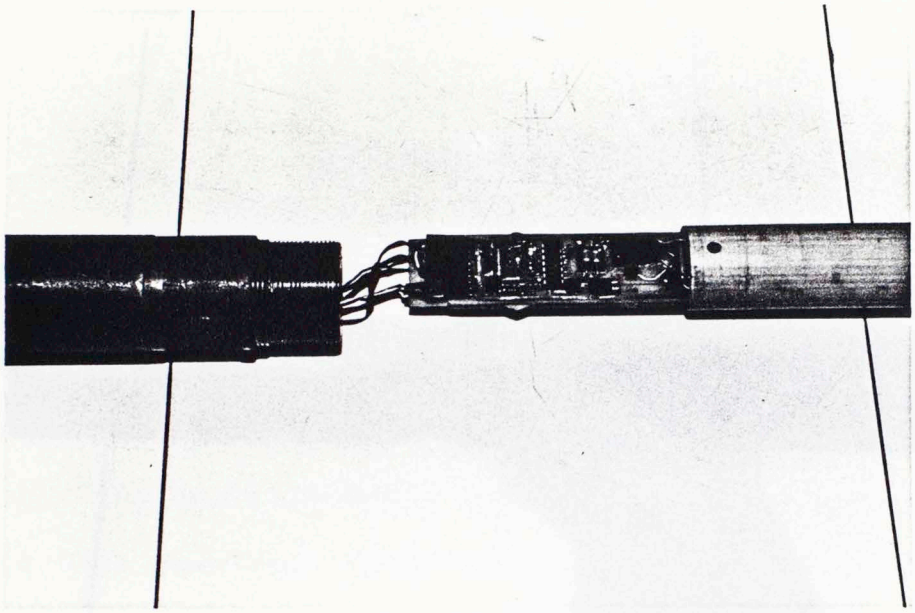

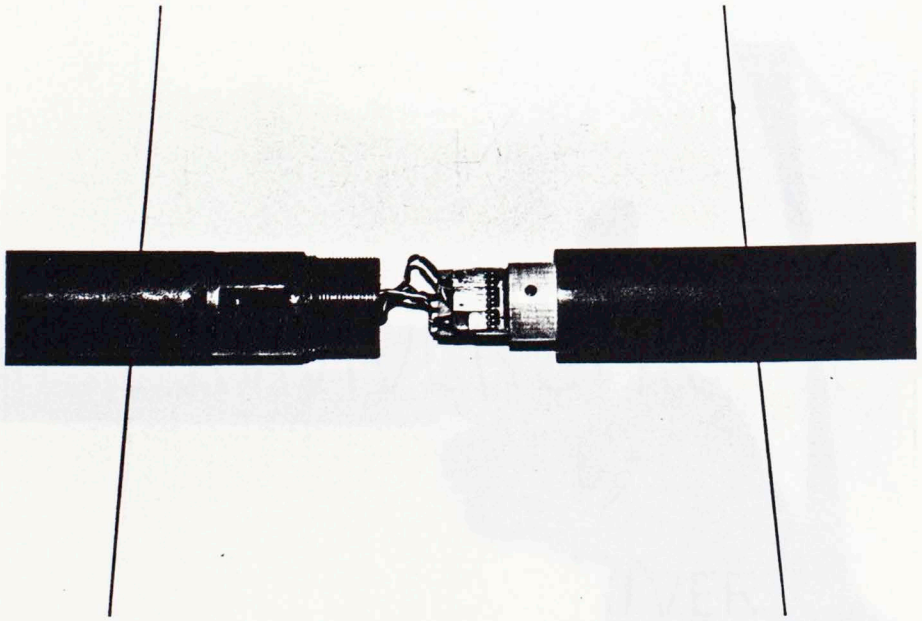

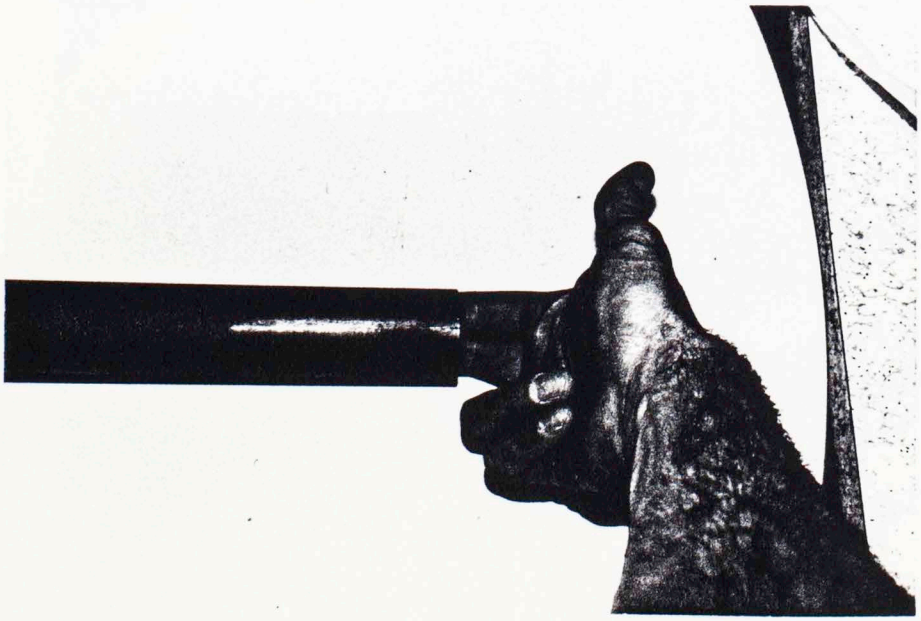

APPENDIX D

APPLICATION NOTES

The photographs on the next page show the correct configuration for reading and writing the apparatus circuit board, via the data recovery board shown in Appendix E.

The data recovery board is driven by a BASIC program to be found on Disk 1 under the filename DATREC.BAS.

The highly interactive program is also listed in Appendix E.

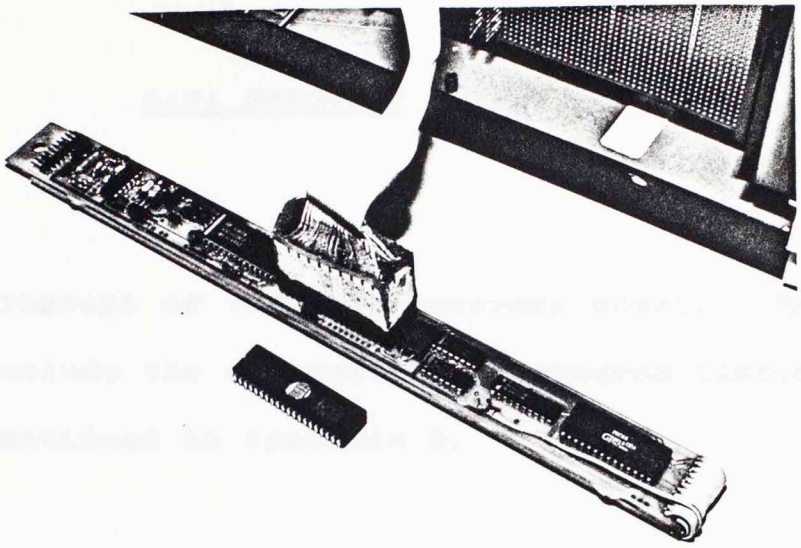

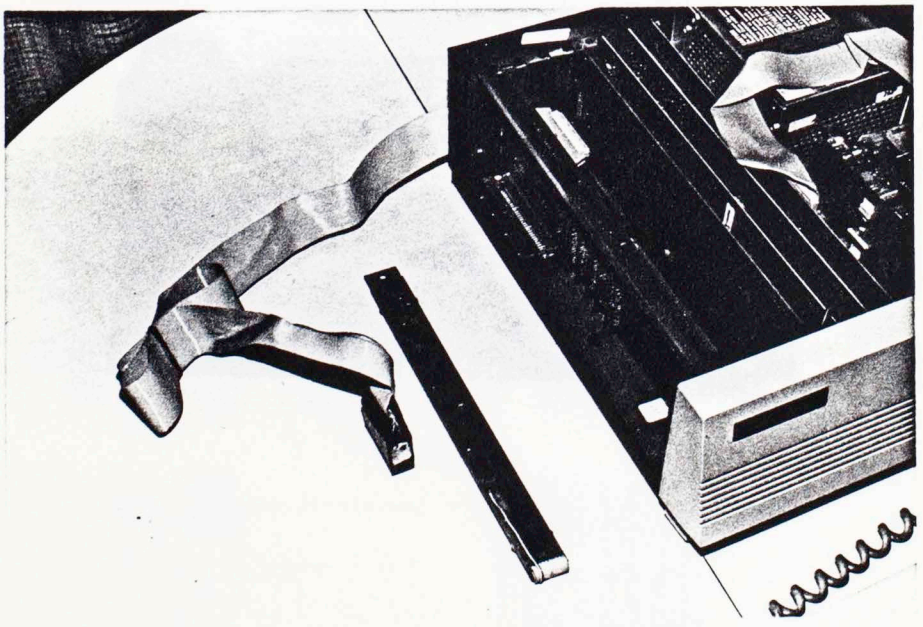

APPENDIX E

DATA RECOVERY BOARD

Below is a photograph of the data recovery board. The following pages include the schematics and program listing for the software mentioned in Appendix D.

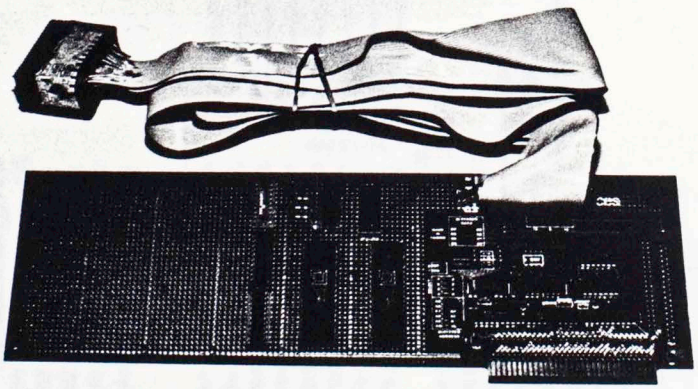

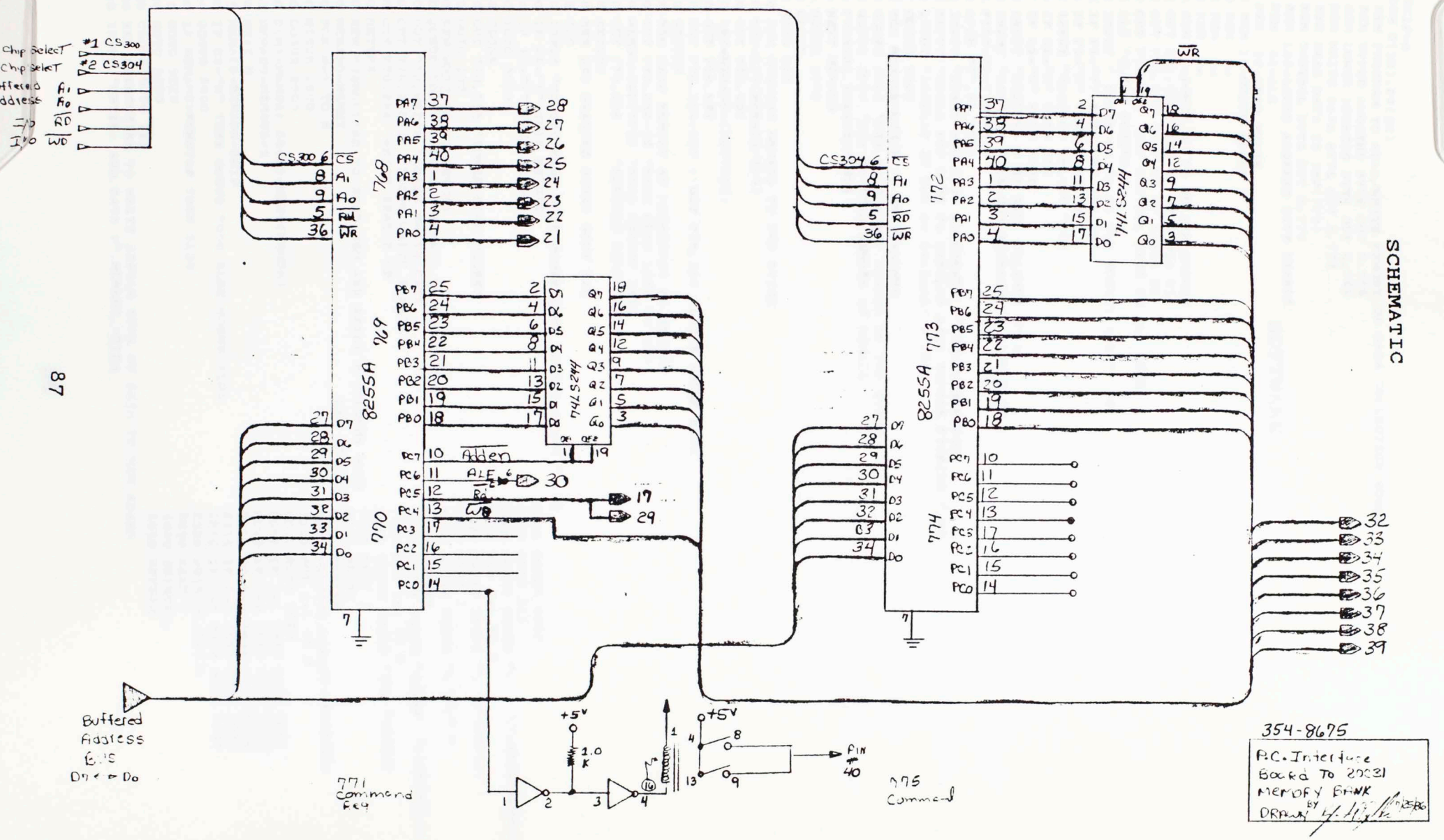

354-8675

P.C. Interface Board To 20031 Memory Bank

DRAWN BY

SOFTWARE

```
2 SKIP=0
5 DIM D(32),D$(32)
10 REM PROGRAM TO READ/WRITE MEMORY ON DATA COLLECTION BOARD
20 REM UPPER ADDRESS BYTE OUT X,768
30 REM LOWER ADDRESS BYTE OUT X,769
40 REM WRITE DATA BYTE OUT X,772
50 REM READ DATA IN INP(773)
60 REM CONTROL BYTE OUT X,770
70 REM 128=LOWER ADDRESS BYTE ENABLE
80 REM  64=ALE
90 REM  32=READ PULSE
100 REM 16=WRITE PULSE
110 REM  8=
120 REM  4=
130 REM  2=
140 REM  1=POWER ON TO 40 PIN SOCKET
150 OUT 771,128 'SET UP OF 8255A U1
160 OUT 775,130 'SET UP OF 8255A U2
170 OUT 770,255 'SET CONTROL BYTE TO ALL ONES
180 CLS 'CLEAR SCREEN
190 INPUT " POWER ON TO 40 PIN SOCKET Y/N ", P$
200 IF P$="Y" THEN OUT 770,254
210 IF P$="N" THEN GOTO 190
215 INPUT "Read or Write? ",Q$
216 IF Q$="R" THEN 218
217 IF Q$="W" THEN 6000
218 INPUT "DESIRED # OF DATA COLUMNS >";N
220 INPUT "NAME OF FILE FOR STORAGE ON DISK ",F$
230 FIL$=F$+".PRN"
240 OPEN "O",#1,FIL$
250 INPUT "START AND STOP ADDRESSES >",MEMST,MEMSTOP
265 INPUT "WOULD YOU LIKE TO DISPLAY DATA BEFORE STORING ",P$
266 INPUT "DISPLAY IN Hex or Decimal? >",B$
267 GOSUB 5000
270 FOR MEMADD=MEMST TO MEMST+MEMRD
280 GOSUB 1000 'SUB TO CONVERT MEMADD TO TWO BYTES
290 GOSUB 2000 'SUB TO READ MEMORY AT MEMADD
300 PRINT#1,MEMADD;MEMDA
310 NEXT MEMADD
315 GOSUB 3000
320 CLOSE
330 GOTO 220
1000 REM CONVERT MEMADD TO TWO BYTES
1010 UBY=INT(MEMADD/256)
1020 OUT 768,UBY
1030 LBY=MEMADD-(UBY*256)
1040 OUT 769,LBY
1050 OUT 770,254-192 : OUT 770,254 'LATCH LOWER BYTE
1060 RETURN
2000 REM READ MEMORY AS ADDRESSED BY MEMADD
2010 OUT 770,254-32 'MAKE READ LINE GO LOW
2020 MEMDA=INP(773) 'READ MEMORY DATA
2030 OUT 770,254    'RESTORE READ LINE
2040 RETURN
3000 REM END READING POWER DOWN Y/N
3010 CLS
3020 INPUT "MEMORY READ OVER POWER DOWN SOCKET ? Y/N " ,P$
3030 IF P$="N" THEN RETURN
3040 IF P$="Y" THEN 3100
3050 GOTO 3020
3100 CLOSE
3110 OUT 770,255 'POWER DOWN SOCKET
3120 GOTO 190
4000 REM WRITING TO MEMORY
4010 GOSUB 1000 'CONVERTS MEMADD TO TWO BYTES
4020 OUT 772,WRTDA 'LOADS WRITE DATA
4030 OUT 770,254-16 'DROPS WRITE ENABLE
4040 OUT 770,254 'WRITE ENABLE UP
4050 RETURN
5000 REM SUBROUTINE TO READ MEM AND PRINT N COLUMNS WITH
5010 MEMADD=MEMST                                HEX ADDRESS
5020 FOR M=1 TO N
5030 GOSUB 1000
5040 GOSUB 2000
5050 D(M)=MEMDA: D$(M)=HEX$(MEMDA)
5060 MEMADD=MEMADD+1
5070 NEXT M
5075 MEMADD=MEMADD+SKIP
5080 IF B$="H" THEN GOSUB 7000 ELSE GOSUB 7100
5090 GOSUB 8000
5100 IF MEMADD>MEMSTOP THEN 5130
5110 GOTO 5020
5120 GOTO 5020
5130 CLOSE:GOTO 215
6000 REM SUBROUTINE TO WRITE SINGLE BYTE OF DATA TO MEM BOARD
6010 INPUT "ENTER: ADD,DATA >",MEMADD,WRTDA
6020 GOSUB 4000
6030 GOTO 215
7000 PRINT USING "\     \";HEX$(MEMADD-N-SKIP);
7010 FOR I=1 TO N
7020 PRINT USING "\  \";D$(I);
7030 NEXT I
7040 PRINT USING "\ \";" "
7050 RETURN
7100 PRINT USING "#####  ";(MEMADD-N);
7110 FOR I=1 TO N
7120 PRINT USING "### ";D(I);
7130 NEXT I
7140 PRINT
7150 RETURN
8000 PRINT#1,MEMADD-(N+SKIP);
8010 FOR I=1 TO N
8011 GOTO 8020
8012 IF I=1 THEN GOTO 8030
8013 IF I=2 THEN GOTO 8030
8014 IF I=3 THEN GOTO 8030
8015 IF I=5 THEN GOTO 8030
8016 IF I=6 THEN GOTO 8030
8020 PRINT#1,D(I);
8030 NEXT I
8040 PRINT#1,
8050 RETURN
```

APPENDIX F

ELECTRICAL CIRCUITS

This appendix contains the complete circuit documentation, including schematics, assembly drawings, power distribution schematic, and printed circuit board artworks.

There are also photographs of the finished assembly and the 8:1 originals from which the artworks were made.

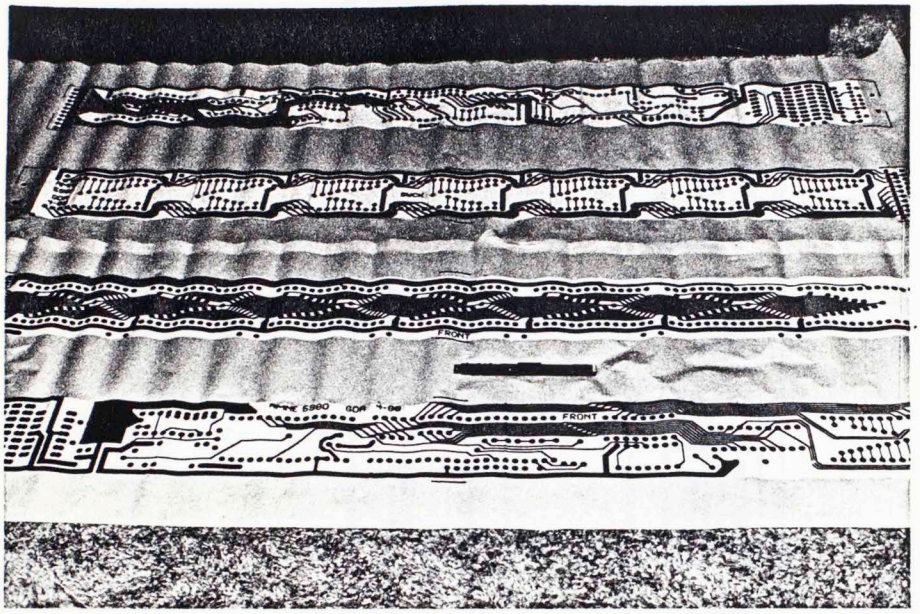
FRONT
FRONT

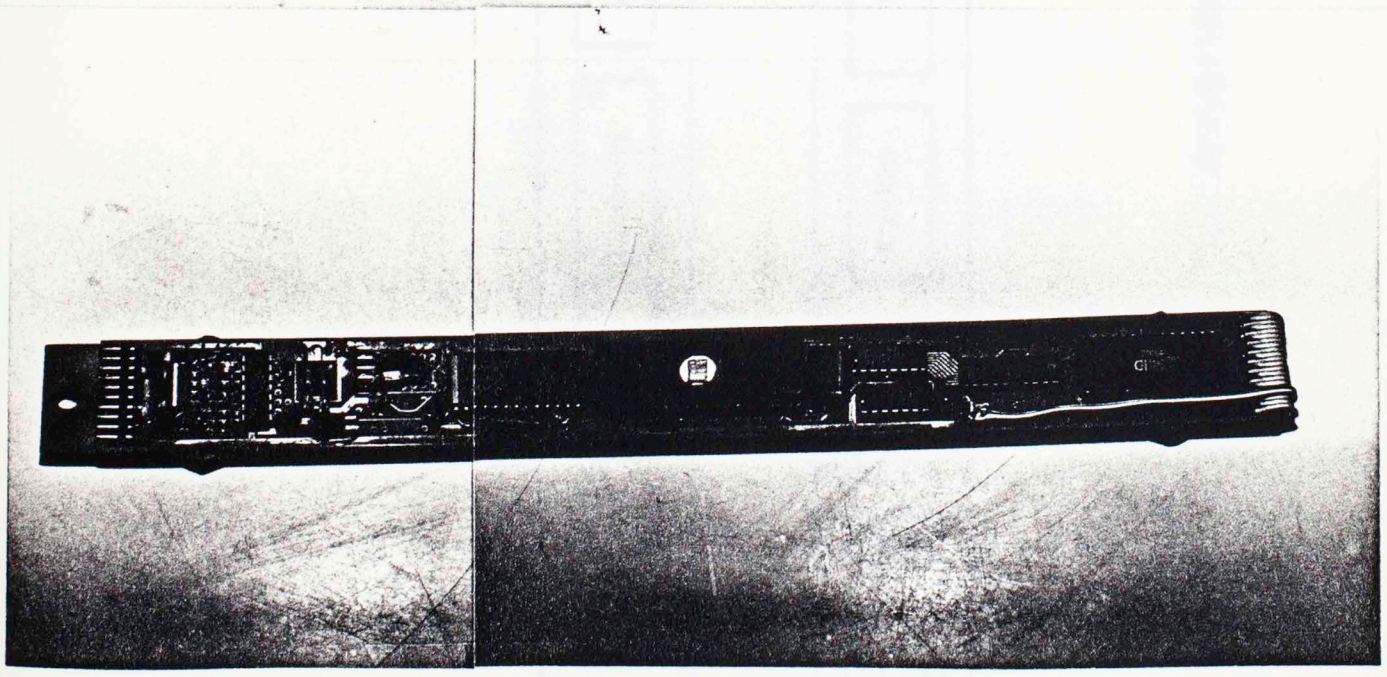

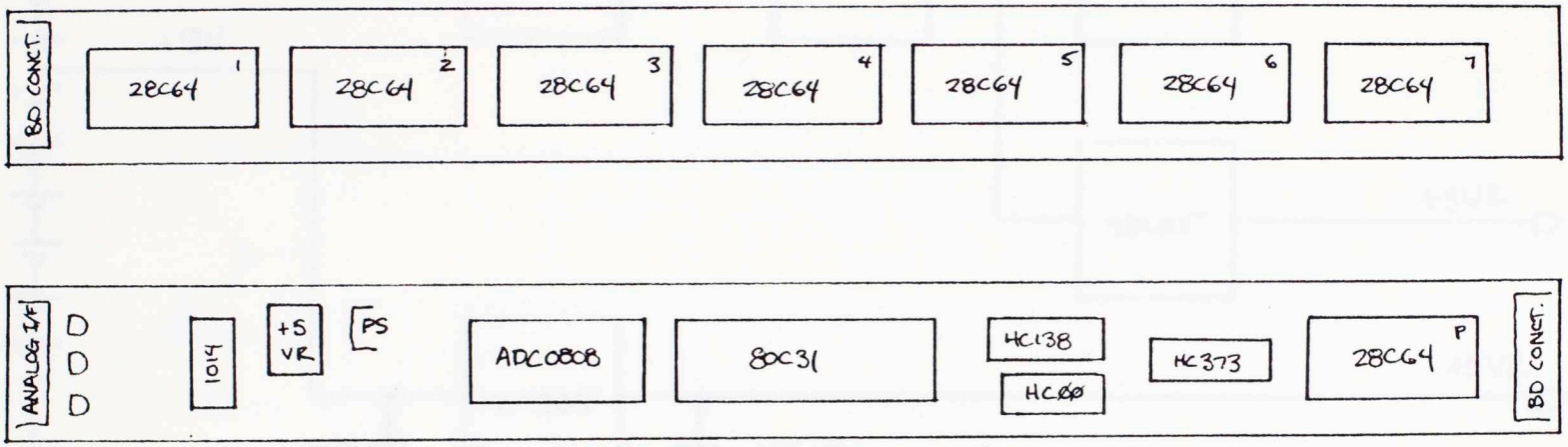

ASSEMBLY DRAWING

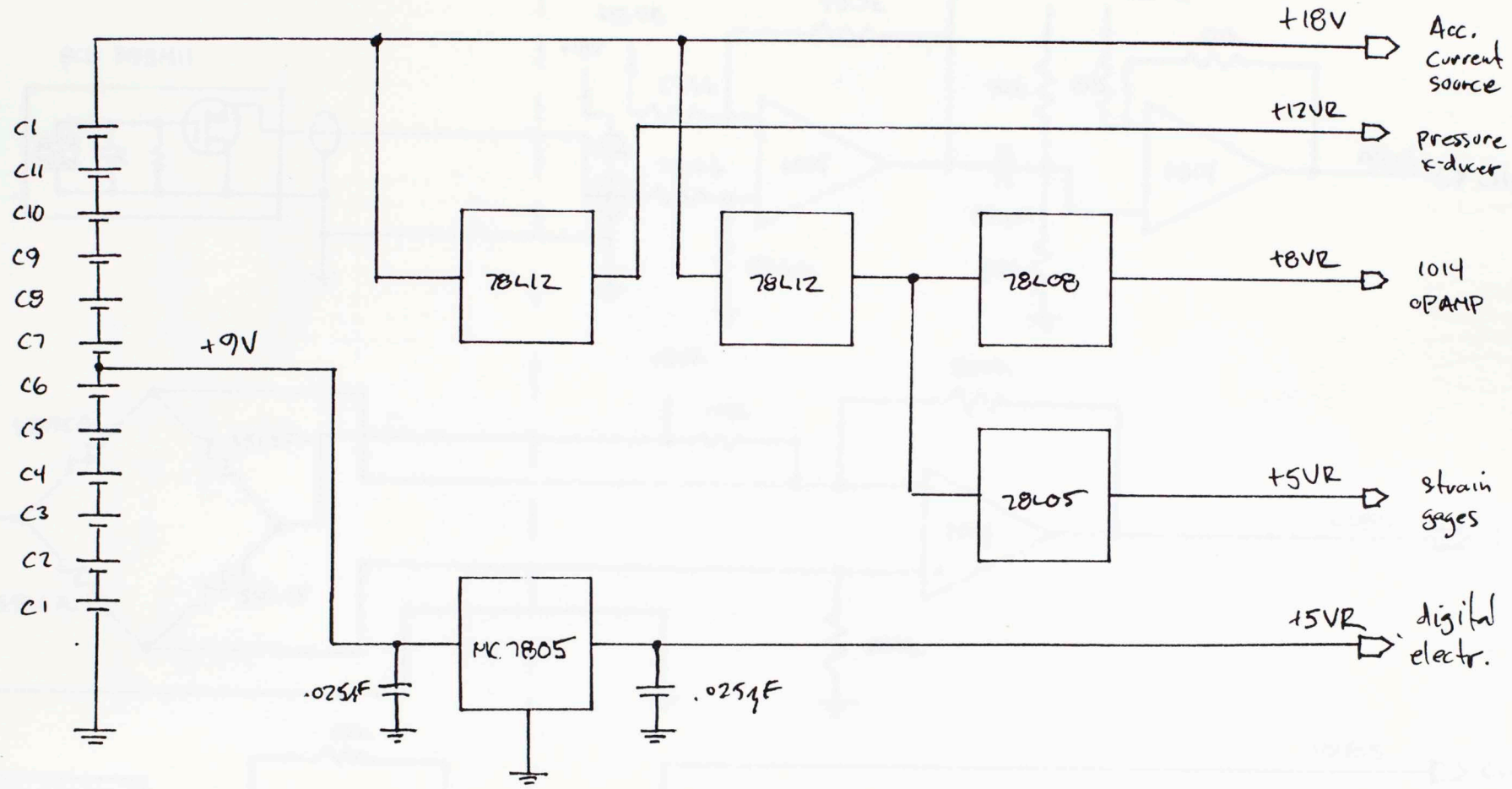

POWER DISTRIBUTION

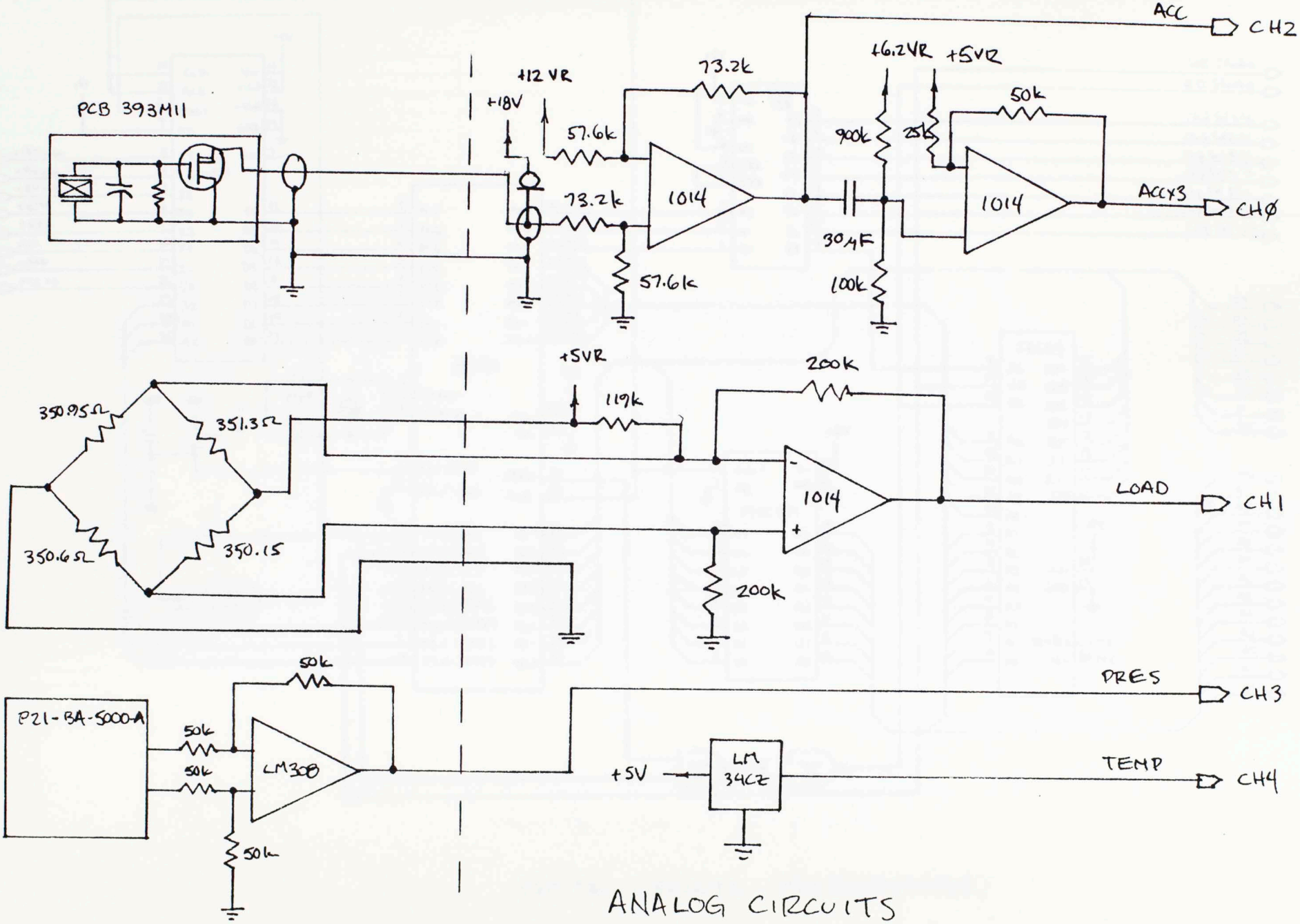

ANALOG CIRCUITS

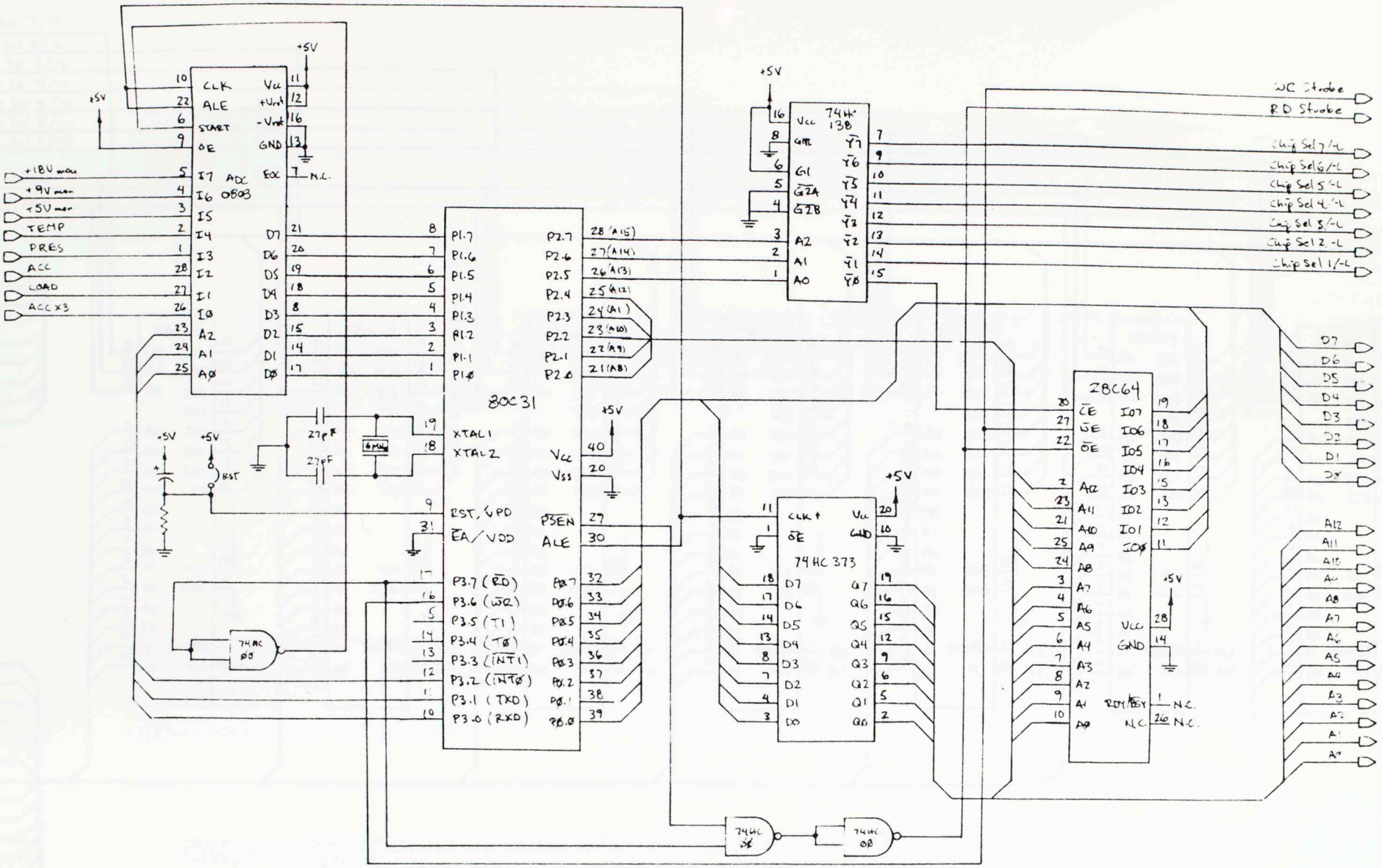

DIGITAL CIRCUITS (MICROCOMPUTER)

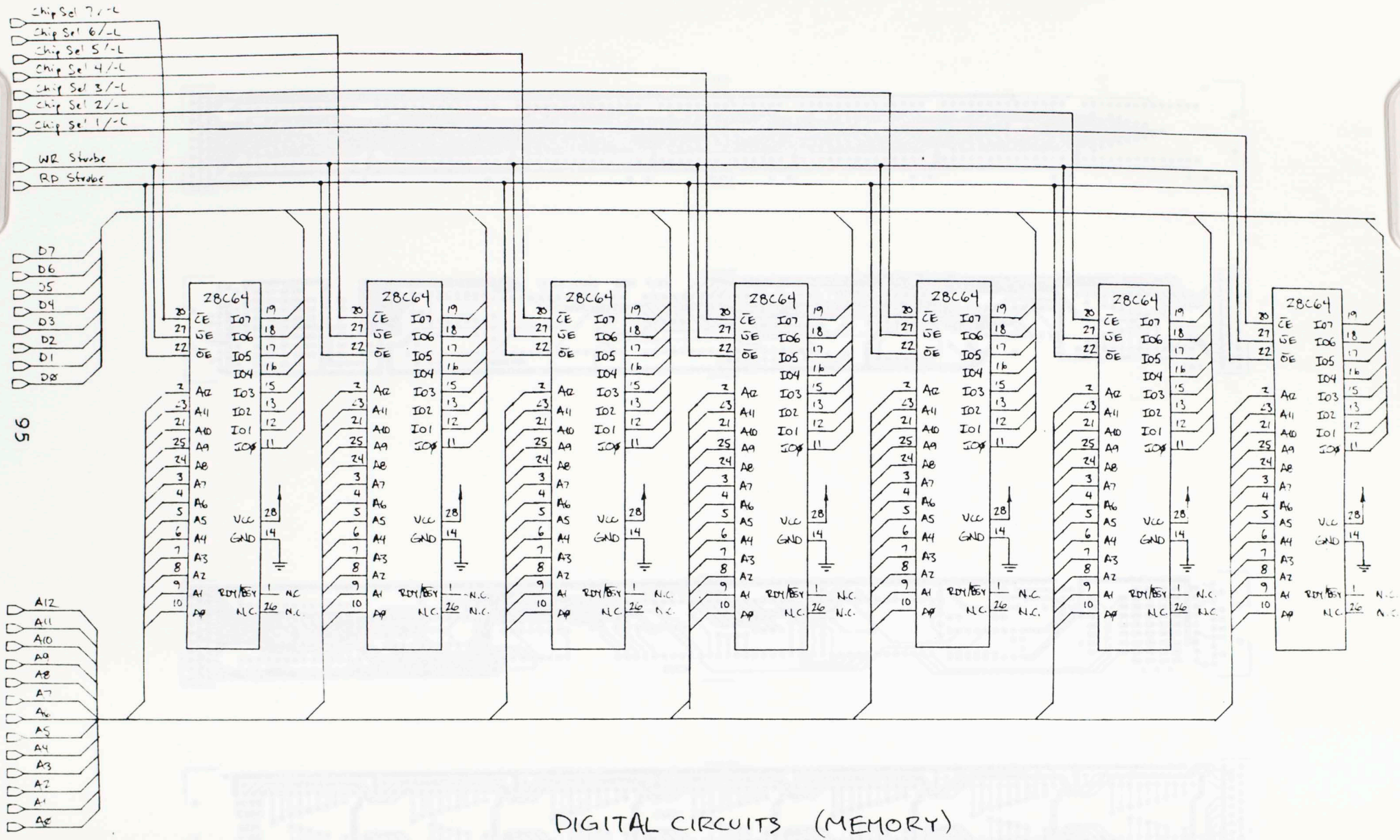

DIGITAL CIRCUITS (MEMORY)

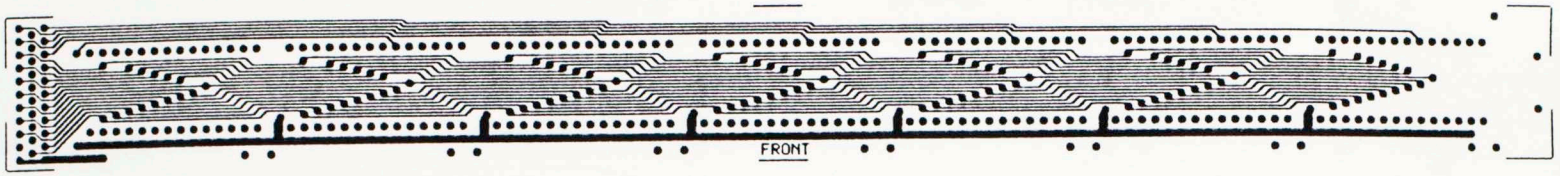
FRONT

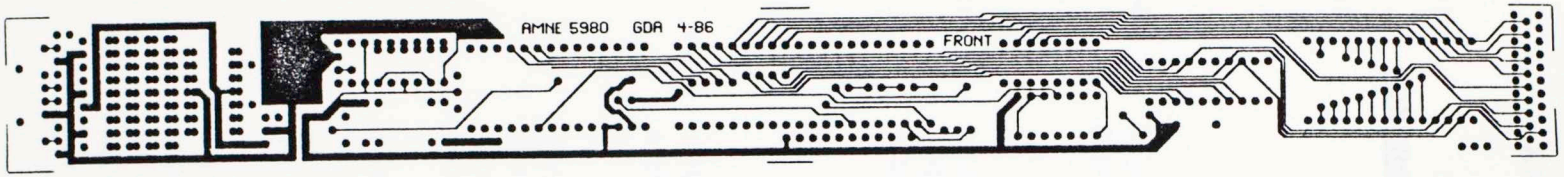
AMNE 5980 GDA 4-86
FRONT

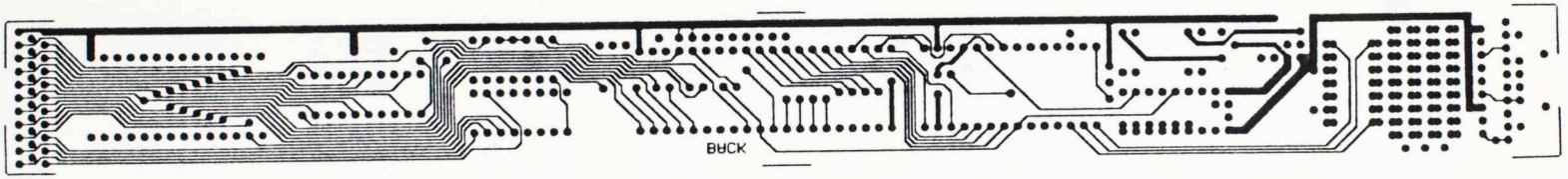
BACK

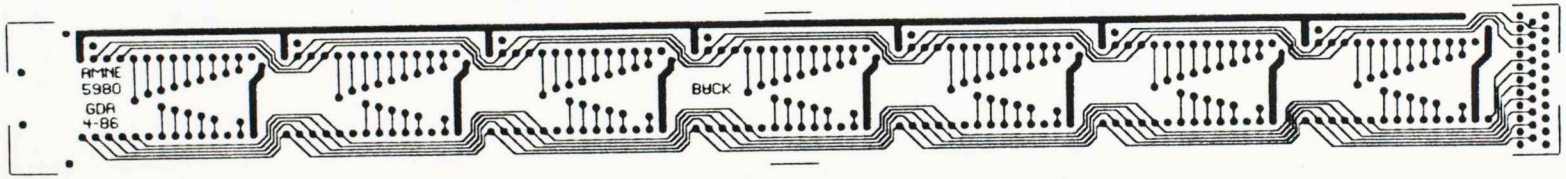
AMNE
5980
GDA
4-86
BACK

APPENDIX G

CONTROLLER FIRMWARE

ASSEMBLY LANGUAGE PROGRAM for DOWNHOLE DATA ACQUISITION SYSTEM

```
CODE        ADD   LABEL      OPCODE            COMMENTS
B1 B2 B3

01 30       000      ORG:    AJMP START

                     ;
                     ;
                     ;
                     ;
7B 01       030   START:     MOV R3,#02H       ;Init. TABLE POINTER
7C 0F       032              MOV R4,#0FH       ;Set # of lines (M) in
                                               ;START/STOP/MODE table
                     ;
                     ;
11 50       034   REDOX:     ACALL DOX         ;Get Nth sampling period
DC FC       036              DJNZ R4 REDOX     ;information, N=max?
01 38       038   DONE:      AJMP DONE         ;END
                     ;
                     ;
                     ;
                     ;
                     ;
EB          050   DOX:       MOV A,R3          ;Fetch HI byte of
11 7E       051              ACALL MOVC        ;STARTADD
F5 83       053              MOV DPH,A
                     ;
0B          055              INC R3            ;increment TABPTR
EB          056              MOV A,R3          ;Fetch LO byte of
11 7E       057              ACALL MOVC        ;STARTADD
F5 82       059              MOV DPL,A
                     ;
0B          05B              INC R3            ;increment TABPTR
EB          05C              MOV A,R3          ;Fetch HI byte of
11 7E       05D              ACALL MOVC        ;STOPADD
FA          05F              MOV R2,A
                     ;
0B          060              INC R3            ;increment TABPTR
EB          061              MOV A,R3          ;Fetch LO byte of
11 7E       062              ACALL MOVC        ;STOPADD
F9          064              MOV R1,A
                     ;
0B          065              INC R3            ;increment TABPTR
EB          066              MOV A,R3          ;Fetch MODE byte
11 7E       067              ACALL MOVC
F5 28       069              MOV 28,A
                     ;
31 00       06B              ACALL DO          ;Execute Nth samp period
```

```
                ;
0B      06D             INC R3          ;advance TABPTR to next
0B      06E             INC R3          ;line in table
0B      06F             INC R3
0B      070             INC R3
                ;
22      071             RET             ;next N
                ;
                ;
83      07E     MOVC:   MOVC A,@A+PC
22      07F             RET
                ;
                ;
```

SAMPLE POINTER TABLE

ADD	SAMPLE PERIOD	START BYTE HI LO	STOP BYTE HI LO	MODE	Initial Delay Set XH XL	Initial Delay (min)
080	OA:	XH XL	29 60	88		
088	A:	30 00	48 00	24		
090	AB:	29 60	29 B0	24	20 00	300
098	B:	48 00	60 00	24	20 F0	270
0A0	BC:	29 B0	2A 00	88	21 E0	240
0A8	C:	60 00	78 00	24	22 D0	210
0B0	CD:	2A 00	2A 50	88	23 C0	180
0B8	D:	78 00	90 00	24	24 B0	150
0C0	DE:	2A 50	2A A0	88	25 A0	120
0C8	E:	90 00	A8 00	24	26 90	90
0D0	EF:	2A A0	2A F0	88	27 80	60
0D8	F:	A8 00	C0 00	24	28 70	30
0E0	FG:	2A F0	2E 40	88	29 10	10
0E8	G:	C0 00	00 00	42	29 58	1
0F0	GZ:	23 40	30 00	88		

MODE DEFINITION: 88=Channels 0-7, 1/60 Hz each
24=Channels 0-3, 40 Hz each
42=Channels 0-1, 20 Hz each

```
CODE       ADD  LABEL      OPCODE           COMMENTS
B1 B2 B3
-------------------------------------------------------------------------

                                           ;DO is the main routine
                                           ;and executes calls to
                                           ;three routines that
                                           ;sample and save data and
                                           ;wait app. sampling delay
31 40      100 DO:         ACALL SAMPSTOR
31 70      102             ACALL SAVE
31 20      104             ACALL BLINK
31 28      106             ACALL DELAY
           ;
           ;
EA         108             MOV A,R2        ;Test for DPTR=STOPADD,
B5 83 05   109             CJNE A,DPH CHI  ;first the HI bytes, if
E9         10C             MOV A,R1        ;equal,
B5 82 04   10D             CJNE A,DPL CLO  ;then the LO
22         110             RET             ;DPTR=STOPADD, exit DO
           ;
           ;
00         111 CHI:        NOP             ;continue since inequal
00         112             NOP             ;balance path with that
00         113             NOP             ;if HI bytes were equal
           ;
21 00      114 CLO:        AJMP DO         ;take another sample set
           ;
           ;
           ;
           ;
C2 B4      120 BLINK:      CLR P3.4        ;Blink LED  (2mS)
31 B0      122             ACALL 2ms
D2 B4      124             SET B P3.4
22         126             RET
           ;
           ;
20 45 06   128 DELAY:      JB 45 CALL40Hz  ;Test MODE for sampling
20 46 06   12B             JB 46 CALL20Hz  ;rate (required overhead
20 47 06   12E             JB 47 CALL60s   ;wait)
           ;
31 C0      131 CALL40Hz:   ACALL FILL40Hz  ;call for 40 Hz overhead
22         133             RET             ;delay
           ;
31 D0      134 CALL20Hz:   ACALL FILL20Hz  ;call for 20 Hz overhead
22         136             RET             ;delay
           ;
```

```
CODE       ADD  LABEL      OPCODE              COMMENTS
B1 B2 B3
-------------------------------------------------------------------------
                ;
31 E0       137 CALL60s:   ACALL FILL60s       ;call for 60 second
22          139            RET                 ;overhead delay
                ;
                ;
                                                ;SAMPSTOR samples the
                                                ;A/D channels defined by
                                                ;the MODE byte and stores
                                                ;them temporarily in uP
                                                ;RAM until they can be
                                                ;saved as a group in the
                                                ;EEPROM memory by SAVE
                ;
78 20       140 SAMPSTOR:  MOV R0,#20H         ;initialize RAM pointer
                ;
74 F8       142 NEXSAMP:   MOV A,#F8H          ;mask upper five bits
48          144            ORL A,R0
                ;
F5 B0       145            MOV P3,A            ;output A/D address
E0          147            MOVX A,@DPTR        ;latch add and activate
                                                ;WR strobe to start conv.
31 A0       148            ACALL 200us         ;wait for end of convrsn.
A6 90       14A            MOV @R0,P1          ;store data byte from A/D
                ;
08          14C            INC R0              ;inc RAM/ pointer and mov
E8          14D            MOV A,R0            ;into ACC to test for CH#
                ;
20 43 06    14E            JB 43 TESTACC3      ;test MODE byte for CH#
20 42 0B    151            JB 42 TESTACC2      ;desired per set and go
20 41 0E    154            JB 41 TESTACC1      ;to appr. test branch
                ;
                ;
00          157 TESTACC3:  NOP                 ;MODE said #CH=8, after
00          158            NOP                 ;balancing branch timing
00          159            NOP                 ;test ACC.3 to see if max
00          15A            NOP                 ;CH has been reached
30 E3 E4    15B            JNB ACC.3 NEXSAMP   ;If LO, sample next CH
22          15E            RET                 ;If HI, set done. Proceed
                ;
                ;
00          15F TESTACC2:  NOP                 ;repeat above for #CH=4
00          160            NOP
30 E2 DE    161            JNB ACC.2 NEXSAMP
22          164            RET
                ;
30 E1 DA    165 TESTACC1:  JNB ACC.1 NEXSAMP   ;repeat above for #CH=2
22          168            RET
                ;
                ;
```

```
                        ;
                        ;
                        ;
                                                    ;Subroutine SAVE follows
                                                    ;same logic as SAMPSTOR
                                                    ;only to save in EEPROM
                                                    ;the data stored sequen-
                                                    ;in RAM
                        ;
78 20        170 SAVE:      MOV R0,#20
                        ;
E6           172 NEXSAVE:   MOV A,@20          ;get data byte from RAM
F0           173            MOVX @DPTR,A       ;save it to EEPROM at
                        ;                      ;data pointer address
31 B0        174            ACALL 2msec        ;wait 1+ EEPROM WR cycle
                        ;
A3           176            INC DPTR           ;increment data pointer
08           177            INC R0             ;(rest same as SAMPSTOR)
E8           178            MOV A,R0
                        ;
20 43 06     179            JB 43 TESTACC3
20 42 0B     17C            JB 42 TESTACC2
20 41 0E     17F            JB 41 TESTACC1
                        ;
00           182 TESTACC3:  NOP
00           183            NOP
00           184            NOP
00           185            NOP
30 E3 E9     186            JNB ACC.3 NEXSAVE
22           189            RET
                        ;
00           18A TESTACC2:  NOP
00           18B            NOP
30 E2 E3     18C            JNB ACC.2 NEXSAVE
22           18F            RET
                        ;
30 E1 DF     190 TESTACC1:  JNB ACC.1 NEXSAVE
22           193            RET
```

TIMERS

```
7D 2E        1A0 200us:     MOV R5,#2EH        ;load least sig. tmr byte
7E 01        1A2            MOV R6,#01H        ;load next sign. tmr byte
7F 01        1A4            MOV R7,#01H        ;load most sign. tmr byte
31 F0        1A6            ACALL TIMER        ;call timer to execute
22           1A8            RET                ;200 microsecond delay
                        ;
                        ;
```

```
7D EF     1B0 2ms:          MOV R5,#EFH
7E 02     1B2               MOV R6,#02H
7F 01     1B4               MOV R7,#01H       ;call timer to execute
31 F0     1B6               ACALL TIMER       ;2 millisecond delay
22        1B8               RET
                ;
                ;
7D FF     1C0 FILL40Hz:     MOV R5,#FFH
7E 0D     1C2               MOV R6,#0DH
7F 01     1C4               MOV R7,#01H
31 F0     1C6               ACALL TIMER       ;call timer to execute
22        1C8               RET               ;delay combining with
                ;                             ;program overhead to
                ;                             ;produce 25 mS total
7D FF     1D0 FILL20Hz:     MOV R5,#FFH
7E 2A     1D2               MOV R6,#2AH
7F 01     1D4               MOV R7,#01H
31 F0     1D6               ACALL TIMER       ;execute 20 Hz (50 mS)
22                          RET               ;overhead
                ;
                ;
7D FF     1E0 FILL60s:      MOV R5,#FFH
7E FF     1E2               MOV R6,#FFH
7F E4     1E4               MOV R7,#E4H
31 F0     1E6               ACALL TIMER       ;execute 1/60 Hz (60 sec)
22                          RET               ;overhead
                ;
                ;
                ;
DD FE     1F0 TIMER:        DJNZ R5 TIMER     ;perform timer intervals
DE FC     1F2               DJNZ R6 TIMER     ;by decrementing registrs
DF FA     1F4               DJNZ R7 TIMER     ;until all zeroes.
22        1F6               RET
                ;
                ;
```

ROUTINE FOR IN-SYSTEM PROGRAMMING OF PROGRAM MEMORY THROUGH ICE

```
90 00 00 200 START1:      MOV DPTR #0000H ;init data pointr to 0000
E4       203 CONT:        CLR A           ;clear base register
93       204              MOVC A,@A+DPTR  ;get program mem byt from
F0       205              MOVX @DPTR,A    ;ICE mem and write to
31 B0    206              ACALL 2ms       ;data acqu. bd. prog. mem
A3       208              INC DPTR        ;get ready for next byte
E5 83    209              MOV A,DPH       ;test data pointer for 1k
30 E2 F5 20B              JB E2 CONT      ;copied, no, copy nex byt
31 20    20E              ACALL BLINK     ;yes, blink LED & quit
61 10    210 DONE1:       AJMP DONE1
```

APPENDIX H

DISK FILE LISTINGS

The following disk files can be found in the cover of this document.

```
 Volume in drive A is DISK 1
 Directory of  A:\

MASTER    WK1    116052  11-14-86    1:58a
FCALA282  WK1     24166   1-01-80    1:10a
DATREC    BAS      2637   1-01-80   12:03a
RUN828G   PRN    139646   1-01-80   12:55a
        4 File(s)     77824 bytes free
```

```
 Volume in drive A is DISK 2
 Directory of  A:\

RUN828A   PRN     41941   1-01-80    1:13a
RUN828B   PRN     41925   1-01-80    2:24a
RUN828C   PRN     41954   1-01-80    1:56a
RUN828D   PRN     41923   1-01-80    1:42a
RUN828E   PRN     41864   1-01-80    1:25a
RUN828F   PRN     41742   1-01-80    1:08a
RUN828OA  PRN     21437   1-01-80   12:18a
        7 File(s)     89088 bytes free
```